

2009

EPIGENETIC REGULATION OF ZEB2 IN BREAST CANCER

Jenna Marie Pilon

Follow this and additional works at: <https://ir.lib.uwo.ca/digitizedtheses>

Recommended Citation

Pilon, Jenna Marie, "EPIGENETIC REGULATION OF ZEB2 IN BREAST CANCER" (2009). *Digitized Theses*. 4004.

<https://ir.lib.uwo.ca/digitizedtheses/4004>

This Thesis is brought to you for free and open access by the Digitized Special Collections at Scholarship@Western. It has been accepted for inclusion in Digitized Theses by an authorized administrator of Scholarship@Western. For more information, please contact wlsadmin@uwo.ca.

EPIGENETIC REGULATION OF *ZEB2* IN BREAST CANCER

(Spine Title: Epigenetic Regulation of *ZEB2* in Breast Cancer)

(Thesis format: Monograph)

by

Jenna Marie Pilon

Graduate Program in Biochemistry



A thesis submitted in partial fulfillment of the requirements
for the degree of Master of Science

The School of Graduate and Postdoctoral Studies
The University of Western Ontario
London, Ontario, Canada

©Jenna M. Pilon 2009

ABSTRACT

Epithelial-mesenchymal transition (EMT) has been implicated in the process of breast cancer metastasis, and ZEB2 has been implicated in EMT. Some evidence exists suggesting that epigenetic DNA methylation modifications may be involved in EMT; however, the specific contribution of DNA methylation to *ZEB2* regulation is poorly understood. I hypothesize that aberrant hypomethylation of the *ZEB2* promoter results in increased expression of *ZEB2* in cells that have gone through EMT. I observed decreased *ZEB2* promoter methylation and increased *ZEB2* expression *in vitro* in mesenchymal-like breast cancer cells. Functional assays performed by treating cells with epigenetic inhibitors revealed *ZEB2* demethylation that correlated with *ZEB2* re-expression in a cell line sub-population. As well, a region flanking the *ZEB2* gene was defined as having promoter activity, and this activity was sensitive to *in vitro* DNA methylation. These results support my hypothesis that DNA methylation may be involved in the regulation of *ZEB2* expression.

Keywords: ZEB2, epigenetics, breast cancer, epithelial-mesenchymal transition, DNA methylation

CO-AUTHORSHIP

All experimental work presented in this thesis was performed by Jenna Pilon, with the exception of MDA-MB-468-GFP and MDA-MB-468-LN panels in Figure 3.3. This work was performed by Joseph Andrews and was included for the continuity of the thesis.

ACKNOWLEDGEMENTS

I would like to thank everyone who has supported and aided me throughout the progress of my degree. First of all, I would like to thank my supervisor, David Rodenhiser, for allowing me to find my own path and for always encouraging my thinking and for challenging me. I would also like to thank Ann Chambers for her continual support, and for treating me as one of her own students. I would like to thank the other members of my supervisory committee, Alan Tuck and Mellissa Mann for their guidance and instrumental help.

I would like to thank Joseph Andrews for introducing me to the techniques of the laboratory and dealing with my obsessive organization. I would also like to thank the members of the Chambers lab for all of their help and support, and for treating me as a labmate, with a special mention to David Dales, Brigitte Goulet, Wendy Kennette, Jen Mutrie and Leslie Souter, without whom I would have never made it through the last year. I would also like to thank members of the VRL, and especially my amazing friends- Alysha, Brenna, Courtney, Erin, Katie, Kristin, Julia, Matt, Rohann, - for dealing with me and helping me with my troubleshooting, and for making my time in London memorable. I would also like to thank all of my friends from home for their support during this time.

I would like to thank my family who have always supported me and encouraged me, and for their attempts to understand what I am doing throughout this journey.

Finally, I would like to thank my partner, Matthew Gray, for everything. Thank you for listening to my daily disasters and frustrations, and sharing in my triumphs. Thank you for supporting me and helping me throughout the last two years and thank you for being here for me when I have needed you the most.

TABLE OF CONTENTS

CERTIFICATE OF EXAMINATION	ii
ABSTRACT	iii
CO-AUTHORSHIP	iv
ACKNOWLEDGEMENTS	v
TABLE OF CONTENTS	vi
LIST OF TABLES	x
LIST OF FIGURES	xi
LIST OF ABBREVIATIONS	xiv
CHAPTER 1 – INTRODUCTION	1
1.1 BREAST CANCER AND THE IMPORTANCE OF METASTASIS	1
1.1.1 Breast Cancer	1
1.1.2 The Metastatic Cascade	2
1.2 THE IMPORTANCE OF EPITHELIAL-MESENCHYMAL TRANSITION	3
1.2.1 Normal Epithelium	4
1.2.2 Epithelial versus Mesenchymal Cells	5
1.2.3 The EMT Process	6
1.2.4 EMT in Development	7
1.2.5 EMT in Cancer Metastasis	7
1.3 THE IMPORTANCE OF EPIGENETICS	10

1.3.1	An Overview of Epigenetics	11
1.3.2	Normal Functions of DNA Methylation	15
1.3.3	DNA Methylation in Cancer	16
1.3.4	Epigenetic Drugs as Tools	20
1.4	THE METASTASIS PROJECT	22
1.4.1	The Metastasis Project	22
1.4.2	Candidate Genes	23
1.5	THE RELEVANCE OF ZEB2 TO EMT	24
1.5.1	Molecular Functions of ZEB2	24
1.5.2	ZEB2 in Developmental Disease	32
1.5.3	ZEB2 in Cancer	33
1.5.4	The Complex Regulation of <i>ZEB2</i>	35
1.6	HYPOTHESIS AND SUMMARY OF FINDINGS	39
CHAPTER 2 – MATERIALS AND METHODS		41
2.1	Cell Culture	41
2.2	Three-Dimensional (3D) Matrigel Culture	42
2.3	Bisulfite Mutagenesis and Genomic Sequencing	43
2.4	Reverse Transcription Polymerase Chain Reaction (RT-PCR)	52
2.5	5-Aza-2'-Deoxycytidine and Trichostatin A Treatment	55
2.6	Cell Microscopy	56
2.7	Promoter Construct Cloning	56
2.8	Luciferase Reporter Assays	57

2.9 Plasmid Methylation	58
2.10 Plasmid 'Patch' Methylation	59
2.11 Statistical Analysis	60
CHAPTER 3 – RESULTS	61
3.1 <i>ZEB2</i> was Expressed in Mesenchymal Cell Lines but not in Epithelial Cells	61
3.2 Region hPr Possessed Promoter Activity	64
3.3 <i>ZEB2</i> CpG Island 1 and CpG Island 2 were Hypomethylated in Mesenchymal Cells Compared to Epithelial Cells	65
3.4 The <i>ZEB2</i> Promoter was Differentially Methylated in the MDA-MB-468-GFP and MDA-MB-468-LN Cell Lines	74
3.5 <i>ZEB2</i> Expression and CpG Island 1 Methylation were Similar in 2D and 3D Culture	77
3.6 <i>ZEB2</i> Methylation was Resistant to Demethylation by 5-Aza and TSA Treatment in MDA-MB-468-GFP Cells	80
3.7 <i>ZEB2</i> Methylation was Resistant to Demethylation By 5-Aza and TSA Treatment in MCF-7 Cells	93
3.8 <i>In Vitro</i> Methylation of hPr Diminished Promoter Activity	105
CHAPTER 4 – DISCUSSION	117
4.1 Summary of Thesis Findings	117
4.2 Expression of <i>ZEB2</i> in Mesenchymal Cells	118

4.3 The <i>ZEB2</i> Promoter	120
4.4 DNA Methylation in the Regulation of <i>ZEB2</i>	122
4.5 Future Directions	131
4.6 Conclusions	134
REFERENCES	136
CURRICULUM VITAE	149

LIST OF TABLES

Table 2.1 Primers used for bisulfite mutagenesis and genomic sequencing	48
Table 2.2 Primers used for cloning and sequencing	51
Table 2.3 Primers used for RT-PCR	54

LIST OF FIGURES

Figure 1.1 Parallels between metastasis and epithelial-mesenchymal transition	9
Figure 1.2 DNA methylation and chromatin remodelling	13
Figure 1.3 The contribution of DNA methylation to cancer	18
Figure 1.4 Ingenuity Pathway Analysis of genes associated with epithelial-mesenchymal transition	26
Figure 1.5 The putative role of ZEB2 in epithelial-mesenchymal transition	30
Figure 1.6 <i>ZEB2</i> gene and putative promoter region	37
Figure 2.1 <i>ZEB2</i> gene and location of primers for bisulfite cloning and promoter cloning	46
Figure 3.1 <i>ZEB2</i> was overexpressed in cells with a predominant mesenchymal Phenotype	63
Figure 3.2 Region hPr had promoter activity in mesenchymal cells	67
Figure 3.3 CpG island 1 was differentially methylated in human cancer cells	69
Figure 3.4 CpG island 2 was differentially methylated in human cancer cells	73
Figure 3.5 The <i>ZEB2</i> promoter was differentially methylated in MDA-MB-468-GFP and MDA-MB-468-LN cells	76
Figure 3.6 No differences in <i>ZEB2</i> expression or CpG island 1 methylation were observed in cells grown in 2D and 3D culture	79
Figure 3.7 MDA-MB-468-GFP cells were proliferating during some 5-aza-2'deoxyctidine and Trichostatin A treatment conditions	83
Figure 3.8 5-aza-2'deoxyctidine and Trichostatin A treatment did not alter the expression of <i>ZEB2</i> in MDA-MB-468-GFP cells	85

Figure 3.9 MDA-MB-468-GFP cells were proliferating during some 5 day 5-aza-2'deoxyctidine and Trichostatin A treatment conditions	88
Figure 3.10 MDA-MB-468-GFP cells were proliferating during some 7 day 5-aza-2'deoxyctidine and Trichostatin A treatment conditions	90
Figure 3.11 5-aza-2'deoxyctidine and Trichostatin A treatment for 5 and 7 days did not alter expression of <i>ZEB2</i> in MDA-MB-468-GFP cells	92
Figure 3.12 MDA-MB-468-GFP cells were resistant to demethylation of CpG island 1 by 5-aza-2'deoxyctidine and Trichostatin A	95
Figure 3.13 MDA-MB-468-GFP cells were resistant to demethylation of CpG island 2 by 5-aza-2'deoxyctidine and Trichostatin A	97
Figure 3.14 MDA-MB-468-GFP cells were resistant to demethylation of 5'to Exon 1 by 5-aza-2'deoxyctidine and Trichostatin A	99
Figure 3.15 MCF-7 cells were proliferating during 5-aza-2'deoxyctidine and Trichostatin A Treatment	102
Figure 3.16 Specific 5-aza-2'deoxyctidine and Trichostatin A treatment altered the expression of <i>ZEB2</i> in MCF-7 cells	104
Figure 3.17 MCF-7 cells were partially resistant to demethylation of CpG island 1 by 5-aza-2'deoxyctidine and Trichostatin A	107
Figure 3.18 MCF-7 cells were partially resistant to demethylation of CpG island 2 by 5-aza-2'deoxyctidine and Trichostatin A	109
Figure 3.19 MCF-7 cells were resistant to demethylation of 5' to Exon 1 by 5-aza-2'deoxyctidine and Trichostatin A	111
Figure 3.20 <i>In vitro</i> methylation of Region hPr reporter plasmid diminished	

promoter activity

114

Figure 3.21 'Patch' methylation of Region hPr decreased promoter activity

116

LIST OF ABBREVIATIONS

°C	Degree Celcius
2D	Two Dimensional
3D	Three Dimensional
5-aza	5-aza-2'deoxycytidine
Ac	Acetylation
AKA	Also Known As
ALP	Alkaline Phosphatase
αMEM	Minimum Essential Media Alpha Modified
β-gal	β-galactosidase
bHLH	Basic Helix-loop-helix motif
β-ME	β-mercaptoethanol
BMP	Bone Morphogenetic Protein
Bp	Base pair
BSA	Bovine Serum Albumin
CD20	Membrane-spanning 4-domains, subfamily A, member 1 (AKA MS4A1)
CDH1	E-cadherin
CDH3	P-cadherin
cDNA	Complementary Deoxyribonucleic Acid
CID	CtBP Binding Sites
c-jun	Jun Oncogene
CLDN4	Claudin 4
Cm	Centimetre
CMV	Cytomegalovirus
c-MYB	Myeloblastosis Viral Oncogene
CpG	the dinucleotide sequence 5'-cytosine-guanine-3'
CST6	Cystatin E/M
CtBP	C-terminal Binding Protein 1
C-terminal	Carboxyl-terminus
CX26	Connexin 26
δEF-1	delta-crystallin enhancer-binding protein (AKA ZEB1)
DKK3	Dickkopf Homolog 3
DMEM	Dulbecco's Modified Eagle Medium
DMEM/F12	Dulbecco's Modified Eagle Medium: Nutrient Mixture F12
DNA	Deoxyribonucleic Acid
DNaseI	Deoxyribonuclease 1
DNMT	DNA Methyltransferase
DNMT1	DNA Methyltransferase 1
DNMT3A	DNA Methyltransferase 3A
DNMT3B	DNA Methyltransferase 3B
dNTP	Deoxynucleotide Triphosphate
dNTPs	Dinucleotides
E8.5	Embryonic Day 8.5
E9.5	Embryonic Day 9.5

ECM	Extracellular Matrix
EDTA	Ethylenediaminetetraacetic acid
EGFR	Epidermal Growth Factor Receptor
EMT	Epithelial-Mesenchymal Transition
ER	Estrogen Receptor
ETS1	V-ets erythroblastosis virus E26 oncogene homolog 1
FBS	Fetal Bovine Serum
FGF	Fibroblast Growth Factor
g	Gram
GAPDH	Glyceraldehyde-3-phosphate Dehydrogenase
GFP	Green Fluorescent Protein
GLI1	Glioma-associated oncogene homolog 1
H2A	Histone 2A
H2B	Histone 2B
H3	Histone 3
H3K27	Histone 3 Lysine 27
H3K36	Histone 3 Lysine 36
H3K4	Histone 3 Lysine 4
H3K79	Histone 3 Lysine 79
H3K9	Histone 3 Lysine 9
H4	Histone 4
H4K20	Histone 4 Lysine 20
HCC	Hepatocellular Carcinoma
HDAC	Histone Deacetylase
HEPES	4-(2-hydroxyethyl)-1-piperazineethanesulfonic acid
HER2	Human Epidermal Growth Factor Receptor 2
HGF	Hepatocyte Growth Factor
HIF-1	Hypoxia-inducible Factor 1
HSCR	Hirschsprung's Disease
hTERT	Human Telomerase Reverse Transcriptase
IPA	Ingenuity Pathway Analysis
IRES	Internal Ribosome Entry Site
kb	Kilobases
LB	Luria-Bertani
MBD	Methyl-binding Domain
MDCK	Madin-Darby Canine Kidney
MEF2C	Myocyte Enhancer Factor 2C
MET	Mesenchymal-Epithelial Transition
MET	Mesenchymal-Epithelial Transition Factor (AKA HGF Receptor: HGFR)
µg	Microgram
mg	Milligram
MgCl ₂	Magnesium Chloride
miR200	MicroRibonucleic Acid 200
miR205	MicroRibonucleic Acid 205
miRNA	MicroRibonucleic Acid (AKA MicroRNAs)
µL	Microlitre

mL	Millilitre
mM	Millimolar
mm	Millimetre
MMP	Matrix Metalloproteinase
MMP-1	Matrix metalloproteinase 1
MMP-2	Matrix metalloproteinase 2
mRNA	Messenger Ribonucleic Acid
MT1-MMP	(AKA MMP14: Matrix metalloproteinase 14)
MYOD1	Myogenic Differentiation 1
NaPi	Sodium Phosphate pH7.4
NAT	Natural Antisense Transcript
ng	Nanogram
NK- κ B	Nuclear Factor Kappa-light-chain-enhancer of Activated B Cells
nM	Nanomolar
N-terminal	Amino-terminus
Oct	Octamer Transcription Factor
ONPG	<i>ortho</i> -Nitrophenyl- β -galactoside
OptiMEM	Opti- Minimum Essential Media
P/CAF	p300/CBP-associated factor
P1	Mouse <i>Zeb2</i> promoter 1
P2	Mouse <i>Zeb2</i> promoter 2
P3	Mouse <i>Zeb2</i> promoter 3
PBS	Phosphate Buffered Saline
Pc2	Polycomb 2 homolog (AKA E3 SUMO-protein ligase CBX4)
PCR	Polymerase Chain Reaction
PKP2	Plakophilin 2
PR	Progesterone Receptor
rpm	Revolutions Per Minute
RNA	Ribonucleic Acid
RPMI	Roswell Park Memorial Institute medium
RT-PCR	Reverse Transcription Polymerase Chain Reaction
SAH	S-(5'-deoxy-5'-adenosyl)-l-homocysteine
SAM	S-adenosyl Methionine
SIP1	Smad Interacting Protein 1 (AKA ZEB2 and ZFHx1b)
SPI1	Spleen Focus Forming Virus (SFFV) Proviral Integration Oncogene
TB	Terrific Broth
TCF3	Transcription Factor 3
TGF β	Transforming Growth Factor Beta
TSA	Trichostatin A
U	Unit
VP16	Herpes simplex virus protein vmw65
WNT	Wingless and Int Signaling
WNT4	Wingless-type MMTV integration site family, member 4
WNT5A	Wingless-type MMTV integration site family, member 5A
ZEB1	Zinc finger E-box Binding homeobox 1 (AKA δ EF-1)
ZEB2	Zinc finger E-box Binding homeobox 2 (AKA SIP1 and ZFHx1b)

Zfh-1	<i>Drosophila</i> Zinc Finger Homeodomain 1
ZFHX1b	Zinc finger E-box Binding homeobox 2 (AKA ZEB2 and SIP1)
ZO	Zona Occludens
ZO-3	Zona Occludens 3

CHAPTER 1 - INTRODUCTION

1.1 BREAST CANCER AND THE IMPORTANCE OF METASTASIS

Cancer is a multistep process involving the transformation of normal human cells into highly malignant cells. Cancerous cells can generate their own growth signals and are insensitive to growth inhibitory signals. They can evade programmed cell death and have limitless replicative potential. They also may develop sustained angiogenesis and are capable of tissue invasion and metastasis (Hanahan and Weinberg, 2000). These characteristics are thought to be common among cancer cells. However, this process can occur in different types of cells and tissues, giving rise to an extensive array of cancer types, each with their own unique properties and clinical consequences.

1.1.1 Breast Cancer

Breast cancer is the most common cancer among Canadian women. In 2009, an estimated 22,700 women will be diagnosed with breast cancer and 5,400 will die of it (Canadian Cancer Society's Steering Committee: Canadian Cancer Statistics 2009. Toronto: Canadian Cancer Society). There are many types of mammary carcinoma, but the majority of breast cancers are epithelial-in-origin, and often arise at the junction between the terminal duct and lobule (Sims et al., 2007; Wellings et al., 1975). It was originally thought that breast cancer progression occurred in a simple multi-step fashion. However, it is evident that this process is quite complex, involving many genetic and signalling alterations. Because of this, the classification of breast cancer can be difficult. Clinically, breast carcinomas are classified by stage and grade, and it has become

increasingly important to examine the expression of molecular markers, such as human epidermal growth factor receptor 2 (HER2), estrogen receptor (ER) and progesterone receptor (PR) (Simpson et al., 2005). As well, mutations of known genes are often screened, especially in tumours of patients with a family history of breast cancer (Szabo and King, 1995). Together, these classifications can help aid in the diagnosis and prognosis of patients, and aid in the selection of treatments. However, it is important to understand that the majority of deaths due to breast cancer are not due to the primary tumour itself, but are due to the spread of disease, or metastasis, to distant organs. Despite this fact, little is understood of the mechanisms underlying metastatic progression, and very few biological markers exist to differentiate tumours with metastatic potential.

1.1.2 The Metastatic Cascade

The process of metastasis is intricate, and in order to develop a metastatic tumour, a series of steps must have been completed (Chambers et al., 2002). Initially, angiogenesis must occur during the growth of the primary tumour. This is the process in which the primary tumour develops a blood supply to support its metabolic needs as it grows. This can then provide a route for cancer cells to escape from the primary tumour, a process known as intravasation (Wyckoff et al., 2000). Cancer cells can also enter the circulatory system through an indirect mechanism, by first entering through the lymphatic system. Once in circulation, these cells must be able to survive until they can arrest in a new organ. They must extravasate out of the circulation, into a distant tissue. These steps are highly inefficient, and only a small subset of these cells actually survives throughout

the process. Once in a distant organ, these cells have many fates. Many will die, some remain dormant, and a few cells may initiate growth. New blood vessels must be created in order to sustain the growth of these cells (Chambers et al., 2002).

Cells often metastasize from a primary tumour to specific organs. Breast cancer cells often metastasize to bone, liver, brain and lungs (Chambers et al., 2002). This may be due in part, to patterns of the circulatory system (Ewing, 1928). However, this can also be partially explained by the 'seed and soil' theory of cancer spread, in which the success of a cancer cell depends on the environment of the secondary organ (Paget, 1989). Thus, not only are characteristics of cancer cells important in metastatic progression, but the interaction between cancer cells and their environment can also play a role. It is clear that the process of metastasis is quite complex, and undoubtedly, this process relies on a wide range of molecular and behavioural alterations of cancer cells.

1.2 THE IMPORTANCE OF EPITHELIAL-MESENCHYMAL TRANSITION

The process in which epithelial cells lose many of their physical characteristics (i.e. becoming more mesenchymal-like and gaining motility) is known as epithelial-mesenchymal transition (EMT). The EMT process appears to be conserved throughout evolution, and has been shown to be important in development. More recently, this process has been thought to help contribute to metastasis (Thiery, 2002), as the majority of breast cancers are epithelial-in-origin (Wellings et al., 1975).

1.2.1 Normal Epithelium

Epithelial cells form thin layers, joined by multiple types of junctions. Cell-cell adhesion junctions and cell-basement membrane junctions are pivotal in the maintenance of the epithelial phenotype. These cells are also highly polarized, and this apico-basal polarity is defined by the localization of the junctional proteins, the polarity of the actin cytoskeleton and the presence of the basal lamina (Berx et al., 2007).

Tight junctions, gap junctions, adherens junctions and desmosomes are all found between epithelial cells. Tight junctions provide a physical barrier that restricts paracellular transport. These are found at the boundary between the apical and lateral surface domains. Claudins are the essential transmembrane protein of these junctions, while zona occludens (ZO) proteins are highly enriched at the cytoplasmic face. Adherens junctions provide adherent strength, and are localized to the basal side of tight junctions. The cadherin family of proteins is very important in this junction. E-cadherin is the main cadherin found in epithelial cells, and interaction between E-cadherin on the surfaces of adjacent cells provides strong cell-to-cell adhesion. Cytoplasmically, catenins link E-cadherin to the actin cytoskeleton. ZO proteins have also been found in these junctions. Gap junctions are cell-to-cell channels which allow small molecules to be exchanged between neighbouring cells and connexins are the most integral protein of these junctions. Desmosomes help to resist shearing forces, and are crucial for tissue integrity. These junctions form a continuum of cells within tissues by linkage of their membrane proteins, desmocollin and desmoglein, to intermediate filaments, via desmoplakins. Epithelial cells also maintain contact with the basement membrane through integrin heterodimers (Giepmans and van Ijzendoorn, 2009).

Epithelial cells are motile, but because of their organization, they remain within this epithelial layer, and thus only move in two dimensions. Normally, these cells do not detach and move away from the epithelial layer. When grown in culture, these cuboidal cells grow as clusters of cells, maintaining maximal contact with cells surrounding them (Overton, 1977; Thiery and Sleeman, 2006).

1.2.2 Epithelial versus Mesenchymal Cells

Mesenchymal cells are phenotypically different from epithelial cells. These cells are not polarized, and do not form an organized layer of cells. They only maintain focal contact with neighbouring cells, and do not associate with the basal lamina. When grown in culture, these cells are spindle-shaped and fibroblastic in phenotype, and are often highly motile (Overton, 1977; Thiery and Sleeman, 2006).

Epithelial cells can be distinguished from mesenchymal cells in several ways. Not only do they differ phenotypically, but their molecular compositions also differ. E-cadherin, the adherens junction protein, is highly expressed in epithelial cells, and is not present in mesenchymal cells (Giepmans and van Ijzendoorn, 2009; Yoshida-Noro et al., 1984). The expression of other junctional proteins is also lower in mesenchymal cells compared to epithelial cells. Mesenchymal cells express intermediate filaments, such as vimentin, specific cadherins such as N-cadherin, and cytoskeletal proteins and extracellular matrix components, such as fibronectin (Berx et al., 2007; Franke et al., 1979; Franke et al., 1978; LaGamba et al., 2005).

1.2.3 The EMT Process

A process known as epithelial-mesenchymal transition (EMT) occurs when epithelial cells lose many of their epithelial characteristics, and become more mesenchymal-like in their properties, becoming more motile. This process was initially thought to only occur during development, but has also been shown to occur in adult, differentiated tissues (Greenburg and Hay, 1982, 1988). This process can also reverse, in a process known as mesenchymal-epithelial transition (MET), where mesenchymal cells regain an epithelial-like phenotype (Thiery, 2002). EMT is triggered by extracellular signals such as extracellular matrix (ECM) components and soluble growth factors like transforming growth factor beta (TGF β). In response to these ligands, receptor-mediated signalling triggers the activation of intracellular effector molecules, which then coordinates the disassembly of the junctional complexes and the changes in cytoskeletal organization that occur during EMT. This can also result in the activation of transcriptional regulators, such as zinc finger E-box binding homeobox 2 (ZEB2), Snail and Slug, which can regulate changes in the expression of many genes important in EMT. The main target of downregulation is E-cadherin by these factors. Not only does this result in the loss of adherens junctions, but also in a loss in E-cadherin mediated signalling. E-cadherin also binds to β -catenin (Ozawa et al., 1989), and plays a role in sequestering the nuclear signalling capabilities of β -catenin (Bienz, 2005). EMT also involves a reorganization of contact with the basement membrane, and a change occurs from cadherin-based adhesion to integrin-based adhesion. Cross talk between E-cadherin and integrins helps coordinate this transition (Thiery and Sleeman, 2006).

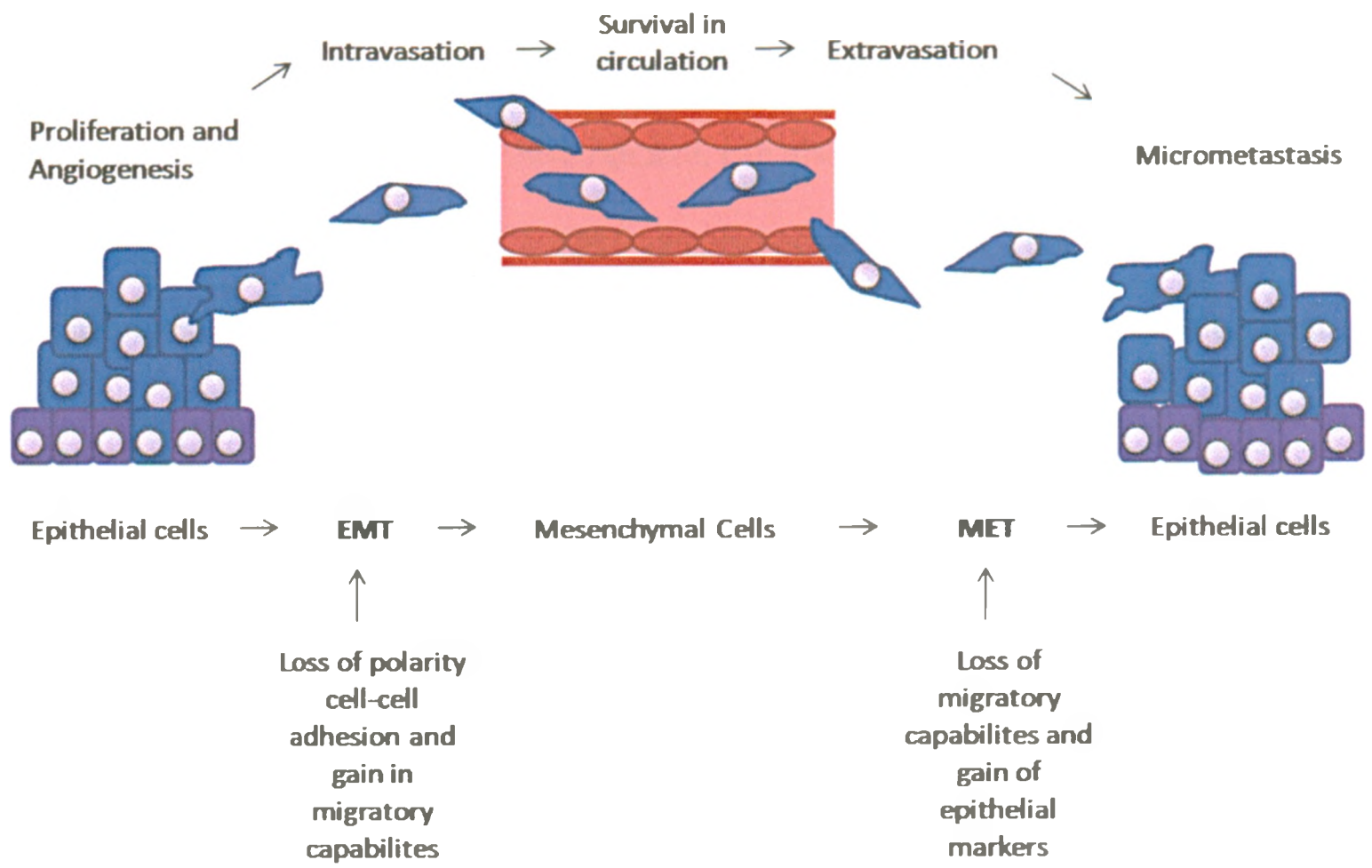
1.2.4 EMT in Development

Epithelial-mesenchymal transition is crucial during development. During embryogenesis, epithelial sheets can convert into mesenchymal cells, allowing for the formation of the three-layered embryo through gastrulation. Multiple pathways can contribute to this, such as the fibroblast growth factor (FGF) receptor-1 signaling and the wingless and Int (WNT) signalling pathway. EMT is also important in the development of many structures, such as the brain, where neural-crest cells undergo EMT within the dorsal neural epithelium and migrate before differentiating. This process involves signalling through bone morphogenic protein (BMP), WNT and FGF. As well, endocardial EMT is regulated through the TGF β and NOTCH signalling pathways during the formation of the cardiac valve (Thiery and Sleeman, 2006).

1.2.5 EMT in Cancer Metastasis

Epithelial-mesenchymal transition also plays an important role in tumour progression (Figure 1.1). EMT may enhance the metastatic capabilities of cancer cells, through the acquired mobility associated with this transition. There are many known inducers of EMT in the context of cancer. Loss of E-cadherin expression plays a significant role in EMT induction, and can occur in several ways. The aberrant expression of transcriptional repressors of E-cadherin, such as Snail, Slug, ZEB2 and transcription factor 3 (TCF3), can contribute to EMT (Bolos et al., 2003; Cano et al., 2000; Comijn et al., 2001; Eger et al., 2005; Perez-Moreno et al., 2001). Alternatively, mutations in E-cadherin can cause the absence, or truncation, of the E-cadherin protein in

Figure 1.1 Parallels between metastasis and epithelial-mesenchymal transition. For metastasis to occur, a cell must escape the primary tumour (known as intravasation), invade into circulating blood or lymph vessels, and survive in the circulation. It can then arrest in capillaries and escape to a distant tissue (known as extravasation) where it must survive and sustain growth, forming a micrometastasis. To gain the migratory capabilities required for invasion, epithelial cells may lose their characteristics and become more mesenchymal like, through epithelial-mesenchymal transition (EMT). In contrast, once cells have travelled to distant tissues, they may lose their migratory capabilities and become more epithelial-like through mesenchymal-epithelial transition (MET). Modified from: (Thiery and Sleeman, 2006; Tse and Kalluri, 2007).



an early stage of disease (Berx et al., 1995). As well, it has been shown that a large number of receptor tyrosine kinases and growth factors can induce EMT (Thiery, 2002). For instance, activation of mesenchymal-epithelial transition factor (MET) by hepatocyte growth factor (HGF) can initiate many signalling cascades resulting in enhanced cell scattering, migration, invasion and metastasis (Benvenuti and Comoglio, 2007). Activation of other tyrosine kinase receptors such as receptors for fibroblast growth factor, insulin-like growth factor and the epidermal growth factor receptor (EGFR) family has also been shown to induce EMT (Thiery, 2002; Valles et al., 1990). As well, TGF β , an important inducer of EMT in development, can also induce EMT in cancer cells (Caulin et al., 1995; Thiery, 2002). EMT can also occur through NOTCH, WNT and hedgehog signalling. Many of these signalling pathways are important in development, and it is evident that aberrant signalling of these pathways can lead to cancer progression. Alterations in signalling pathways due to inactivating mutations, altered expression of transcription factors, aberrant receptor activation, and more recently observed, aberrant epigenetic marks, can all contribute to the complex process of cancer progression (Esteller, 2008; Thiery and Sleeman, 2006).

1.3 THE IMPORTANCE OF EPIGENETICS

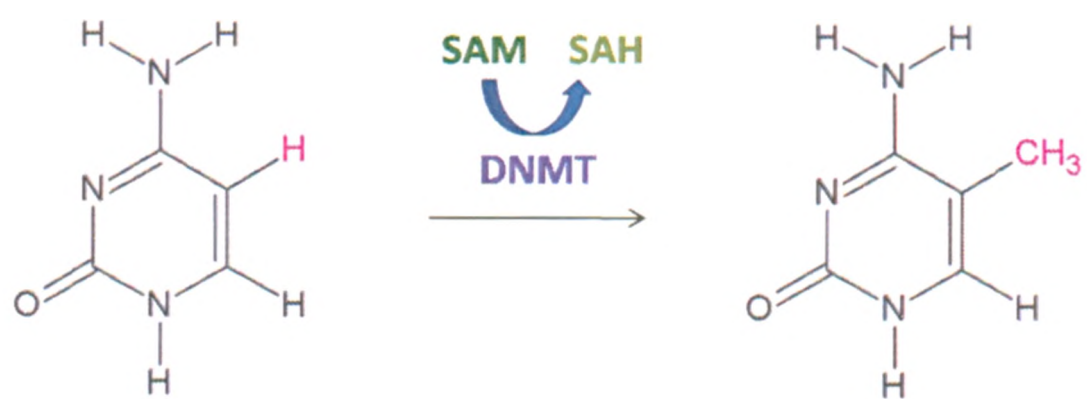
While it is evident that the complex processes of metastasis and epithelial-mesenchymal (EMT) are influenced by a variety of genetic alterations, such as chromosome copy number changes and genetic mutations, the emerging field of epigenetics may also contribute important insights into these processes.

1.3.1 An Overview of Epigenetics

Chromatin consists of nucleosome units, which consists of DNA wrapped around clusters of proteins known as histones, with DNA linker regions in between. These units fold into fibres, which in turn, fold into more compact fibres. This allows chromatin to be efficiently compacted (Peterson and Laniel, 2004). However, the structure of chromatin can be altered to either permit or prevent gene transcription. An open, active conformation of chromatin allows for transcription factor and transcription machinery accessibility. Chromatin can also be condensed, which renders it inactive, and this tends to be refractory to transcription (Figure 1.2). The epigenetic modifications that control these chromatin states include DNA methylation and histone modifications (Rountree et al., 2001). Epigenetics is defined as changes in gene function without a change in the DNA sequence itself, thereby providing an extra level of regulation, impacting gene expression (Rodenhiser and Mann, 2006).

Nucleosomes are composed of four histone pairs, H2A, H2B, H3 and H4, which form an octamer. These globular proteins act as a spool around which approximately 150 bp of DNA is wrapped. Modifications of histones occur on histone tails, which are unstructured, N-terminal regions of these proteins. There are at least eight types of histone modifications, the most studied of which are methylation, phosphorylation and acetylation. At least 60 different residues have been found to contain these modifications. Histone modifications can directly influence chromatin structure, and can recruit other proteins to histone clusters, with distinct modifications associated with each chromatin state. Silent chromatin (heterochromatin) is associated with low levels of histone

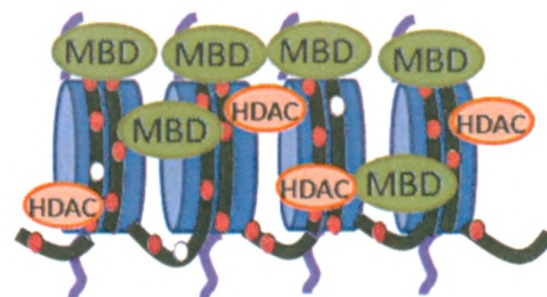
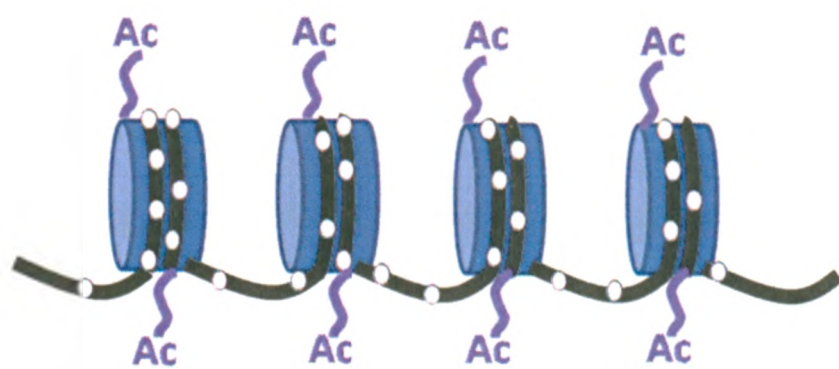
Figure 1.2 DNA methylation and chromatin remodelling. DNA methylation occurs on cytosines of cytosine/guanine pairs (CpGs). DNA methyltransferases (DNMTs) transfer methyl groups (CH₃) from methyl donor S-adenosylmethionine (SAM) to the fifth carbon of cytosine. This process results in the conversion of SAM to S-(5'-deoxy-5'-adenosyl)-L-homocysteine (SAH). This form of epigenetic modification, along with histone modifications, control chromatin remodelling. Open chromatin is associated with low levels of DNA methylation (open, white circles), high levels of histone acetylation (Ac) and H3K4 histone methylation. Closed chromatin is associated with high levels of DNA methylation (closed, red circles), as well as the recruitment of methyl-binding proteins (MBDs), histone deacetylase complexes (HDACs) and H3K9, H3K27 and H4K20 histone methylation. Modified from: (Gronbaek et al., 2007).



OPEN CHROMATIN



CLOSED CHROMATIN



acetylation and high levels of histones methylated at specific sites, such as H3K9, H3K27 and H4K20. In contrast, active chromatin (euchromatin) is associated with high levels of histone acetylation and trimethylation at H3K4, H3K36 and H3K79. As well, there are a multitude of different enzymes responsible for catalyzing these modifications.

Acetyltransferases acetylate histones, whereas histone deacetylases remove acetyl groups from histones. Similarly, methyltransferases add methyl groups to histones, while demethylases remove them. Many of these enzymes have specificity as to the particular residue they modulates (Kouzarides, 2007).

The second type of modification important in chromatin structure is DNA methylation. DNA methylation occurs at sites of cytosine and guanine pairs, known as CpG pairs, or CpGs, where a methyl group is covalently added to the 5' carbon of cytosine. There are three main DNA methyltransferases (DNMTs) that are responsible for transferring methyl groups onto DNA from the methyl donor S-adenosyl methionine (SAM). DNMT1 is responsible for maintaining the methylation pattern through replication, adding methyl groups to the newly synthesized strands of DNA (Bestor, 1992; Leonhardt et al., 1992), whereas DNMT3A and DNMT3B are responsible for *de novo* methylation, and thus are capable of adding new methyl groups onto DNA (Okano et al., 1999). Often, CpGs are found clustered together in highly CpG-rich regions known as CpG islands (Gardiner-Garden and Frommer, 1987). CpG islands are often seen in the promoter regions of genes: approximately 60% of all genes have CpG islands associated with them. High levels of CpG methylation within the promoter region of genes, whether in conventional CpG islands or not, is often associated with transcriptional repression. This is because methyl groups can physically hinder the binding of transcription factors.

as well as recruit methyl-binding proteins, which can then recruit other proteins such as corepressors (Guil and Esteller, 2009).

It is still under debate as to the order in which epigenetic modifications occur on chromatin. There is evidence that DNA methylation occurs first, which then recruits methyl-binding proteins and histone deacetylases to the chromatin (Stirzaker et al., 2004; Vaissiere et al., 2008). Conversely, there is also evidence that DNA methylation plays a role in locking the chromatin into an inactive state, and therefore occurs after other epigenetic modifications (Bachman et al., 2003; Vaissiere et al., 2008). However, despite this debate, it is clear that together these two types of epigenetic modifications, histone modifications and DNA methylation, act to modulate chromatin structure and transcriptional activity.

1.3.2 Normal Functions of DNA Methylation

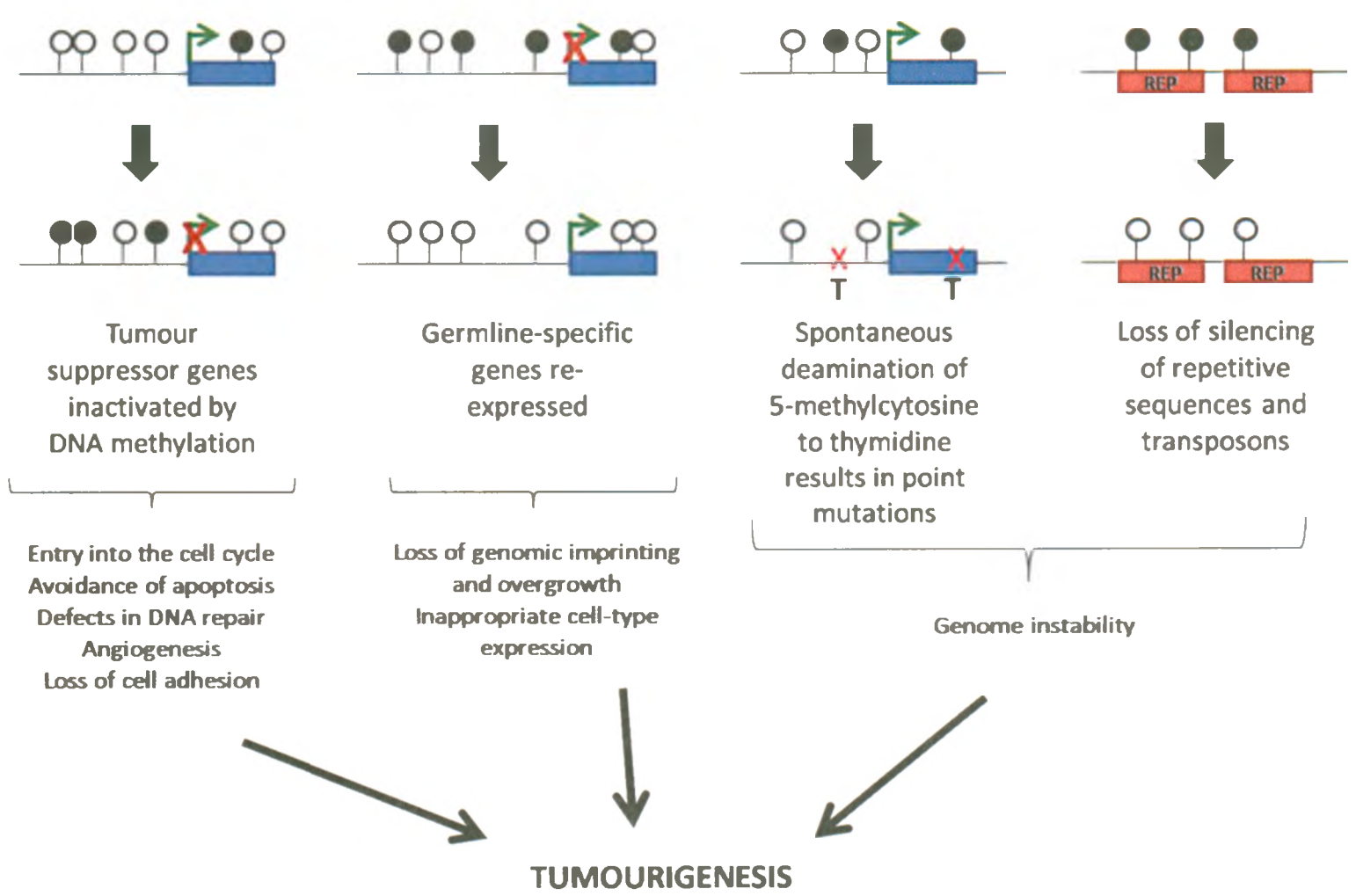
DNA methylation has an extremely important role in development. After fertilization, the paternal genome undergoes rapid demethylation (and changes in histone modifications). The maternal genome is gradually demethylated, and a new set of embryonic methylation patterns are created (Monk et al., 1987). DNA methylation is important in genomic imprinting, a process that distinguishes between maternal or paternal inheritance so that only one allele is expressed (Verona et al., 2003). DNA methylation is also important in X-chromosome inactivation, a process in which one of the two copies of the X-chromosome in a female is inactivated (Heard et al., 1997), and tissue-specific gene expression (Song et al., 2005).

DNA methylation also plays an important role in the maintenance of genomic stability. Repetitive genomic sequences are normally highly methylated, potentially to prevent chromosomal rearrangements, translocations and the reactivation of transposons (Lo and Sukumar, 2008; Schorderet and Gartler, 1992).

1.3.3 DNA Methylation in Cancer

It is well known that genetic alterations and gene expression changes can contribute to cancer. More recently, it has been shown that epigenetic alterations can also contribute to this disease. DNA methylation can contribute to cancer in a variety of ways (Figure 1.3). First, deamination of 5-methylcytosine can result in transitional mutations at methylated CpG dinucleotides (Coulondre et al., 1978). Secondly, it has also been observed that DNA methylation patterns are dramatically altered in cancer cells. A progressive overall loss of methylation, combined with increased methylation in the promoter regions of specific genes, has been shown to contribute to the aberrant behaviour of these cells (Esteller, 2008; Feinberg et al., 1988; Gronbaek et al., 2007; Lo and Sukumar, 2008; Rountree et al., 2001). Hypomethylation of DNA in cancer cells often occurs in repetitive regions, or gene-poor regions, of the genome, and in the coding regions and introns of genes (Esteller, 2008; Weber et al., 2005). Thirdly, hypomethylation of a genome can have dramatic effects on a cell, causing genomic instability, leading to mitotic recombination, causing deletions and translocations, as well as chromosomal rearrangements (Eden et al., 2003; Qu et al., 1999). Fourthly, hypomethylation can reactivate transposable elements further disrupting the genome,

Figure 1.3 The contribution of DNA methylation to cancer. During cancer progression, an overall decrease in methylation is often seen which can result in genomic instability and the expression of oncogenes. An increase in methylation specifically at the promoters of genes during cancer progression is also seen, and can result in the repression of tumour suppressor genes. Furthermore, spontaneous deamination of 5-methylcytosine can result in point mutations. Modified from: (Esteller, 2007).



cause a loss of imprinting, and cause a loss of gene silencing (Bourc'his and Bestor, 2004; Esteller, 2008). Finally, hypomethylation of gene promoters can also lead to aberrant gene expression, disrupting tissue-specific expression of many genes, causing alterations in transcription and signalling (Gronbaek et al., 2007).

In the same respect, hypermethylation of particular regions of the genome can be detrimental. One of the most dramatic effects of DNA methylation alterations in cancer is hypermethylation of gene promoter regions. This can cause silencing of a variety of individual genes important in the cell cycle, DNA repair, cell-to-cell interactions, apoptosis and angiogenesis, including tumour-suppressors (Herman and Baylin, 2003). More recently, it has also been shown that hypermethylation of sequences encoding microRNAs can cause aberrant repression of genes important in cell cycle, DNA repair and cell-to-cell interactions (Guil and Esteller, 2009).

Abnormal DNMT behaviour may contribute to considerable changes in DNA methylation patterns found in cancers. Indeed, DNMT over-expression has been found in numerous cancers (Rountree et al., 2001). It has also been suggested that disruption of the DNMT complex due to the loss of binding partners is another potential factor for carcinogenesis (Rountree et al., 2001).

More recently, the contribution of aberrant DNA methylation to the process of metastasis has been identified. The majority of the work in this field has focused on DNA methylation patterns in the promoters of genes whose expression is altered both *in vitro*, in aggressive cell lines, and *in vivo*, in tumours demonstrating lymph node metastasis and in metastatic lesions (Rodenhiser, 2009).

Studying how altered methylation patterns contribute to cancer and metastasis will help us gain a better understanding of the development of this disease, while identifying the methylation status of a particular gene may be used as a diagnostic, or prognostic factor, or to help predict the response to treatment by some patients.

1.3.4 Epigenetic Drugs as Tools

The emergence of epigenetic modifications as contributors to cancer and metastasis has led to the development of drugs that alter these epigenetic modifications, many of which are currently being used both in the clinic, and for research purposes. There are two main types of epigenetic drugs: demethylating agents, and histone deacetylase inhibitors.

The two most studied demethylating agents are 5-azacytidine (Vidaza) and 5-aza-2'-deoxycytidine (Decitabine). These drugs are analogues to cytosine, and therefore can be incorporated into DNA in the place of cytosine. These inhibitors are capable of covalently binding to DNA methyltransferases (DNMTs). Thus, when these drugs are present, DNMTs are trapped and unable to transfer methylation groups to DNA. Thus, during transcription, loss of methylation is seen with these inhibitors (Jones and Taylor, 1980). Despite the similarity of these drugs, they do not possess the same efficacy. 5'-aza-2'-deoxycytidine is a more potent inhibitor of DNMTs, as this analogue is only incorporated into DNA, whereas 5-azacytidine is capable of being incorporated into both RNA and DNA (Hellebrekers et al., 2007). Both drugs have been approved in the United States as therapeutic agents for the treatment of myelodysplastic syndrome, a pre-leukemia disease. However, both of these drugs are highly unstable in neutral aqueous

solutions. Thus, another cytosine analogue, Zebularine, has also been developed, which has increased stability, lower toxicity and is highly selective for tumour cells (Cheng et al., 2004). In addition, non-nucleotide DNMT inhibitors have been developed recently, which bind to the active site of all DNMTs and disrupt the interaction between the enzymes and their target sites (Brueckner et al., 2005; Segura-Pacheco et al., 2003). The anti-cancer effect of these drugs can for the most part be attributed to the re-expression of tumour suppressor genes, initially silenced by hypermethylation (Lo and Sukumar, 2008).

The second clan of epigenetic drug is histone deacetylase (HDAC) inhibitors. Because it has been shown that abnormal recruitment of HDACs to the promoter region of tumour suppressor genes can lead to cancer (Lo and Sukumar, 2008), it seems logical that inhibiting these enzymes may have functional benefits to the treatment of cancer (Lo and Sukumar, 2008). A number of both synthetic and natural inhibitors have been developed or isolated, and can be classified as hydroxamates, short-chain fatty acids, cyclic peptides, benzamides, or anilides. These inhibitors have been shown to have anti-cancer effects, eliciting such responses as apoptosis, cell-cycle arrest, immune modulation and anti-angiogenesis affects. These effects occur both through histones and non-histone proteins (Bolden et al., 2006).

Interestingly, epigenetic drugs are also currently being used as experimental tools for research. An increasing number of studies report the use of 5-aza-2'-deoxycytidine (5-aza) as a method of studying the contribution of DNA methylation to the regulation of a particular gene of interest, or in whole-genome studies (Chiurazzi et al., 1999; Hesson et al., 2009; Kongkham et al., 2008; Meng et al., 2007; Rivenbark et al., 2006; Seder et al., 2009; Veeck et al., 2008; Veeck et al., 2006; Zhang et al., 2005). As well, Trichostatin A

(TSA), a HDAC inhibitor, is often used to understand the contribution of acetylation to the regulation of gene expression. In fact, both 5-aza and TSA are often used concurrently to allow for a maximally open chromatin structure, and often, these drugs work synergistically to alter the expression of many genes thought to be regulated by DNA methylation and histone modifications (Chiurazzi et al., 1999; Meng et al., 2007; Veeck et al., 2008; Zhang et al., 2005).

1.4 THE METASTASIS PROJECT

Metastasis is responsible for the majority of deaths due to breast cancer, but despite this clinical importance, the biology behind this process is poorly understood.

1.4.1 The Metastasis Project

To study the process of metastasis, a family of cell lines has been created by the Chambers Lab (Vantghem et al., 2005). The MDA-MB-468 breast adenocarcinoma cell line, originally isolated from a 51-year old black female patient with metastatic adenocarcinoma of the breast, was stably transfected with green fluorescent protein (GFP), resulting in the MDA-MB-468-GFP cell line that stably expresses GFP (Vantghem et al., 2005) to allow investigation of these cells in a xenograft model system. This cell line was orthotopically injected into the mammary fat pads of nude mice, and tumours were formed. One mouse developed a lung metastasis despite the low metastatic potential of the MDA-MB-468-GFP cell line. The cells of the lung metastasis were isolated from the lung and grown in culture (MDA-MB-468-LN) (Vantghem et al., 2005). These two cell lines differ in morphology: the parental MDA-MB-468-GFP cells

have an epithelial phenotype, whereas the daughter MDA-MB-468-LN cells appear more spindle-shaped, have a higher proliferation rate, and form a greater number of non-spherical colonies in 3-dimensional Matrigel (Pandit et al., 2009; Vantghem et al., 2005). The differences between these two related cell lines led to at least three pertinent questions. 1) What genes are differentially expressed between these two cell lines? 2) Do differences in DNA methylation at the promoter contribute to the differences in gene expression? 3) Can these altered gene expression patterns and DNA methylation patterns contribute to the differences in morphology and behaviour of these cells? To address these questions, promoter tiling microarray analyses have been performed using genomic DNA from the MDA-MB-468-GFP and MDA-MB-468-LN cells grown in 2D culture, to detect DNA methylation changes between these two cell lines. Quantitative real-time polymerase chain reaction (PCR) has been performed using cDNA from both the MDA-MB-468-GFP and MDA-MB-468-LN cells grown in 2D culture, to examine the expression of genes identified as having differential promoter methylation between these two cell lines (Rodenhiser et al., 2008).

1.4.2 Candidate Genes

In an effort to narrow the potential gene targets identified from these arrays, Ingenuity Pathways Analysis (IPA) software has been used to identify functional categories and canonical pathways most significant to the genes that have been found to be altered in our data sets. Because of the drastic morphology difference seen between these two cell lines, a network of genes previously identified as being important in EMT (Lee et al., 2006) was analyzed by IPA, and the methylation status of these genes has

been overlaid onto the network (Figure 1.4). As well, biological relationships between genes and gene products found to be altered in our data sets was demonstrated by creating multiple networks related to the EFGR, TGF β , TNF and MYC genes. The resulting network identified multiple genes that are important in EMT or these signalling pathways, and identified those with altered DNA methylation patterns between the two cell lines. Epidermal growth factor receptor (EGFR), the lysosomal cysteine protease inhibitor cystatin M (CST6), ZEB2, Slug and E-cadherin were genes that displayed distinct promoter methylation and gene expression patterns in each cell line. The methylation status of these genes has been confirmed through bisulfite genomic sequencing, and expression has been confirmed by quantitative real-time PCR (Rodenhiser et al., 2008).

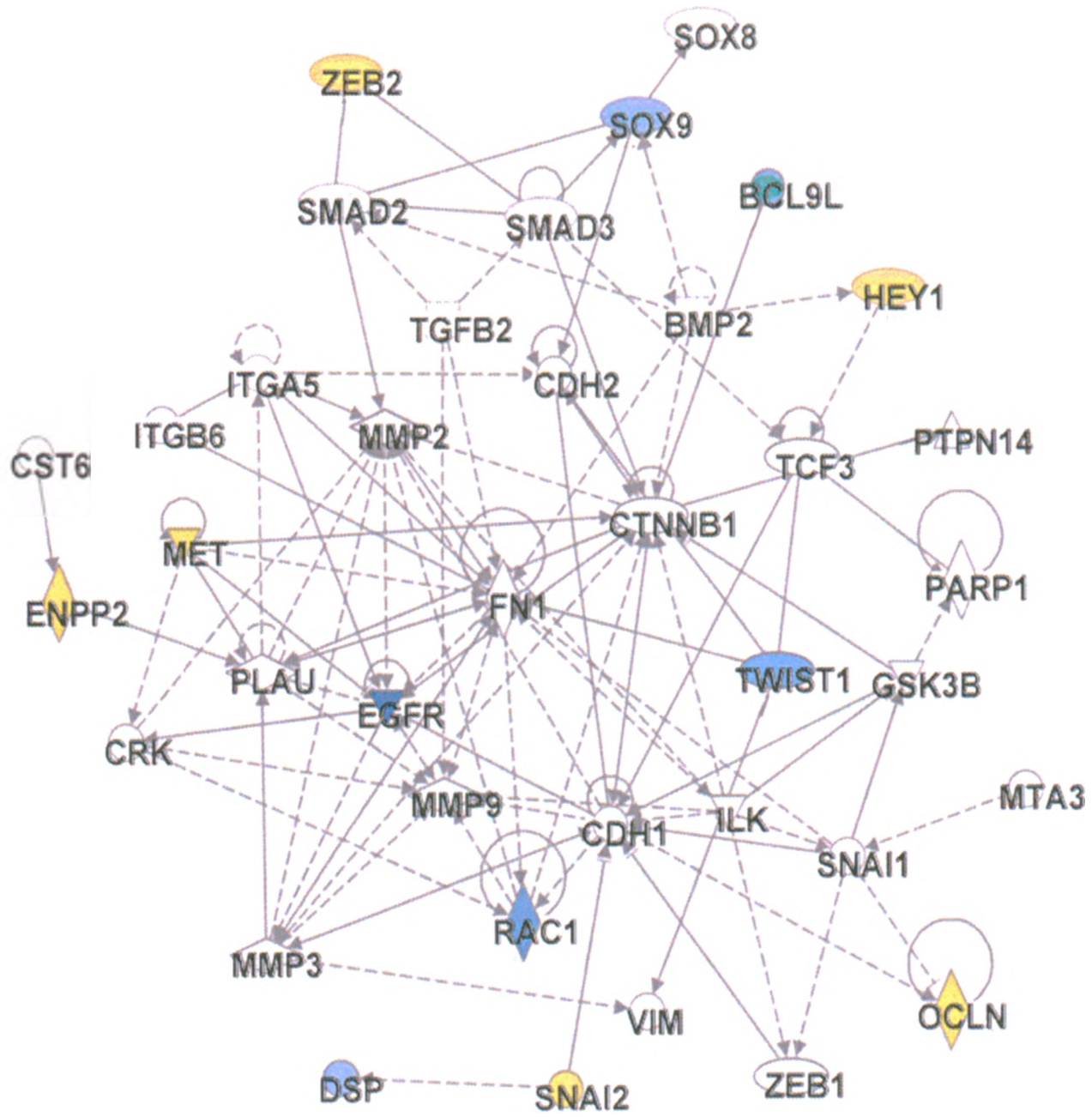
1.5 THE RELEVANCE OF ZEB2 TO EMT

One of the targets whose gene expression and methylation patterns at the promoter differed between the two cell lines was *ZEB2*. A considerable amount of literature had focused on the importance of *ZEB2* in development, and the involvement of *ZEB2* in EMT. Therefore, *ZEB2* was selected as a relevant gene for further study in the context of EMT and to understand the contribution of DNA methylation to its regulation.












1.5.1 Molecular Functions of ZEB2

ZEB2, also known as SMAD-interacting protein-1 (SIP1) and zinc finger E-box binding homeobox 2 (ZFHX1b), was originally identified through two independent



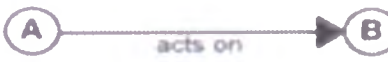

Figure 1.4 Ingenuity Pathway Analysis of genes associated with epithelial-mesenchymal transition. This network is a graphical representation of the molecular relationships between 35 genes associated with epithelial-mesenchymal transition. Node colour indicates the degree of hypermethylation (blue) or hypomethylation (yellow) above the significance cutoff. Nodes are displayed using various shapes that represent the functional classes of the gene products as shown in the key (Rodenhiser et al., 2008).



IPA Node Types

-  Cytokine
-  Enzyme
-  G-protein Coupled Receptor
-  Growth Factor
-  Ion Channel
-  Kinase
-  Peptidase
-  Phosphatase
-  Transcription Regulator
-  Transporter
-  Other

IPA Edge Types

-  binding only
-  inhibits
-  acts on
-  inhibits AND acts on

Note: "Acts on" and "Inhibits" edge may also include a binding event

————— direct interaction

- - - - - indirect interaction

experiments; as a SMAD-interacting protein (hence the SIP1 nomenclature) through a yeast two-hybrid screen (Verschueren et al., 1999), and as a *Drosophila* protein zinc finger homeodomain 1 (*zfh-1*) homolog, expressed in the central nervous system (Postigo and Dean, 2000). ZEB2 was the second member of the zinc finger E-box binding homeobox/delta-crystallin enhancer-binding protein/zinc finger homeodomain 1 (ZEB/ δ EF-1/*zfh-1*) family of vertebrate zinc finger/homeodomain proteins to be identified.

ZEB2 has similar gene structure and sequence to its mammalian homolog *ZEB1*, and it has been postulated that both of these genes originated late in evolution from a single *zfh-1* gene (Postigo and Dean, 2000). The ZEB2 protein contains two zinc finger domains located at the N-terminus and C-terminus, a central homeodomain (Postigo and Dean, 2000; Verschueren et al., 1999), a SMAD-binding domain located between the homeodomain and N-terminal zinc finger domain (Verschueren et al., 1999), and four CtBP binding sites (CID) (Postigo and Dean, 2000).

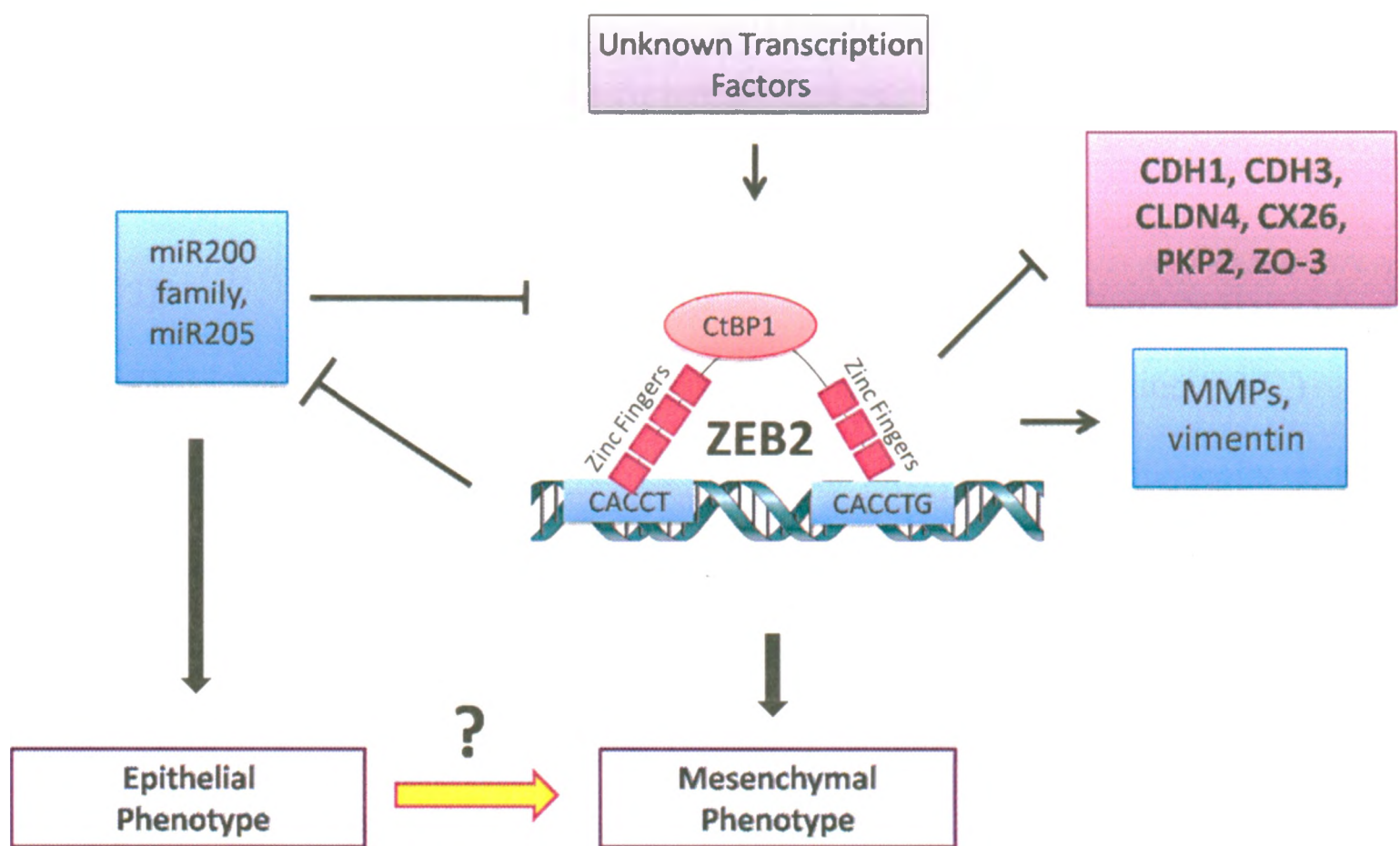
ZEB2 mRNA is expressed in fetal brain, liver and kidney, similar to *ZEB1*. The expression patterns of *ZEB1* and *ZEB2* are also similar in adult tissue, with expression in the spleen, skeletal muscle, bladder, placenta, and other muscular and nervous system tissues. However, *ZEB2* is more abundant in the heart and brain (Postigo and Dean, 2000; Verschueren et al., 1999) than *ZEB1*. Although *ZEB2* is found in many adult tissues, it is not detected in the prostate, testis, ovary, pancreas, thyroid, salivary and mammary glands (Cacheux et al., 2001). Thus, while it does appear that these two proteins have similar expression patterns, they are not equally expressed everywhere, and their functions are most likely not compensatory in neural development. In fact, *Zeb2* null

mice (Higashi et al., 2002) exhibit defects as early as embryonic day 8.5 (E8.5), and die at E9.5 (Van de Putte et al., 2003).

ZEB2 functions as a transcription regulator and can bind to DNA. ZEB2 binds specifically to the sequence 5'-CACCT through both its zinc fingers, similar to ZEB1, and can bind to the CATTG E box sequence (but not all E-box sequences) (Postigo and Dean, 2000; Verschuere et al., 1999). ZEB2 interacts with the co-repressor C-terminal binding protein 1 (CtBP-1), and is capable of repressing the activity of a large number of transcriptional activators, such as the Myeloblastosis viral oncogene (c-MYB), the ETS family protein spleen focus forming virus (SFFV) proviral integration oncogene (SPI1), nuclear factor kappa-light-chain-enhancer of activated B cells (NF- κ B), myocyte enhancer factor 2C (MEF2C), Herpes simplex virus protein vmw65 (VP16), TCF3 and myogenic differentiation 1 (MYOD1) (Postigo and Dean, 2000). It is thought that an individual ZEB2 binds each zinc finger to an independent sequence. Thus, ZEB2 binds a bipartite element (composed of one CACCT and one CACCTG sequence) where the N-terminal zinc finger cluster binds to one sequence, and the C-terminal zinc finger cluster binds to the other (Figure 1.5). The integrity of this bipartite element is crucial for the high-affinity binding of ZEB2 (Remacle et al., 1999).

As alluded to previously, ZEB2 is capable of binding to several SMAD proteins, and this occurs after activation of these SMADs by specific type I receptors (Verschuere et al., 1999). Interestingly, ZEB1 can also bind to these SMADs, but ZEB2 binds more efficiently. ZEB2 represses TGF β –mediated activation of the p21, p15 and Jun oncogene (c-jun) promoters, whereas ZEB1 synergizes with TGF β to activate transcription of the same reporters. The opposing acts of ZEB1 and ZEB2 are also observed in BMP-

Figure 1.5 The putative role of *ZEB2* in epithelial-mesenchymal transition. In cells with an epithelial phenotype, microRNAs (miRNAs) are present which are capable of downregulating the expression of *ZEB2*. However, *ZEB2* is often found to be overexpressed in cells of a more mesenchymal phenotype. When *ZEB2* is overexpressed in these cells, it can downregulate the microRNAs (miRNAs) that regulate it (miR200 family, miR205), through a negative feedback loop, and can downregulate genes important in cell-cell junctions, such as E-cadherin (CDH1), P-cadherin (CDH3), claudin 4 (CLDN4), connexin 26 (CX26), plakophilin 2 (PKP2) and zona occludens 3 (ZO-3). *ZEB2* can also cause the upregulation of genes associated with the mesenchymal phenotype, such as matrix metalloproteinases (MMPs) and vimentin. The repression of these genes may involve the interaction between *ZEB2* and its co-repressor C-terminal binding protein 1 (CtBP1).



mediated signalling (Postigo, 2003). However, it has recently been suggested that ZEB2 does not require the binding to SMADs to inhibit BMP signalling (Nitta et al., 2007). The ability of the ZEB proteins to act on these signalling pathways requires the formation of an R-SMAD-SMAD4 complex. As well, ZEB2 inhibits the ability of BMP-2 to induce alkaline phosphatase (ALP) and ZEB2 also inhibits TGF β mediated growth arrest (Postigo, 2003; Tylzanowski et al., 2001). It has also been shown that the difference in ZEB behaviour with respect to SMAD signalling is due to the differential recruitment of coactivators and corepressors. As mentioned previously, ZEB2 binds to CtBP, as does ZEB1. However, ZEB1 is also capable of binding to p300 and p300/CBP-associated factor (P/CAF), which promotes the formation of an active SMAD complex (Postigo et al., 2003).

ZEB2 has also been implicated in epithelial-mesenchymal transition (EMT) (Figure 1.5). It has already been demonstrated that the integrity of epithelial cells relies on the maintenance of proper cell-cell junctions. E-cadherin plays a pivotal role in maintaining these associations, and downregulation of E-cadherin is often associated with epithelial-mesenchymal transition. ZEB2 is capable of downregulating E-cadherin by binding both zinc fingers to E2 boxes in the E-cadherin gene promoter (Comijn et al., 2001; Imamichi et al., 2007; Miyoshi et al., 2004). This is also true in TGF β induced EMT, where ZEB2 interaction with SMAD proteins is essential for full repression of E-cadherin (Comijn et al., 2001). The process of E-cadherin repression by ZEB2 was shown to occur independently of CtBP (van Grunsven et al., 2003). However, it was demonstrated that ZEB2 is sumoylated by polycomb 2 homolog (Pc2), causing partial disruption of E-cadherin repression (Long et al., 2005). ZEB2 has also been shown to

repress genes coding for proteins of tight junctions, desmosomes and gap junctions (Vandewalle et al., 2005). ZEB2 regulates vimentin, and ZEB2 has been demonstrated to activate a vimentin promoter construct (Bindels et al., 2006). It is clear that ZEB2 is involved in many molecular pathways, influencing development and disease.

1.5.2 ZEB2 in Developmental Disease

In both mouse and *Xenopus*, the importance of ZEB2 for normal brain development has been clearly demonstrated. ZEB2 is activated in the early gastrula stage in *Xenopus*, and ZEB2 mRNA is found in mice at E8.5 in the neuroepithelium (Eisaki et al., 2000; Van de Putte et al., 2003; van Grunsven et al., 2000). ZEB2 expression levels closely follow the maturation of the neural plate, and ZEB2 transcripts are seen in premigratory and migrating neural crest cells (Van de Putte et al., 2003). Experiments with mutant embryos have demonstrated that ZEB2 is essential for the development of vagal neural crest and migration of cranial neural crest cells (Van de Putte et al., 2003). ZEB2 is involved in the positioning of somite boundaries in the mouse embryo (Maruhashi et al., 2005), is essential for the development of the hippocampus and dentate gyrus (Miquelajauregui et al., 2007), and a role for ZEB2 as an activator in development has been suggested (Yoshimoto et al., 2005). All of these findings discussed illustrate the critical function of ZEB2 in neural development. Thus, it is no surprise that mutations of this gene can lead to abnormal developmental consequences. In humans, deletions and mutations in ZEB2 has been identified as a cause of Mowat-Wilson syndrome. This syndrome was first delineated in 1998, with patients having characteristic facial features, such as deep set large eyes, broad nasal bridge, triangular jaw and prominent chin. in

association with mental retardation and microcephaly. Most of these patients also have Hirschsprung (HSCR) disease, and share musculoskeletal features, congenital heart disease and renal structure abnormalities. These patients are developmentally delayed with absent or minimal speech, and delayed gross motor skills, and brain abnormalities (Mowat et al., 1998). In a recent review of the literature, it was suggested that a total of 192 cases of Mowat-Wilson syndrome have been reported (Garavelli et al., 2009). The majority of *ZEB2* mutations leading to this disease are frameshift mutations and nonsense mutations, and sometimes large gene deletions. However, a few splice site mutations, missense mutations, and other types of mutations have been observed (Garavelli et al., 2009). This demonstrates the importance of *ZEB2* in development, and the cause of disease due to *ZEB2* abnormalities.

1.5.3 ZEB2 in Cancer

The role of *ZEB2* in EMT has been further demonstrated by *in vitro* studies (Figure 1.5). *ZEB2* is highly abundant in E-cadherin negative cancer cells (Comijn et al., 2001; Miyoshi et al., 2004), and is expressed in migratory and invasive breast cancer cells (Bindels et al., 2006). Functional experiments *in vitro* have demonstrated the effects of expression of *ZEB2*. Conditional *ZEB2* expression in MDCK canine epithelial cells disrupted cell-cell adhesion, decreased unidirectional migration and increased invasion (Comijn et al., 2001; Vandewalle et al., 2005). This has been further demonstrated in a colon cancer cell line, DLD1, where conditional expression of *ZEB2* caused a drastic morphological change from an epithelial phenotype to a more mesenchymal like phenotype, and caused the loss of aggregation and increased invasion (Comijn et al.,

2001). *ZEB2* stable transfectants in hepatocellular carcinoma cell lines have also shown an increase in invasion, but no change in proliferation. An increase in the expression of several matrix metalloproteinases (MMP-1, MMP-2 and MT1-MMP) has also been observed (Miyoshi et al., 2004). Expression of *ZEB2* in the squamous carcinoma cell line A431 has demonstrated a switch from a proliferative to an invasive state. Transition into S-phase of the cell cycle is inhibited by *ZEB2* via direct cyclin D1 downregulation (Mejlvang et al., 2007). The reduction of the *ZEB2* transcript in diffuse-type gastric cancer results in significant decrease in invasion, and causes reduced expression of several genes, such as *WNT5A*, and an upregulation of *WNT4* (Ohta et al., 2008). However, one seemingly contradictory report indicates that *ZEB2* can act as a molecular switch between replicative immortality and replicative senescence fates in hepatocellular carcinoma cells (HCC), acting as a repressor of human telomerase reverse transcriptase (hTERT). *ZEB2* has been shown to be expressed in non-tumour liver samples, but its expression was decreased in corresponding HCC samples (Ozturk et al., 2006).

A number of clinical studies have also implicated the role of *ZEB2* in invasive cancers. *ZEB2* is expressed in both intestinal-type gastric cancer and diffuse-type gastric cancer, but correlation with E-cadherin downregulation has only been seen in the latter (Ohta et al., 2008; Rosivatz et al., 2002). High levels of E-cadherin and low levels of *ZEB2* have been observed in normal pancreatic tissue, whereas high levels of *ZEB2* and low levels of E-cadherin have been seen in some pancreatic tumour tissues (though an inverse correlation between *ZEB2* and E-cadherin has been seen in the majority of tumour tissues analyzed) (Imamichi et al., 2007). *ZEB2* expression is abundant in some spindle cell carcinomas, and either no change, or decreased *ZEB2* expression, has been

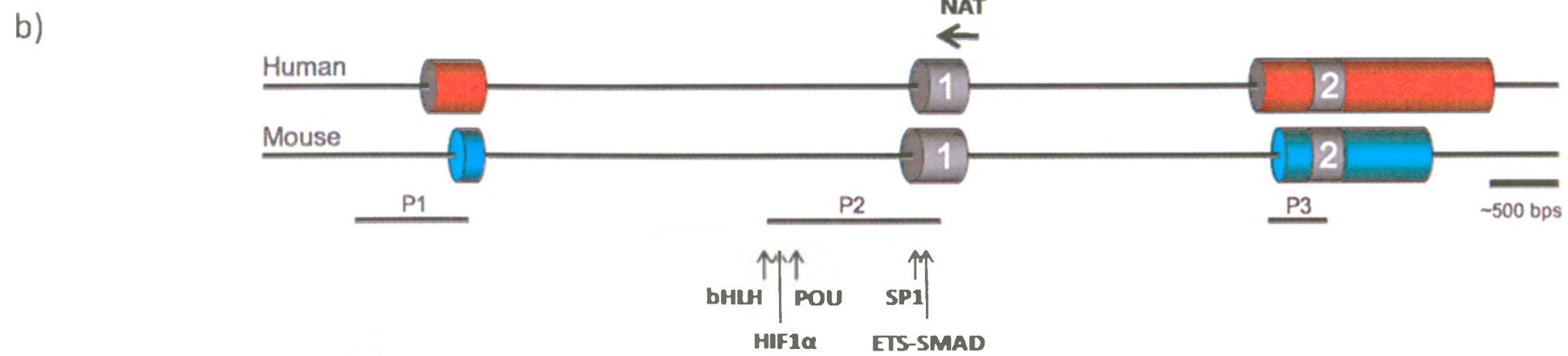
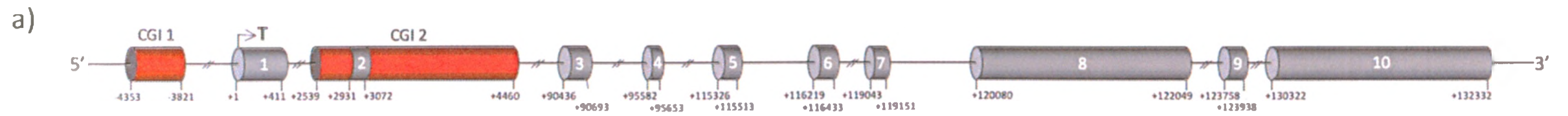
found in squamous cell carcinomas (Kojc et al., 2009). *ZEB2* is overexpressed in a large number of esophageal squamous cell carcinoma cells (Isohata et al., 2009). *ZEB2* is also expressed in breast carcinomas and ovarian carcinomas, with a high *ZEB2*/E-cadherin ratio in the former, compared to the latter. Higher expression of *ZEB2* levels correlates with high MMP-2 expression in ovarian carcinomas. Higher *ZEB2* levels have been found in ovarian carcinomas that have been obtained prior to chemotherapy when compared with disease recurrence specimens. Finally, a high *ZEB2*/E-cadherin ratio predicts poor survival, suggesting that the *ZEB2*/E-cadherin ratio may be a prognostic marker in patients with ovarian carcinoma (Elloul et al., 2005). These findings have been further validated through gene expression array analysis of eight early stage and 35 advanced stage ovarian cancer tissues, where high *ZEB2* levels have been associated with a poor prognosis (Yoshihara et al., 2009). As well, *ZEB2* is absent from normal ovarian surface epithelium, and expression increases stepwise in benign, borderline and malignant tumours (Yoshida et al., 2009).

1.5.4 The Complex Regulation of *ZEB2*

While the molecular functions of *ZEB2* are well defined, much less is known about how the *ZEB2* gene itself is regulated.

The human *ZEB2* gene is found on chromosome 2q22, and is composed of 10 exons and 9 introns (Figure 1.6a). Exon 1 is untranslated, and translation starts within Exon2. Through analysis of the mouse *ZEB2* gene, it was identified that RNA from different mouse tissues and cell lines show the presence of different splice forms.

Figure 1.6 *ZEB2* gene and putative promoter region. a) The human *ZEB2* gene consists of 10 exons (grey cylinders) and 9 introns (black lines between blue cylinders) and spans over approximately 132,000bp. The transcriptional start site is indicated by a horizontal arrow (+1 bp). Two CpG islands (red cylinders) are found in the proximity of the *ZEB2* gene. CGI 1 is found downstream of the *ZEB2* transcriptional start site, and CGI 2 spans the first intron, Exon 2 and the second intron. b) The 5' region of the human *ZEB2* gene is similar to the 5' region of the mouse *ZEB2* gene. Human and mouse exons are represented by grey cylinders, human CpG islands are represented by red cylinders, and mouse CpG islands are represented by blue cylinders. Three mouse *ZEB2* regions (P1, P2 and P3) have promoter activity, with P2 having the highest activity (Nelles et al., 2003). Putative transcription factor binding sites of basic helix-loop-helix motif (bHLH factors), hypoxia-inducible factor 1 (HIF-1), POU, SP1 and V-ets erythroblastosis virus E26 oncogene homolog 1 (ETS)/SMAD at P2 are indicated with arrows (Katoh, 2009). The *ZEB2* natural antisense transcript (NAT) is indicated by a horizontal arrow.



indicating the existence of nine untranslated exons upstream of the first translated exon. Three promoters have been identified for the mouse gene (P1, P2 and P3; Figure 1.6a). P1, upstream of the most 5' untranslated exon, and P3, upstream of the first translated exon, show weak promoter activity. P2, upstream of exon 1, shows high promoter activity (Nelles et al., 2003). It has been suggested that at least two of these promoters, P1 and P2, do exist in humans (through integrative genomic analysis) and that human *ZEB2* transcripts are generated from both promoters. However, the majority of transcription occurs at the P2 promoter (Katoh, 2009). However, to date, these promoter regions have not been confirmed experimentally for the human *ZEB2* gene.

Many factors have been suggested to play a role in *ZEB2* regulation, such as NF- κ B, ETS1 induced by TGF β , Snail, Churchill, Glioma-associated oncogene homolog 1 (GLI1) in hedgehog signalling, and hypoxia-inducible factor 1 (HIF-1) (Chua et al., 2007; Criswell and Arteaga, 2007; Isohata et al., 2009; Krishnamachary et al., 2006; Ohta et al., 2008; Sheng et al., 2003; Shirakihara et al., 2007; Takkunen et al., 2006). Due to the lack identification of the *ZEB2* promoter, promoter binding has not been validated through promoter association methods. However, a recent paper demonstrated conserved transcription factor binding sites for ETS-SMAD, HIF-1, NF- κ B, basic helix-loop-helix motif (bHLH) factors and POU/Octamer transcription factor (OCT) factors, 5' to Exon1, or within the *ZEB2* gene (Figure 1.6b) (Katoh, 2009), suggesting that perhaps some of the above factors may play a role in *ZEB2* regulation.

Interestingly, antisense transcripts of the mouse *ZEB2* gene have been identified, complicating the regulation landscape (Nelles et al., 2003). An antisense transcript for the human *ZEB2* gene has also been identified, and it has been suggested that this transcript

is expressed upon Snail induced EMT. This natural antisense transcript (NAT) can then prevent the proper splicing of the *ZEB2* transcript and result in the maintenance of a large intron located in the 5' untranslated region (between exon 1 and exon 2). This intron contains an internal ribosome entry site (IRES), and maintenance of this intron results in increased production of ZEB2 protein (Beltran et al., 2008).

Recently, more information regarding the regulation of *ZEB2* by microRNAs (miRNAs) has come to light. The miR200 family and miR205 have both been shown to regulate EMT by targeting *ZEB2* (and *ZEB1*), and their expression is reduced in a large number of cancers, coinciding with increased *ZEB2* expression and EMT (Bracken et al., 2008; Christoffersen et al., 2007; Cochrane et al., 2009; Gandellini et al., 2009; Gregory et al., 2008; Kong et al., 2009; Korpala et al., 2008; Park et al., 2008; Tryndyak et al., 2009). Interestingly, a double-negative feedback loop has been demonstrated between *ZEB2* and the microRNA200 family, where *ZEB2* is able to repress the expression of these miRNAs in mesenchymal cells (Bracken et al., 2008). Thus, the contribution of miRNAs to the regulation of *ZEB2* may be important in its differential expression during EMT (Figure 1.5).

1.6 HYPOTHESIS AND SUMMARY OF FINDINGS

It is clear from its complex regulation that further investigation is required to fully understand the regulation of *ZEB2* transcription. Evidence from promoter tiling arrays and gene expression arrays performed by our lab suggests that DNA methylation may contribute to the regulation of *ZEB2* (Rodenhiser et al., 2008), and to the differential expression of *ZEB2* seen between epithelial and mesenchymal cells. **I hypothesize that**

aberrant hypomethylation of the *ZEB2* promoter results in increased expression of *ZEB2* in cells that have gone through epithelial –mesenchymal transition.

In order to address this hypothesis, the specific objectives of my project were:

Objective 1: To determine whether *ZEB2* expression and methylation differ between cells of mesenchymal nature compared to those of epithelial nature, and to determine whether expression and methylation of *ZEB2* are inversely correlated in these cells.

Objective 2: To determine whether DNA methylation plays a causative role in *ZEB2* transcriptional regulation.

Objective 3. To determine the critical regions of the *ZEB2* promoter.

The results I present in this thesis show that DNA methylation and *ZEB2* expression correlate, and indicate that DNA methylation may contribute to *ZEB2* expression. However, the CpG islands proximal to the *ZEB2* gene are at least partially resistant to demethylation by a demethylating agent. I have identified a region of the *ZEB2* gene that possesses promoter activity, and have demonstrated that this region is differentially methylated *in vitro*. Furthermore, methylation of this promoter region *in vivo* can diminish promoter activity. These data suggest that DNA methylation of the *ZEB2* promoter and its CpG islands may play a role in the transcriptional regulation of this gene, offering a possible mechanism for the aberrant expression of *ZEB2* observed in cells which have gone through EMT.

CHAPTER 2 - MATERIALS AND METHODS

2.1 Cell Culture

Human mammary carcinoma MDA-MB-468-GFP, MDA-MB-468-LN (Vantyghem et al., 2005), and the MDA-MB-435 cell line were obtained from the lab of Dr. Ann Chambers at the London Regional Cancer Program and were maintained in minimum essential media alpha modified (α MEM) (Gibco, Burlington, ON) supplemented with 10% fetal bovine serum (FBS; Sigma, Oakville, ON). MCF-7 cells were obtained from the Chambers lab and were maintained in Dulbecco's modified Eagle medium (DMEM) (Gibco) supplemented with 10% FBS. T47D (American Type Culture Collection) and MDA-MB-231 cells, a gift from the Allan lab, were maintained in Dulbecco's modified Eagle medium: nutrient mixture F:12 (DMEM/F12) (Gibco), supplemented with 10% FBS. HCC1806 cells (American Type Culture Collection) were maintained in Roswell Park Memorial Institute medium (RPMI) 1640 supplemented with L-glutamine (0.3 g/L), sodium bicarbonate (2.0 g/L) (Gibco), and 10% FBS. The 21T series cell lines (21PTci, 21NTci, 21MT-1) were obtained from the Chambers lab, which were originally obtained from Vimla Band (Dana Farber Cancer Institute). These cells were maintained in culture in α -MEM supplemented with 10% FBS, 2 mM L-glutamine (Invitrogen), insulin (1 mg/mL) (Sigma Chemical, St. Louis, MO), epidermal growth factor (12.5 ng/mL) (Sigma), hydrocortisone (2.8 mM) (Sigma), 10 mM 4-(2-hydroxyethyl)-1-piperazineethanesulfonic acid (HEPES) (Invitrogen), 1 mM sodium pyruvate (Invitrogen), 0.1 mM nonessential amino acids (Invitrogen) and 50 mg/mL gentamicin reagent (Invitrogen). The 21PT and 21NT-derived cell lines designated

21PTci and 21NTci, contain an empty neo-selection vector (Tuck et al., 1999). All cells were maintained in a humidified incubator at 37°C with 5% CO₂.

2.2 Three-Dimensional (3D) Matrigel Culture

MDA-MB-468-GFP and MDA-MB-468-LN cells were grown in 3D Matrigel, in triplicate, for both RNA and DNA extraction. Matrigel (BD Biosciences, Mississauga, ON) was allowed to thaw overnight, and p1000 tips were cooled overnight, at 4°C. To plate, Matrigel was maintained on ice and mixed carefully, ensuring no bubbles were introduced. Matrigel (1 mL) was plated in 1 well of a 12-well plate (BD Falcon, Oakville, ON) on ice, using a new tip for each well, to ensure the Matrigel did not solidify in the tip. Plates were incubated at 37°C for one hour to solidify the Matrigel. During this incubation, MDA-MB-468-GFP and MDA-MB-468-LN cells were washed in phosphate buffered saline (PBS), trypsinized [using 0.05% trypsin (Invitrogen) and 0.5mM ethylenediaminetetraacetic acid (EDTA) (Sigma) in PBS] and spun down at 1000rpm. Cells were resuspended in 0.1% BSA (Sigma) and media (α MEM), to a final concentration of 1.3×10^6 cells/mL, ensuring no clumping occurred. Cells (0.75 mL cells/well) were added to a 15 mL conical tube and allowed to cool on ice. Matrigel was carefully mixed, and an equal volume of Matrigel (0.75 mL Matrigel/well) was added to the cells in the conical tube, on ice. This was mixed well, ensuring no bubbles were formed. The 12-well plate was removed from the 37°C incubator, cooled on ice, and 1.5 mL of the Matrigel/cell mixture was added on top of the hardened Matrigel layer. The 12-well plate was incubated at 37°C for 1.5 hours. α MEM with 0.1% BSA was added on top

of the Matrigel/cell layer carefully so as to not disrupt the Matrigel. Media was changed every two days.

Cells were harvested from Matrigel using Cell Recovery Solution (BD Biosciences). PBS, cell recovery solution and 50mL conical tubes (1 per well) were cooled on ice. Cell recovery solution (2 mL) was added to each 50 mL conical tube. Three wells at a time, media was removed from each well, and wells were washed with 500 μ L of PBS twice. A metal scraper was used to scrape around the edges of the Matrigel to loosen it from the plate. A 10 mL pipette was used to remove the Matrigel out of one well, and place it into a cold conical tube, at the bottom, below the cell recovery solution. This was repeated for each well. Cell recovery solution (2 mL) was added to each well, and with the 10 mL pipette, Matrigel was cleaned out of each well, separately, and the liquid was added to the corresponding conical tube. This procedure was repeated for the next 3 wells. Each conical tube was mixed and incubated for 1.5 hours while mixing every half hour. The tubes were spun down at 1200 rpm for 10 minutes at 4°C. The supernatant was removed without disturbing the pellet, and the pellet was resuspended in 500 μ L of PBS. The tube was spun down at 1200 rpm for 10 minutes at 4°C and the supernatant was removed. This pellet was then used for RNA or DNA extraction, as outlined below.

2.3 Bisulfite Mutagenesis and Genomic Sequencing

Unless otherwise stated, cells were grown in T-75 flasks (Corning, Corning, NY) and were trypsinized and centrifuged for 5 minutes at 1000 rpm. Cell pellets were lysed and DNA was extracted using GenElute Mammalian Genomic DNA Miniprep Kit

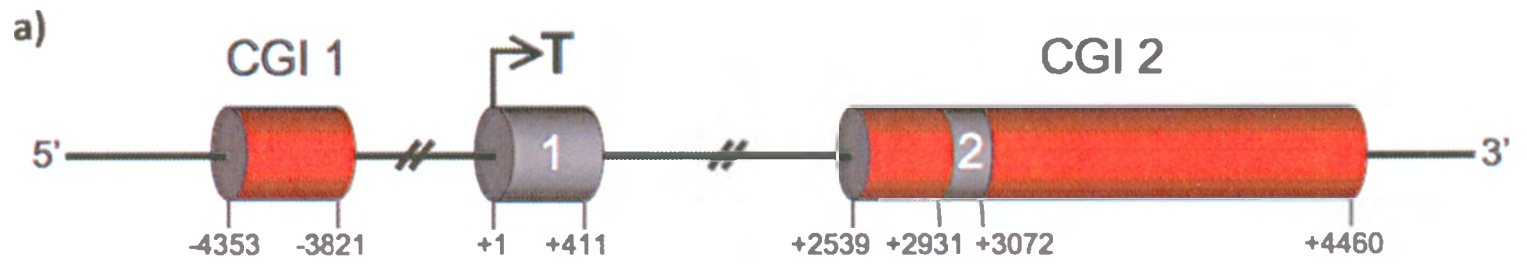
(Sigma). Genomic DNA (2 μ g) was subjected to bisulfite mutagenesis using the Epitect DNA Bisulfite Treatment kit (Qiagen, Mississauga, ON). Primers were manually generated to specifically anneal to bisulfite-converted DNA (Figure 2.1; Table 2.1).

A nested PCR approach was used (unless indicated with * or **; Table 2.1). Outside PCRs were first performed with 1X buffer, 1-2.5 mM $MgCl_2$, 200 μ M dNTPs, 500 nM forward and reverse primers (Sigma-Genosys), 2 μ L of DNA, and 1 U of *Taq* polymerase (Invitrogen) first. The cycling conditions for the outside PCR were: 1 cycle of 94°C for 5 minutes, followed by 5 cycles of 94°C for 1 minute, 55°C for 2 minutes and 72°C for 3 minutes, followed by 35 cycles of 94°C for 30 seconds, 55°C for 2 minutes and 72°C for 2 minutes, followed by 72°C for 10 minutes. PCRs were diluted 1:8 and 2 μ L were used for inside PCRs. Inside PCRs were performed with 1X buffer, 1-2.5 mM $MgCl_2$, 200 μ M dNTPs, 500 nM forward and reverse primers (Sigma-Genosys, Oakville, ON), 2 μ L of DNA, and 2 U of *Taq* polymerase (Invitrogen). The cycling conditions were: 1 cycle of 94°C for 5 minutes, followed by 35 cycles of 94°C for 1 minute, 55°C for 1 minute and 72°C for 1 minute, followed by 72°C for 10 minutes (Table 2.1).

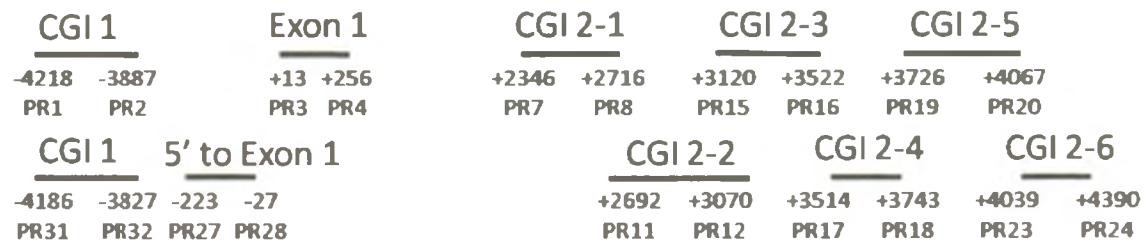
Regions marked with * were amplified with an inside PCR reaction alone. Regions marked with ** were amplified using a high fidelity enzyme in a nested PCR approach: Outside PCRs were performed with 1X Expand High Fidelity^{PLUS} Reaction Buffer (Roche, Mississauga, ON) with 1.5 mM $MgCl_2$, 200 nM dNTPs, 500 nM forward and reverse primers (Sigma-Genosys (Table 2.1)), 2 μ L of converted DNA and 1.25 U of Expand High Fidelity^{PLUS} Enzyme Blend (Roche). The cycling conditions were: 1 cycle of 94°C for 2 minutes, followed by 35 cycles of 94°C for 30 seconds, 52-57°C for 30 seconds and 72°C for 45 seconds, followed by 72°C for 7 minutes. Inside PCR reactions

Figure 2.1 *ZEB2* gene and location of primers for bisulfite cloning and promoter

cloning. a) The most 5' region of the *ZEB2* gene contains 2 CpG islands, CpG island 1 (CGI 1) and CpG island 2 (CGI2) (red cylinders), and Exon 1 and Exon 2 (grey cylinders). The transcriptional start site is indicated by a horizontal arrow. b) The regions cloned for the purpose of bisulfite sequencing are demonstrated with a thick black line, with the region name listed above the primed location. The base pair location of the region cloned, as well as the primer sets utilized for cloning of these regions are also listed below the black line. c) The human promoter (hPr) region amplified for promoter construct cloning is illustrated as a thick black line, with the base pair location and the primer set utilized illustrated below.



b) Bisulfite Primers



c) Promoter Cloning Primers



Table 2.1. Primers used for bisulfite mutagenesis and genomic sequencing. A list of the names of the regions analyzed with their corresponding primers, primer sequence, annealing temperature and product size.

Region	Primer # and Name	Sequence	Annealing Temp	Product Size
* CGI 1	PR1- ZEB2 CpG1 Forward PR2- ZEB2 CpG1 Reverse	TTT TTA AGT TTT AGT GAG ATT GAT AGT CAT TTA ATC TCC AAA AAA AAC CC	55	332 bp
* ZEB2 Exon 1	PR3- ZEB2 Ex1 Forward PR4- ZEB2 Ex1 Reverse	AGA TTT TTT TTT AGA GAG AAA TTT GG TTA TTC CTA CAA AAC AAA TTA AAA CTA	55	244 bp
CGI 2-1	PR5- ZEB2 NAT OUT Forward PR6- ZEB2 NAT OUT Reverse	TGG GGT AAA GGA TAG TGT TTA AAG AGG TAT TAC TAT TTA ATA TAT TAC ACC	55	484 bp
CGI 2-1	PR7- ZEB2 NAT Forward PR8- ZEB2 NAT Reverse	AGG GTG GGG GGA GGA AGA GAT AGT GTT T AAA AAA TCA AAA AAA CAA AAA TTA C	55	371 bp
CGI 2-2	PR9- ZEB2 CpG2-1 OUT Forward (Ex2) PR10- ZEB2 CpG2-1 OUT Forward (Ex2)	GGG GAT GAG AAA AGA TGA GAA CCC TCC TTC TCC CTA AAT CT	55	622 bp
CGI 2-2	PR11- ZEB2 CpG2-1 Forward (Ex 2) PR12- ZEB2 CpG2-1 Reverse (Ex 2)	GTA ATT TTT GTT TTT TTG ATT TTT T TTT TCC TCC TAA AAT TAA CTT ATT TAC	55	378 bp
CGI 2-3	PR13- ZEB2 CpG2-2 OUT Forward PR14- ZEB2 CpG2-2 OUT Reverse	TAA ATA AGT TAA TTT TAG GAG GAA AAA ACT CCG ACA AAA AAC TTT AAA CCT	55	536 bp
CGI 2-3	PR15- ZEB2 CpG2-2 Forward PR16- ZEB2 CpG2-2 Reverse	AGA TTT AGG GAG AAG GAG GGG GAA AGG GAA CTT CGC AAT CTC TCT ACC ACC CCC	55	403 bp
* CGI 2-4	PR17- ZEB2 CpG2-3 Forward PR18- ZEB2 CpG2-3 Reverse	ATT GCG AAG GTA GGA GAG GGG AAT AAC AAA ACC TAC TAA AAA AAA ATC ATC	55	230 bp
* CGI 2-5	PR19- ZEB2 CpG2-4 Forward PR20- ZEB2 CpG2-4 Reverse	TTT TTA GTA GGT TTT GTT TTT AGG T CTC TTA CCA ATC ACT TTT CTC TTT TAT TC	55	342 bp
CGI 2-6	PR21- ZEB2 CpG2-5 OUT Forward PR22- ZEB2 CpG2-5 OUT Reverse	TTT AGG TAT TAT TTT AAA TAA AAT TTT TAC TCC TTC CAA CAC CTC ACA CTA	55	478 bp
CGI 2-6	PR23- ZEB2 CpG2-5 Forward PR24- ZEB2 CpG2-5 Reverse	GAA TAA AAG AGA AAA GTG ATT GGT AAG AG CTA AAA AAA AAT TAC TCC AAA TAA ACC	55	352 bp
** 5' Exon 1	PR25- 5' Ex1 Forward PR26- Fbisulfite Reverse (Outside)	AGAGAATTTTGTTTTAGAAGTTGTATTGA G CCAAATTTCTCTAAAAAAAATCT	57	408 bp
** 5' Exon 1	PR27- Fbisulfite Forward PR28- 5' Ex1 Reverse (Inside)	TTTTAGTTTTTGGAATGGTGTGTAT ATAAAAAAATAAAAATCCACCTCC	56	197 bp
** CGI 1	PR29- JP-1F PR30- JP-1R (Outside)	GTAGGAGGGAGATTTTTGGT CCAACAACTTCAAAACCCAA	52	655 bp
** CGI 1	PR31- JP-2F PR32- JP-2R (Inside)	TGGAGGAGGTTTTTTTAGGT CTCTACCACTCCCCCCC	55	360 bp

were diluted 1:8, and outside PCR reactions were performed with 1X Expand High Fidelity^{PLUS} Reaction Buffer (Roche, Mississauga, ON) with 1.5 mM MgCl₂, 200 nM dNTPs, 500 nM forward and reverse primers (Sigma-Genosys (Table 2.1)), 2 µL of 1:8 inside PCR reaction and 2.5 U of Expand High Fidelity^{PLUS} Enzyme Blend (Roche). The cycling conditions were: 1 cycle of 94°C for 2 minutes, followed by 35 cycles of 94°C for 30 seconds, 55-56°C for 30 seconds and 72°C for 45 seconds, followed by 72°C for 7 minutes (Table 2.1).

PCR products were electrophoresed on a 1-1.5% agarose gel and the appropriate band was gel extracted using a QIAEX II Gel Extraction kit (Qiagen). The extracted PCR product was then ligated into the pCR2.1 vector using The Original TA Cloning Kit (Invitrogen). Plasmids were transformed into TOP10 competent bacteria (Invitrogen), and transformed bacteria were spread onto Luria-Bertani (LB) agar plates containing 50 µg/mL ampicillin (Sigma) and 50 µL of 10 mg/mL X-gal (5-bromo-4-chloro-3-indolyl-β-D-galactopyranoside; Sigma) and incubated overnight at 37°C. Potential clones were screened through PCR using the PCR primers used in the initial amplification step. Positive clones were grown up in 2 mL of Terrific Broth (TB) with 100 µg/mL ampicillin overnight at 37°C. Plasmid DNA was isolated using QIAprep Spin Miniprep kit (Qiagen) and sequenced using the T7 promoter primer at the Robarts Research Institute DNA Sequencing Facility (<http://www.robarts.ca/gateway.php?id=26>). Alternatively, some clones were screened through PCR using M13 primers (Table 2.2), performed with 1X buffer, 1.5 mM MgCl₂, 200 µM dNTPs, 500 nM forward and reverse primers (Sigma-Genosys, Oakville, ON), 2 µL of DNA, 2 U of *Taq* polymerase, and a bacterial colony (Invitrogen). The cycling conditions were: 1 cycle of 94°C for 10 minutes, followed by

Table 2.2. Primers used for cloning and sequencing. A list of the primers that were used for the cloning of the *ZEB2* promoter fragment hPr, or for sequencing of the pCR2.1 vector and pGL3-basic vector, as well as the primer sequence.

Primer # and Name	Primer Sequence	Usage
PR49- M13 Forward PR50- M13 Reverse	CGC CAG GGT TTT CCC AGT CAC GAC TCA CAC AGG AAA CAG CTA TGA C	pCR2.1 colony PCRs
PR51- RVprimer3	CTA GCA AAA TAG GCT GTC CC	pGL3-basic sequencing
PR52- GLprimer2	CTT TAT GTT TTT GGC GTC TTC CA	pGL3-basic sequencing
PR53- PROMBASH5	AGC TAC GCG TCT GCG AAG TCT TGT TTG TAG TTT TG	Fragment F cloning
PR54- PROMBASH8	AGC TGA GCT CAA GAA AAA AAT AAC AAT AAG AGA AAG GG	Fragment F cloning

30 cycles of 94°C for 45s, 57°C for 30s and 72°C for 1.5 minute, followed by 72°C for 10 minutes. Positive samples were sent as unpurified PCR samples to McGill University and Genome Quebec Innovation Centre Sequencing Services (<http://www.genomequebecplatforms.com/mcgill/services/sequencing/index.aspx?l=e>), where the PCRs were purified and sequenced using the T7 promoter or M13 reverse primers. Sequences were aligned and analyzed using the ClustalW alignment algorithm (<http://www.ebi.ac.uk/Tools/clustalw2/index.html>).

2.4 Reverse Transcription Polymerase Chain Reaction (RT-PCR)

Unless otherwise stated, mammalian cells were grown in T-75 flasks (Corning) and were trypsinized and centrifuged for 5 minutes at 1000 rpm. Cell pellets were lysed and RNA was extracted using the RNAeasy Kit (Qiagen) and RNA was run on a 1.5% gel to ensure good quality. RNA (1µg) was DNase I (Invitrogen) treated, and cDNA was synthesized using SuperScript II (Invitrogen). PCRs for *ZEB2*, glyceraldehyde-3-phosphate dehydrogenase (*GAPDH*), E-cadherin, vimentin, N-cadherin and fibronectin were performed with 1X buffer, 2.5 mM MgCl₂, 200 µM dNTPs, 500 nM forward and reverse primers (Sigma-Genosys, Table 2.3), 1 µl of cDNA, or cDNA diluted 1:10, and 1 U of *Taq* polymerase (Invitrogen). The cycling conditions were: 1 cycle of 94°C for 4 minutes, followed by 25-35 cycles (Table 2.3) of 94°C for 1 minute, 55-60°C (Table 2.3) for 1 minute and 72°C for 1 minute, followed by 72°C for 10 minutes. PCR products were electrophoresed on a 1.5% gel. Dickkopf homolog 3 (*DKK3*) RT-PCR was performed with 1X buffer, 2.5 µM MgCl₂, 400 nM dNTPs, 400 nM forward and reverse primers (Sigma-Genosys, Table 2.3), 1µL of cDNA and 1.25 U

Table 2.3. Primers used for RT-PCR. A list of the names of the primers that were used for RT-PCR, with their corresponding primer sequence, annealing temperature, number of cycles, and product size.

Primer # and Name	Primer Sequence	Annealing Temp	Cycles	Product Size
PR33- GAPDH RT Forward PR34- GAPDH RT Reverse	CAT GTT CGT CAT GGG TGT GAA CCA ATG GCA TGG ACT GTG GTC ATG AGT	60	25	156 bp
PR35- ZEB2 RT Forward PR36- ZEB2 RT reverse	TGA TGA ACC GGG CTT ACT TGC AGA TTC TTT CTC GTG CTC CTT CTC GCT	60	30	110 bp
PR37- ZEB2 Exon1 Forward PR38- ZEB2 Exon1 Reverse	TTC AAT TAT CCC TCC CCA CA GAC CGT TAT TCC TGC AGA GC	58	35	186 bp
PR39- DKK3 RT Forward PR40- DKK3 RT Reverse (Veeck et al., 2008)	AAG GCA GAA GGA GCC ACG AGT GC GGC CAT TTT GGT GCA GTG ACC CCA	60	35	182 bp
PR41- N-cadherin Forward PR42- N-cadherin Reverse (Ohta et al., 2008)	GGC ATA GTC TAT GGA GAA GT GCT GTT GTC AGA AGT CTC TC	55	30	383 bp
PR43- Vimentin Forward PR44- Vimentin Reverse (Miyoshi et al., 2004)	ACG CCA TCA ACA CCG AGT TCA GTG CCA GAG ACG CAT TGT CAA	55	30	383 bp
PR45- Fibronectin Forward PR46- Fibronectin Reverse (Miyoshi et al., 2004)	AGG AAG CCG AGG TTT TAA CTG TCA GCT ATG GGC TTG CAG GTC	55	30	314 bp
PR47- E-cadherinRT Forward PR48- E-cadherinRT Reverse	TGA GTG TCC CCC GGT ATC TTC CAG TAT CAG CCG CTT TCA GAT TTT	60	30	87 bp

of *Taq* polymerase (Invitrogen). The RT-PCR cycling conditions for *DKK3* were: 35 cycles of 95°C for 1 minute, 60°C for 1 minute and 72°C for 1 minute, followed by 72°C for 10 minutes. PCR products were electrophoresed on a 1.5% gel.

2.5 5-Aza-2'-deoxycytidine and Trichostatin A Treatment

MCF-7 cells were seeded at a density of 2.1×10^4 cells/cm² on a 10 cm plate (Nunc, Rochester, NY), and MDA-MB-468-GFP cells were seeded at a density of 7.1×10^3 cells/cm² on a 15cm plate (Nunc), in duplicate on Day 0. 5-aza-2'-deoxycytidine (5-aza) (Sigma) was added to a final concentration of 1, 2, 5 and 10 μ M in fresh media on days 1, 2 and 3, with the addition of 0.3 μ M Trichostatin A (TSA) (Sigma) on day 3. Control cells were incubated without the addition of 5-aza and TSA, and fresh media was also supplied on Day 1, 2 and 3. Cells were harvested on Day 4. The MDA-MB-468-GFP experiments with 5-aza drug treatment for 5 and 7 days were performed as outlined above, with the addition of 5-aza to a final concentration of 1, 2, 5 and 10 μ M in fresh media for 5 or 7 days, with the addition of TSA on the last day. Fresh media was added to the control cells every day. At appropriate timepoints, cells were harvested using trypsin, and cell suspension was split between two 15 ml conical tubes and centrifuged at 1000 rpm for 5 minutes. One set of cell pellets were snap frozen using dry ice and ethanol, and stored at -80°C for DNA extraction. The other set of cell pellets were lysed and RNA was extracted and RT-PCRs were performed as outlined above.

2.6 Cell Microscopy

An Olympus 1X70 Inverted microscope was used to obtain brightfield pictures of control cells and cells treated with 5-aza and TSA. ImagePro software (MediaCybernetics, Bethesda, MD) was used to obtain the images.

2.7 Promoter Construct Cloning

Primers for Region hPr (human Promoter; -399 to +411) were constructed containing *SacI* and *MluI* cut sites on the forward, and reverse primer, respectively (Sigma-Genosys; Table 2.2). PCR was performed with 1X Expand High Fidelity^{PLUS} Reaction Buffer (Roche, Mississauga, ON) with 1.5 mM MgCl₂, 200 nM dNTPs, 500 nM forward and reverse primers (Sigma-Genosys; Table 2.2), 100 ng of Human Female Genomic DNA (Novagen, Gibbstown, NJ) and 2.5 U of Expand High Fidelity^{PLUS} Enzyme Blend (Roche). The cycling conditions were: 1 cycle of 94°C for 2 minutes, followed by 35 cycles of 94°C for 30 seconds, 58°C for 30 seconds and 72°C for 2 minutes, followed by 72°C for 7 minutes. PCR products were purified using Qiagen PCR Purification Kit (Qiagen), and sequentially digested using *SacI* and *MluI* (New England Biolabs, Pickering, ON), purifying the PCR product between digestions. Region hPr was ligated into pGL3-basic (a kind gift from Dr. F. Dick) at 14°C overnight with 1X T4 DNA ligase buffer and T4 DNA ligase (Invitrogen). Plasmids were transformed into NEBα competent bacteria (New England Biolabs), and transformed bacteria were spread onto LB agar plates containing 50 µg/mL ampicillin and incubated overnight at 37°C. Potential clones were grown up in 5 mL of LB with 50 µg/mL ampicillin overnight at 37°C. Plasmid DNA was isolated using QIAprep Spin Miniprep kit (Qiagen) and

sequenced using GLprimer2 and RVprimer3 pGL3-basic vector primers (Sigma-Genosys) (Table 2.2). One clone identified without mutations was then grown in 25 mL LB with 50 µg/mL ampicillin overnight at 37°C, and plasmid DNA was isolated using PureLink HiPure Plasmid Midiprep Kit (Invitrogen) to use for luciferase assays.

2.8 Luciferase Reporter Assays

MDA-MB-468-LN and MDA-MB-435 cells were plated at a density of 2×10^5 cells per well of a six-well dish (Falcon), and MCF-7 cells were plated at a density of 5×10^5 cells per well of a six-well dish (Falcon), in triplicate, and were transfected 24 hours later. Each well was transfected individually with Lipofectamine 2000 (Invitrogen). Reporter plasmid (2µg; pGL3 or pGL3-hPr) and 200 ng of CMV-β-Gal vector, a kind gift from Dr. F. Dick, was incubated with 250 µL of OptiMEM (Invitrogen), and 6-9 µL Lipofectamine 2000 (Invitrogen) was incubated with 250 uL OptiMEM for 5 minutes. The DNA/OptiMEM mixture was added to the Lipofectamine/OptiMEM mixture, and incubated for 20 minutes. The mixture was then dropped onto cells. Cells were washed with PBS and fresh media was added 5 hours after transfection. Cells were harvested 48 hours after transfection, by the addition of 250 µL of Reporter Lysis Buffer (Promega), and allowed to incubate on ice for 5 minutes. Cells were then frozen at -80°C until the luciferase assay was performed. The luciferase activity of each set of transfections was determined using a Wallac Victor² 1420 Multilabel Counter (Beckman Coulter, Inc., Fullerton, CA) by addition of Luciferase Assay Reagent (Promega, Madison, WI) and determination of the relative amount of Luciferase gene product expressed in each sample. Assays to determine the β-galactosidase (β-Gal) activity of each transfected

group were performed by the addition of β -Gal Assay Buffer (2X Buffer: 200 mM NaPi (sodium phosphate, pH 7.4), 2 mM MgCl_2 , 100 mM beta-mercaptoethanol (β -ME), and 1.33 mg/mL *ortho*-Nitrophenyl- β -galactoside (ONPG) (Bioshop, Burlington, ON) to each sample. Samples were read with a Wallac Victor² 1420 Multilabel Counter. Luciferase activity of each sample was normalized to β -Gal activity, and the results were presented in bar graph form as fold activation of pGL3-hPr activity over pGL3 activity, of the mean of three triplicates (separate transfections performed on the same day and at the same time) of corrected luciferase activity between the pGL3-hPr and pGL3, and were expressed as “Fold Difference” for each cell line.

2.9 Plasmid Methylation

Aliquots of pGL3- and pGL3-hPr reporter constructs (5 μg) were methylated *in vitro* using 12 units of *Sss*I methylase (NEB) supplemented with 160 μM S-adenosylmethionine (SAM) at 37°C for 8 hours. After 4 hours of incubation, the reaction was supplemented with additional SAM. Mock-methylation reactions were also performed, in the absence of *Sss*I methylase and SAM. The methylated and mock-methylated constructs were purified using a Qiagen PCR Purification Kit (Qiagen), and the methylation status of each construct was determined by *Hpa*II (NEB) digestion. These constructs were used in luciferase experiments with MDA-MB-468-LN cells as described above.

2.10 Plasmid ‘Patch’ Methylation

pGL3- and pGL3-hPr (50µg) were sequentially digested with *SacI* (NEB) overnight at 37°C and *MluI* (NEB) at 37°C for 5 hours, purifying the plasmid between digestions using a Qiagen PCR Purification Kit (Qiagen). *MluI* digestion reactions were electrophoresed on a 1% low melting temperature agarose gel and both the pGL3 vector and the fragment corresponding to hPr were gel extracted using a QIAEX II Gel Extraction kit (Qiagen). Aliquots of the hPr fragment were methylated *in vitro* using 12 units of *SssI* methylase (NEB) supplemented with 160µM SAM at 37°C for 8 hours. After 4 hours of incubation, the reaction was supplemented with additional SAM. Mock-methylation reactions were also performed, in the absence of *SssI* methylase and SAM. The methylated and mock-methylated fragments were purified using a Qiagen PCR Purification Kit (Qiagen), and the methylation status of each fragment was determined by *HpaII* (NEB) digestion. These methylated and mock-methylated fragments were ligated into the pGL3 vector previously gel extracted, and ligated overnight at 14°C with 1X T4 DNA ligase buffer and T4 DNA ligase (Invitrogen). Ligation reactions were digested with *EcoRV* (Invitrogen) for 2 hours at 37°C in order to linearize the vector for quantification. Digestion reactions were electrophoresed on a 1% low melting temperature agarose gel and the linearized vector was gel extracted using a QIAEX II Gel Extraction kit (Qiagen) and quantified. Linearized vector (pGL3-hPr-mock and pGL3-hPr-meth) (1.6µg) was ligated overnight at 14°C with 1X T4 DNA ligase buffer and T4 DNA ligase (Invitrogen). Ligation reactions (18.75 µL) containing 0.75 µg of vector were used in duplicate transfections for luciferase experiments. A vector coding for membrane-spanning 4-domains, subfamily A, member 1 (CD20) was used to increase the total DNA

to 2 μg to maintain transfection efficiency. Transfections of MDA-MB-468-LN cells and luciferase assays were performed as described above.

2.11 Statistical Analysis

Differences in the activity of pGL3-basic and pGL3-hPr were analyzed by Student's T-test, for each cell line. Differences in the activity of pGL3mock, pGL3meth, pGL3-hPr-mock and pGL3-hPr-meth were analyzed by Analysis of Variance (ANOVA) based on ranks. The Student Newman Keuls post hoc test was used to determine which groups showed a significant difference. The difference in the activity of pGL3-hPr-mock (Patch) and pGL3-hPr-meth (Patch) was analyzed by Student's T-test.

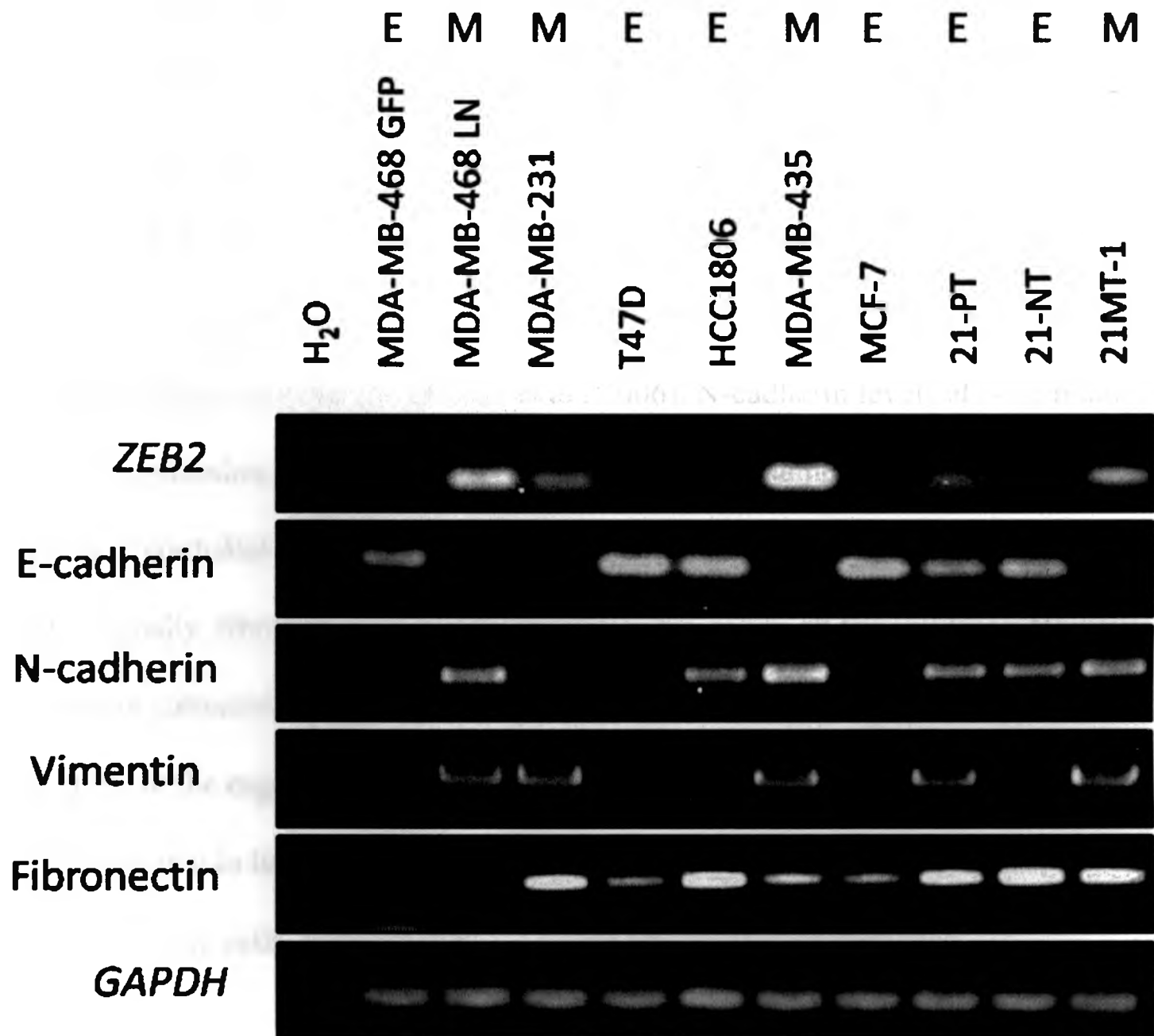
CHAPTER 3 - RESULTS

3.1 *ZEB2* was Expressed in Mesenchymal Cell Lines but not in Epithelial Cells

To understand the function and regulation of *ZEB2*, it was first essential to analyze the expression pattern of *ZEB2* mRNA in various human cancer cell lines. To address this, ten human breast cancer cell lines (MDA-MB-468-GFP, MDA-MB-468-LN, MDA-MB-231, MDA-MB-435, T47D, HCC1806, MCF-7, 21PT, 21NT and 21MT-1 cells), some of an epithelial-like nature, and some of a more mesenchymal-like nature, were grown *in vitro* in two-dimensional (2D) culture. These cells were harvested, RNA was extracted and reverse transcription polymerase chain reaction (RT-PCR) was performed to determine the expression levels of *ZEB2* relative to GAPDH (Figure 3.1). *ZEB2* was expressed in the MDA-MB-468-LN, MDA-MB-435 cell lines, MDA-MB-231, 21-PT and 21MT-1 cell lines. Low expression of *ZEB2* was observed in MDA-MB-468-GFP, T47D, HCC1806, MCF-7 and 21NT cell lines. Therefore, differential expression of *ZEB2* is observed between these ten cell lines.

It has been shown previously that *ZEB2* is a repressor of E-cadherin (Comijn et al., 2001; Imamichi et al., 2007; Miyoshi et al., 2004). To determine whether E-cadherin expression negatively correlated with *ZEB2* expression in our cell lines, RT-PCR was performed. E-cadherin levels were found to be high in cell lines not expressing *ZEB2*, and low in cells expression *ZEB2*. Thus, *ZEB2* and E-cadherin levels are inversely correlating in these cell lines.

Figure 3.1 *ZEB2* was overexpressed in cells with a predominant mesenchymal phenotype. Ten human cancer cell lines were grown in 2D culture and RNA was extracted and converted to cDNA. Levels of *ZEB2*, E-cadherin, N-cadherin, vimentin and fibronectin were analyzed using RT-PCR. Water is shown as a no template control. PT-PCR of *GAPDH* is shown as a positive control. E indicates a cell line with an epithelial phenotype, and M indicates a cell line with a more mesenchymal phenotype.



It has also been previously shown that *ZEB2* was highly expressed in cells which have gone through epithelial-mesenchymal transition (EMT), compared to cells of a more epithelial nature (Bindels et al., 2006; Comijn et al., 2001; Mejlvang et al., 2007; Vandewalle et al., 2005). Although we found that *ZEB2* expression was higher in cells which have a more fibroblastic, spindle-shaped morphology (data not shown), it was important to further illustrate this relationship by analyzing the expression of other mesenchymal markers. Therefore, vimentin, N-cadherin and fibronectin expression levels were analyzed (Figure 3.1). Vimentin expression patterns were found to mimic those of *ZEB2*, which is consistent with previous findings which showed that vimentin and *ZEB2* had similar expression patterns (Bindels et al., 2006). N-cadherin levels also correlated with *ZEB2* expression, but some discrepancies were seen. Namely, N-cadherin was expressed in epithelial-like HCC1806 cells, and absent in mesenchymal-like MDA-MB-231 cells. Finally, fibronectin was differentially expressed in all ten cell lines. However, no consistent pattern of fibronectin expression was seen when compared to cell morphology or the expression of *ZEB2* or other EMT markers. Therefore, this analysis demonstrated that in the ten cell lines analyzed, *ZEB2* was highly expressed in mesenchymal-like cells, and absent in cells with epithelial characteristics.

3.2 Region hPr Possessed Promoter Activity

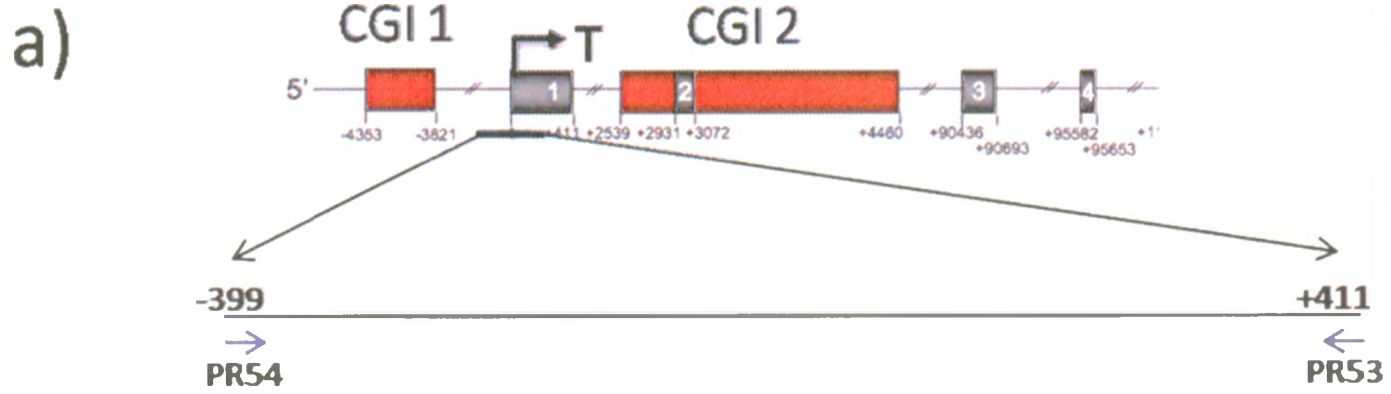
Regulation of the human *ZEB2* promoter has not been well defined. A promoter fragment of *ZEB2* with high activity has been identified in mouse (P2; Figure 1.6b; (Nelles et al., 2003)). However, this region has not been confirmed as the promoter of

human *ZEB2*. Thus, a 810 bp region that spans from -399 bp + to -411 bp was amplified, corresponding to a large portion of mouse P2 promoter (-960 bp to + 297 bp: (Nelles et al., 2003)). This region (which we denote as hPr) was cloned into pGL3-basic. The resulting reporter vector (pGL3-hPr) was then used in luciferase assays. Reporter vectors (pGL3 and PGL3-hPr) were transfected into MCF-7, MDA-MB-468-LN and MDA-MB-435 cells, and were co-transfected with the CMV- β -Gal vector to control for transfection efficiency (Figure 3.2). Region hPr had increased luciferase activity in MCF-7, MDA-MB-468-LN and MDA-MB-435 cells compared to the control pGL3-basic vector. It appeared that the activity of the promoter region was lower in MCF-7 cells than in the other cell lines. MCF-7 cells do not endogenously express *ZEB2* (Figure 3.1). These results suggested that the region from -399 bp to +411 bp is an important regulatory region for *ZEB2* activity.

3.3 *ZEB2* CpG Island 1 and CpG Island 2 were Hypomethylated in Mesenchymal Cells Compared to Epithelial Cells

Despite the contribution of *ZEB2* to EMT, there is still very little known about how *ZEB2* may become deregulated during this process. Promoter tiling arrays have been previously used in our laboratory to analyze DNA methylation patterns in MDA-MB-468-GFP and MDA-MB-468-LN cells. Hypomethylation of the proximal *ZEB2* gene was observed (Rodenhiser et al., 2008) in the MDA-MB-468-LN cells compared to the MDA-MB-468-GFP cells. These results were previously validated by bisulfite genomic sequencing to determine the methylation status of CpG island 1 (CGI 1) of *ZEB2*, in these two cell lines (Figure 3.3) (Rodenhiser et al., 2008). We observed that decreased

Figure 3.2 Region hPr had promoter activity in mesenchymal cells. a) The most 5' region of the *ZEB2* gene contains 2 CpG islands, CpG island 1 and CpG island 2 (red cylinders), surrounding Exon 1 and Exon 2 (grey cylinders). The region hPr is located from -399 bp to +411 bp, spanning from 5' to Exon 1, through the entirety of Exon 1. b) A table of the average relative luciferase units (RLU) for the pGL3-basic and pGL3-hPr plasmids transfected into MCF-7, MDA-MB-468-LN and MDA-MB-435 cell lines, the fold activation of the pGL3-hPr plasmid over the pGL3-basic plasmid, and the P-values for each cell line. c) This region was amplified and cloned into pGL3-basic. pGL3 or pGL3-hPr, along with CMV- β -Gal, were transfected into MCF-7, MDA-MB-468-LN and MDA-MB-435 cells using Lipofectamine 2000. Forty-eight hours after transfection, cells were lysed and luciferase assays were performed. β -Galactosidase assays were performed to normalize for transfection efficiency. Bars represent the fold-difference of promoter activity of pGL3-hPr compared to pGL3, normalized to β -Galactosidase, obtained from three separate transfection experiments for each cell line. Significant luciferase activity differences of pGL3-hPr ($P < 0.05$) compared to pGL3-basic are indicated by (*).



b)

Cell Line	Plasmid	RLU	RLU relative to pGL3-basic (Fold Activation)	P-value
MCF-7	pGL3-basic	8291	1	0.0060
	pGL3-hPr	30386	3.67	
MDA-MB-468-LN	pGL3-basic	588	1	0.0004
	pGL3-hPr	5795	9.86	
MDA-MB-435	pGL3-basic	1473	1	0.0002
	pGL3-hPr	18410	12.49	

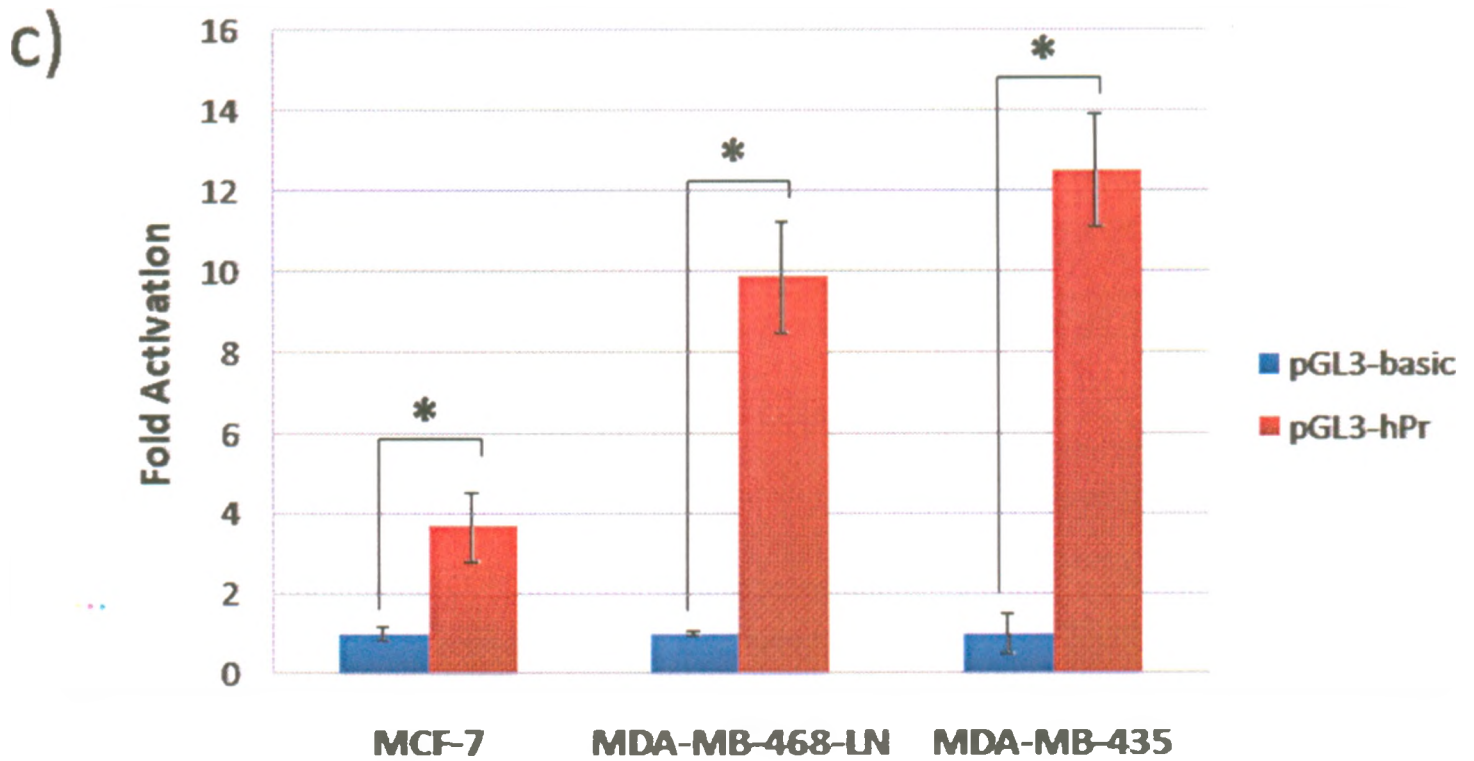
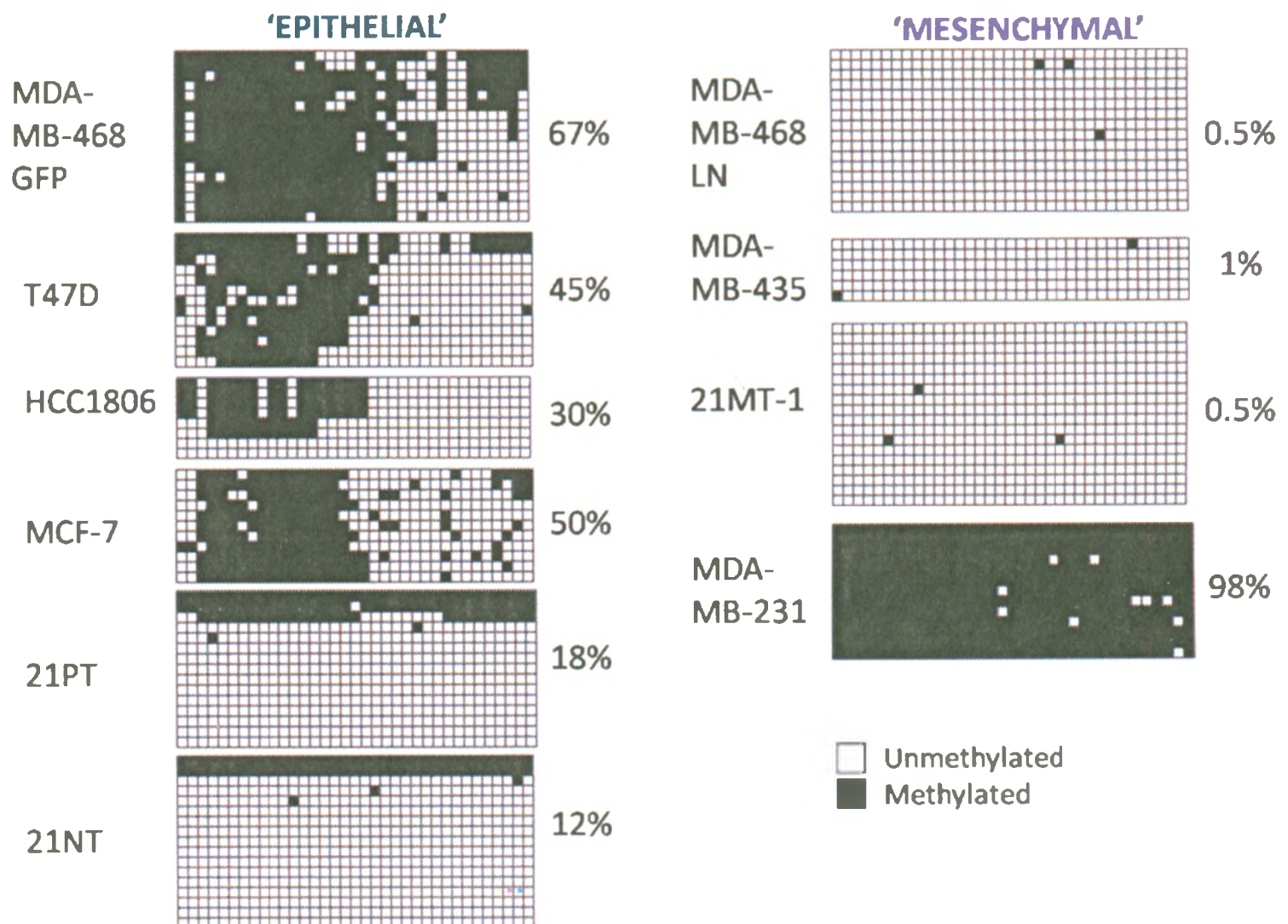
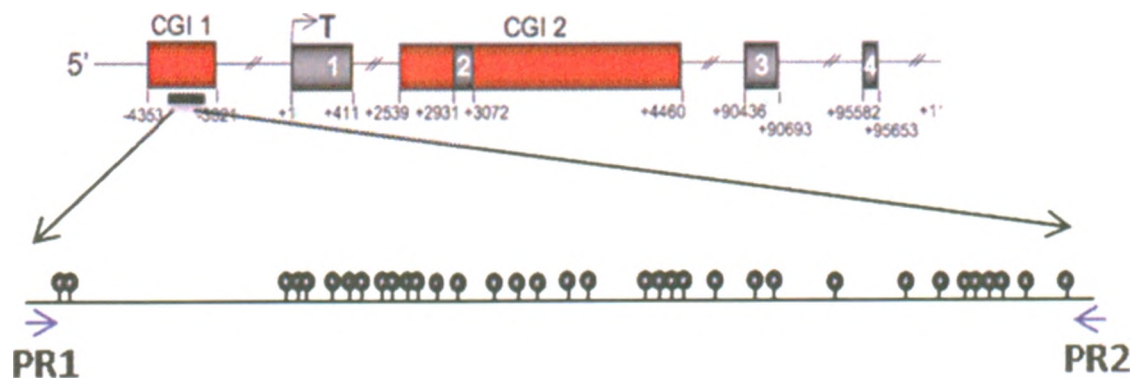


Figure 3.3 CpG island 1 was differentially methylated in human cancer cells. DNA extracted from ten human cancer cell lines, MDA-MB-468-GFP, MDA-MB-468-LN, MDA-MB-231, T47D, HCC1806, MDA-MB-435, MCF-7, 21PTci, 21NTci and 21MT-1ci, was subjected to bisulfite mutagenesis, and CGI 1 was amplified and cloned into pCR2.1. Multiple clones were sequenced for each cell line. Each square represents a CpG. Each row of squares represents a separate cloned PCR sequence. Vertical columns represent each individual CpG analyzed within CGI 1. Open boxes are unmethylated CpGs and closed boxes are methylated CpGs. Percent methylation (%) is indicated beside each methylation diagram.

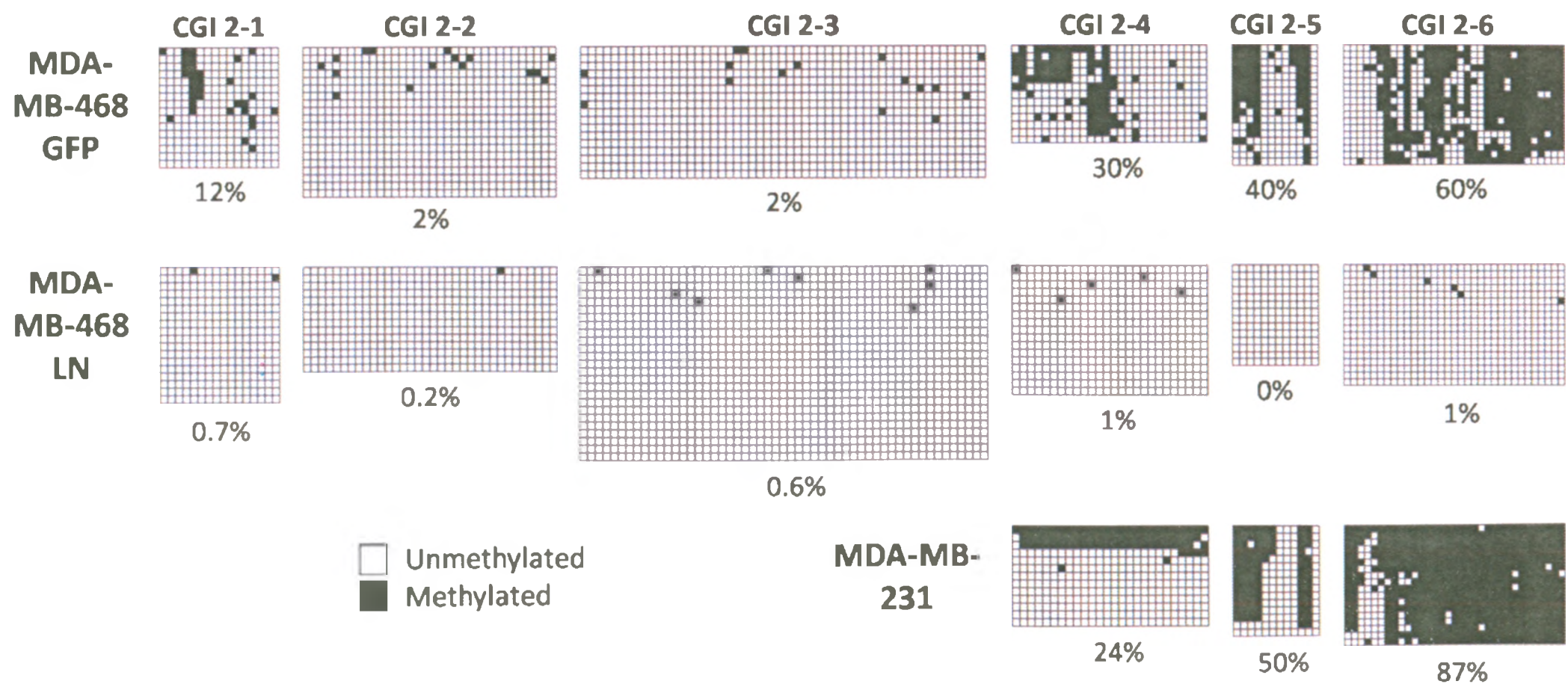
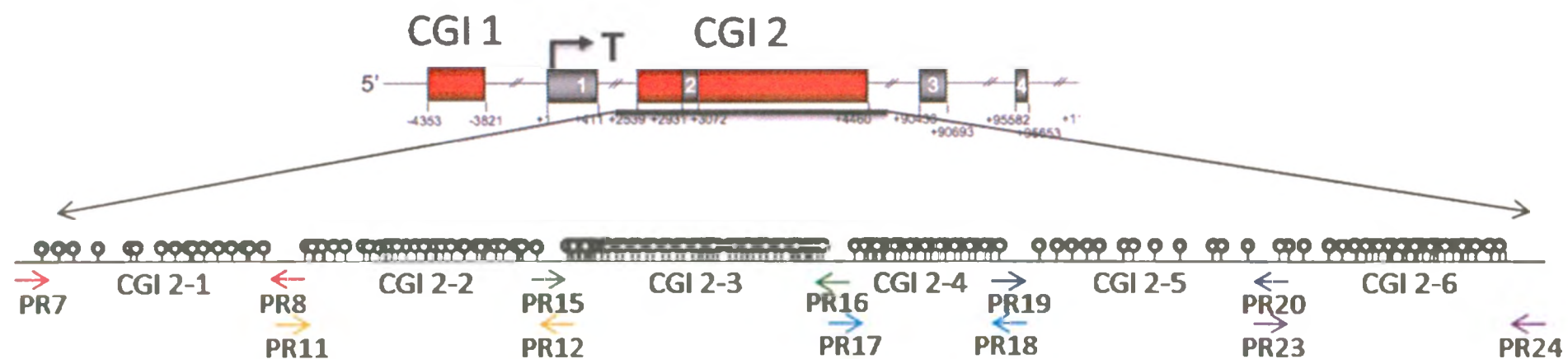


methylation was present in the MDA-MB-468-LN cells and correlated with increased *ZEB2* expression patterns.

Because of this previous work, and the knowledge that CpG islands can be functionally important in the regulation of gene expression, it was important to determine whether *ZEB2* CpG island methylation patterns correlated with *ZEB2* expression patterns in the human cancer cell lines previously tested for *ZEB2* expression (Figure 3.1). Thus, the human breast cancer cell lines, MDA-MB-231, MDA-MB-435, T47D, HCC1806, MCF-7, 21PT, 21NT and 21MT-1 cells, were investigated for methylation at regions surrounding *ZEB2*. First, CGI 1, a region of approximately 527 bp found upstream (-4353 bp to -3821 bp) of the *ZEB2* transcriptional start site, was analyzed to determine its methylation status (Figure 1.6a; Figure 3.3). In MDA-MB-231 cells, this region was almost entirely methylated, whereas this region in MDA-MB-468-GFP, T47D, HCC1806 and MCF-7 cells was highly methylated closer to the 5' end of the CpG island. However, the MDA-MB-468-LN, MDA-MB-435 and 21T series cell lines were mainly hypomethylated at CGI 1. Methylation of a gene promoter is often associated with silencing of the gene. In this particular case, it appeared that cell lines with high levels of *ZEB2* expression (MDA-MB-468-LN, MDA-MB-435, and 21MT-1 cell lines) were hypomethylated, and the majority of cell lines not expressing *ZEB2* (MDA-MB-468-GFP, T47D, HCC1806 and MCF-7) were highly methylated. Therefore, lack of methylation was correlating with increased *ZEB2* expression, especially for those cells with distinctly high or low levels of *ZEB2*. However, there were some discrepancies in this correlation that were mainly seen in cell lines with moderate *ZEB2* expression, such as the MDA-MB-231 and 21NTci cell lines.

Another CpG island (CGI 2) is present within the *ZEB2* gene, downstream of the transcription start site (+2539 bp to +4460 bp). This region, approximately 1922 bp long, spans intron 1, exon 2 and intron 2 (Figure 1.6a). Because it is unknown whether this CpG island plays a role in the regulation of *ZEB2*, it was important to determine the methylation status of this CpG island in multiple cell lines. Therefore, bisulfite mutagenesis and genomic sequencing analysis were performed on DNA from MDA-MB-468-GFP and MDA-MB-468-LN cell lines, for 6 separate regions spanning CGI 2 (CGI 2-1, CGI 2-2, CGI 2-3, CGI 2-4, CGI 2-5 and CGI 2-6) (Figure 3.4). Little difference in methylation patterns were found between the MDA-MB-468-GFP and MDA-MB-468-LN cell lines in the most 5' regions (+2346 bp to + 2522 bp), but differential methylation was seen in regions CGI 2-4 to CGI 2-6. These patterns were consistent with the patterns observed at CGI 1 (Figure 3.3), where the MDA-MB-468-GFP cells had high levels of methylation, and MDA-MB-468-LN cells had very low levels of methylation. Because the MDA-MB-231 cell line expressed *ZEB2*, but was highly methylated at CGI 1, it was important to determine if this discrepancy was also seen at CGI 2. Therefore, the three regions found to be differentially methylated between the MDA-MB-468-GFP and MDA-MB-468-LN cells, CGI 2-4 to CGI 2-6, were also analyzed in the MDA-MB-231 cell line (Figure 3.4). This region was found to be highly methylated in this cell line, which was consistent with the high methylation pattern seen for CGI 1 (Figure 3.3). From these results, it appeared that the methylation status of CGI 1 and CGI 2 were correlated with the expression of *ZEB2* in most cell lines, and that methylation was consistent between these two CpG islands. These CpG islands were hypomethylated, and high

Figure 3.4 CpG island 2 was differentially methylated in human cancer cells. DNA extracted from MDA-MB-468-GFP, MDA-MB-231 and MDA-MB-468-LN cells was subjected to bisulfite mutagenesis, and six regions spanning across CGI 2 (CGI 2-1 to CGI 2-6) were amplified and cloned into pCR2.1. Multiple clones were sequenced for each cell line and each region. Each square represents a CpG. Each row of squares represents a separate cloned PCR sequence. Vertical columns represent each individual CpG analyzed within CGI 2. Open boxes are unmethylated CpGs and closed boxes are methylated CpGs. Percent methylation (%) is indicated below each methylation diagram.

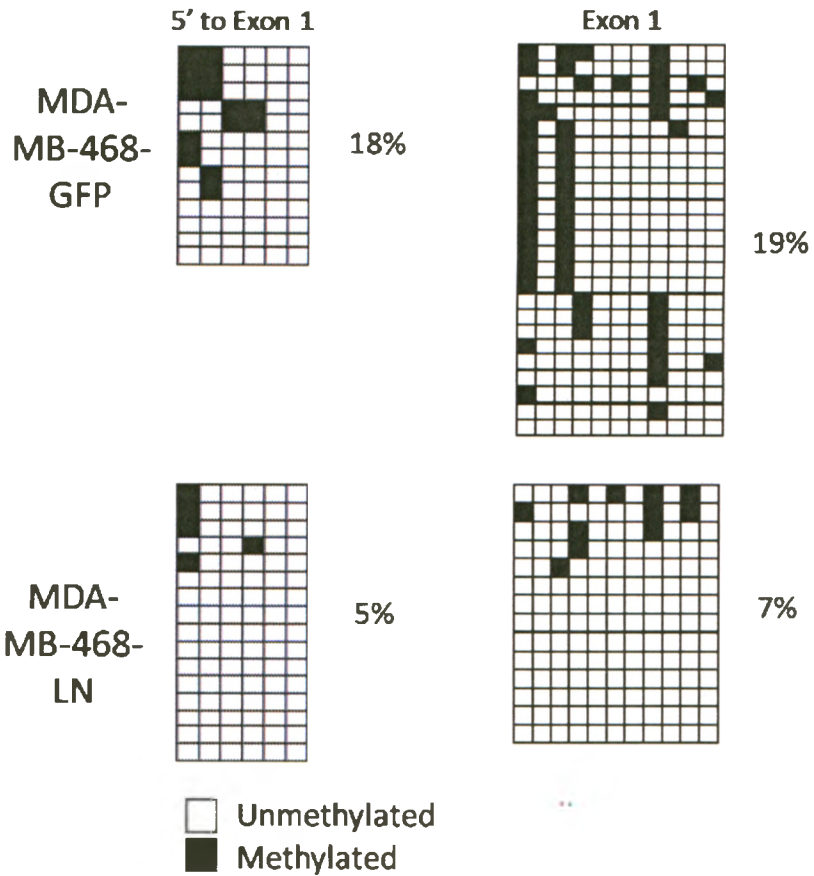
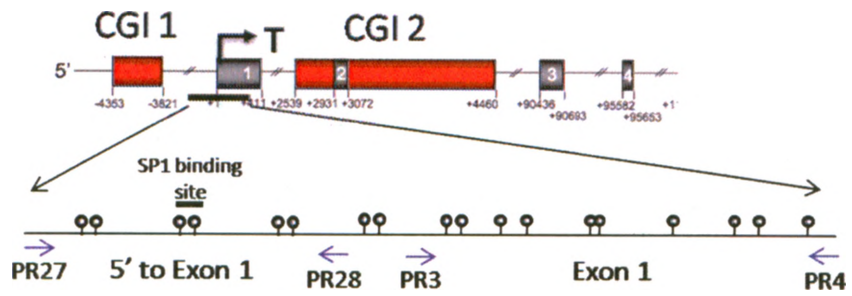


levels of *ZEB2* were observed, in most mesenchymal-like cells (MDA-MB-468-LN, MDA-MB-435 and 21MT-1).

3.4 The *ZEB2* Promoter was Differentially Methylated in the MDA-MB-468-GFP and MDA-MB-468-LN Cell Lines

If methylation is playing a role in the regulation of *ZEB2* expression, differential methylation may be expected at the promoter, between MDA-MB-468-GFP and MDA-MB-468-LN cells. Thus, DNA from these cells were subjected to bisulfite mutagenesis, and the 5' end of this promoter region, 5' to Exon 1 (- 233 bp to -27 bp), was amplified, cloned and sequenced (Figure 3.5). This region was methylated in MDA-MB-468-GFP cells at four of the 6 CpG sites in some of the clones analyzed, mainly at the most 5' CpG sites in this region, while the MDA-MB-468-LN cell line was unmethylated at most CpG sites. Thus, it appeared that this region of the promoter was differentially methylated between these two cell lines. A portion of Exon 1(+13 bp to +256 bp), within this putative promoter, was analyzed for its methylation status in the MDA-MB-468-GFP and MDA-MB-468-LN cell lines. Both cell lines had very low levels of methylation in this region, although there was greater methylation at this region in the MDA-MB-468-GFP cells (Figure 3.5), similar to that seen for the region 5' to Exon 1 (Figure 3.5). Thus, differential methylation of this putative promoter was seen between MDA-MB-468-GFP and MDA-MB-468-LN cells, similar to that seen for CpG island 1 and CpG island 2. The low levels of methylation in the putative promoter of MDA-MB-468-LN cells further suggests a correlation with the increased *ZEB2* expression observed, supporting the notion that DNA methylation may play a role in the regulation of *ZEB2*.

Figure 3.5 The *ZEB2* promoter was differentially methylated in MDA-MB-468-GFP and MDA-MB-468-LN cells. DNA extracted from MDA-MB-468-GFP and MDA-MB-468-LN cells was subjected to bisulfite mutagenesis and region 5' to Exon 1, and Exon 1, were amplified and cloned into pCR2.1. Multiple clones were sequenced for each cell line. Each square represents a CpG. Each row of squares represents a separate cloned PCR sequence. Vertical columns represent each individual CpG analyzed within CpG island 1. Open boxes are unmethylated CpGs and closed boxes are methylated CpGs. The SP1 putative binding site is demonstrated with a solid black line. Percent methylation (%) is indicated beside each methylation diagram.



3.5 *ZEB2* Expression and CpG Island 1 Methylation were Similar in 2D and 3D

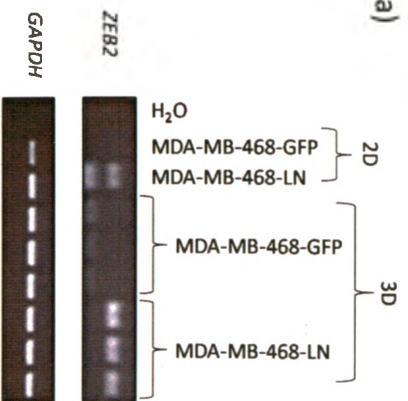
Culture

The previous analyses of *ZEB2* expression and methylation analyses of multiple genomic regions were performed on cells grown in 2D culture. However, the behaviour of cells in an artificial, *in vitro* system was not necessarily reflective of the behaviour of cells *in vivo*. Ultimately, it was critical to understand the importance of methylation in the regulation of *ZEB2* in the context of the clinic. Therefore, it was crucial to determine how physiologically relevant these expression and methylation correlation findings were. Thus, the MDA-MB-468-GFP and MDA-MB-468-LN cell lines were grown in 3D Matrigel, a system that has been shown previously to mimic certain aspects of the physiology of the breast (Petersen et al., 1992; Weaver and Bissell, 1999). Cells were grown in Matrigel for 9 days and cell recovery solution was used to harvest cells from the matrix. Once harvested, RNA and DNA were extracted. RT-PCR was performed to determine the expression of *ZEB2* in cells grown in 3D Matrigel compared with cells grown on 2D tissue culture plastic (Figure 3.6a). It was observed that in both 2D and 3D cultures, the MDA-MB-468-GFP cells did not express *ZEB2*, whereas the MDA-MB-468-LN cells had high levels of *ZEB2* expression.

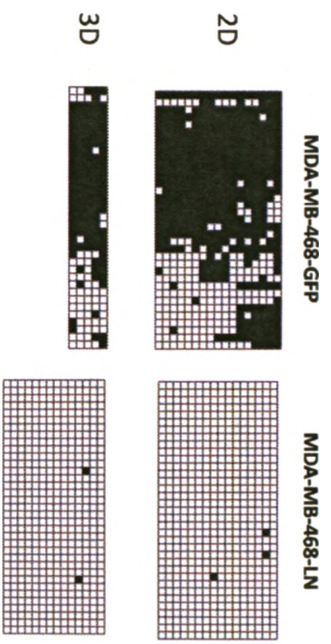
To determine whether methylation patterns were similar in cells grown in 2D and 3D culture, bisulfite genomic analysis was performed on DNA extracted from MDA-MB-468-GFP and MDA-MB-468-LN cell lines grown in 2D culture or 3D Matrigel (Figure 3.6b). It was found that in 3D Matrigel, the MDA-MB-468-GFP cells were highly methylated at CGI 1, and the MDA-MB-468-LN cells were hypomethylated at CGI 1, which was consistent with what was observed in these cells when grown in 2D culture.

Figure 3.6 No differences in *ZEB2* expression or CpG island 1 methylation were observed in cells grown in 2D and 3D culture. MDA-MB-468-GFP and MDA-MB-468-LN cells were grown in 2D culture and in 3D Matrigel. Cells were harvested, and RNA and DNA were extracted. a) RT-PCR was performed to determine the levels of *ZEB2* expression. Water and *GAPDH* are shown as negative and positive controls, respectively. b) Bisulfite mutagenesis and sequencing analysis of CpG island 1 was performed with DNA from cells grown in both 2D and 3D culture. Cells were grown in triplicate in 3D Matrigel wells, and PCRs were performed for each triplicate. Multiple clones were sequenced for each cell line. Each square represents a CpG. Each row of squares represents a separate cloned PCR sequence. Vertical columns represent each individual CpG analyzed within CpG island 1. Open boxes are unmethylated CpGs and closed boxes are methylated CpGs.

a)



b) CGI 1



These results suggest that the expression and methylation analysis of *ZEB2* in 2D culture may be representative of *in vivo* data.

3.6 *ZEB2* Methylation was Resistant to Demethylation by 5-Aza and TSA Treatment in MDA-MB-468-GFP Cells

The methylation pattern of two CpG islands and the putative *ZEB2* promoter correlated with the expression of *ZEB2* in multiple cancer cell lines. To determine whether DNA methylation is a cause or consequence of *ZEB2* repression, the methylation of these DNA regions was manipulated through the use of the demethylating agent 5-aza-2'-deoxycytidine. There are many demethylating drugs that are currently available, for both clinical and experimental use. 5-aza-2'-deoxycytidine (5-aza), which is a cytosine analogue, is the most frequently used drug for experimental purposes. 5-aza is incorporated into DNA, where it covalently binds to DNA methyltransferases and inhibits their catalytic ability to copy methylation patterns during replication (Gabbara and Bhagwat, 1995; Santi et al., 1984). In addition, Trichostatin A (TSA), a deacetylase inhibitor, inhibits the ability of deacetylases to remove acetyl groups from histones, causing chromatin to remain in an open conformation (Yoshida et al., 1990). TSA can often act synergistically with 5-aza to allow maximal re-expression of silent genes (Chiurazzi et al., 1999; Meng et al., 2007; Veeck et al., 2008; Zhang et al., 2005). To understand whether DNA methylation and histone acetylation play a functional role in the regulation of *ZEB2*, 5-aza and TSA were used to reduce DNA methylation patterns in the MDA-MB-468-GFP cell line, which has high levels of CpG island methylation and *ZEB2* putative promoter methylation and very low levels of *ZEB2* expression. By

removing DNA methylation from these highly methylated regions then analyzing changes in *ZEB2* expression, it may be possible to determine whether DNA methylation plays a causal role in regulating the expression of this gene. To this end, MDA-MB-468-GFP cells were either treated with no drug, or 1, 2, 5 or 10 μM 5-aza-2'-deoxycytidine for 3 days. TSA (0.3 μM) was added for the last 24 hours of the 5-aza treatment. To analyze morphological changes between control cells and cells treated with 5-aza and TSA, and to ensure cells were proliferating, brightfield images of cells were taken before 5-aza treatment, 48 hours after 5-aza treatment (before TSA treatment), and before harvesting (72 hours after 5-aza treatment, 24 hours after TSA treatment) (Figure 3.7). No differences in morphology were observed between cells treated with 5-aza and TSA and control cells. MDA-MB-468-GFP cells were able to proliferate in the absence of drug, or in 1 μM and 2 μM 5-aza + TSA, however, 5 μM and 10 μM 5-aza drug treatments resulted in cell death.

To determine the effect of 5-aza and TSA treatment on *ZEB2* expression, RT-PCR was performed (Figure 3.8). No changes in *ZEB2* expression were observed. From this, it was evident that *ZEB2* expression was resistant to demethylation under these drug conditions. As a control, to ensure the drugs were active, and the cells were able to respond to the drugs, I analyzed the expression of *DKK3*, a WNT5a inhibitor. *DKK3* expression has been shown in the literature to be reactivated after 1 μM 5-aza and 0.3 μM TSA treatment in MCF-7 cells (Veeck et al., 2008). Therefore, *DKK3* expression

Figure 3.7 MDA-MB-468-GFP cells were proliferating during some 5-aza-2'deoxyctidine and Trichostatin A treatment conditions. MDA-MB-468-GFP cells were plated at a density of 7.1×10^3 cells/cm² on day 0. Fresh 5-aza-2'deoxyctidine (1, 2, 5 and 10 μ M) was added on day 1, 2 and 3, with the addition of Trichostatin A for the last 24 hours, and cells were harvested on day 4. Brightfield images of cells were obtained before treatment (0 days), and 2 days and 3 days after drug treatment. White bars represent 100 μ m.

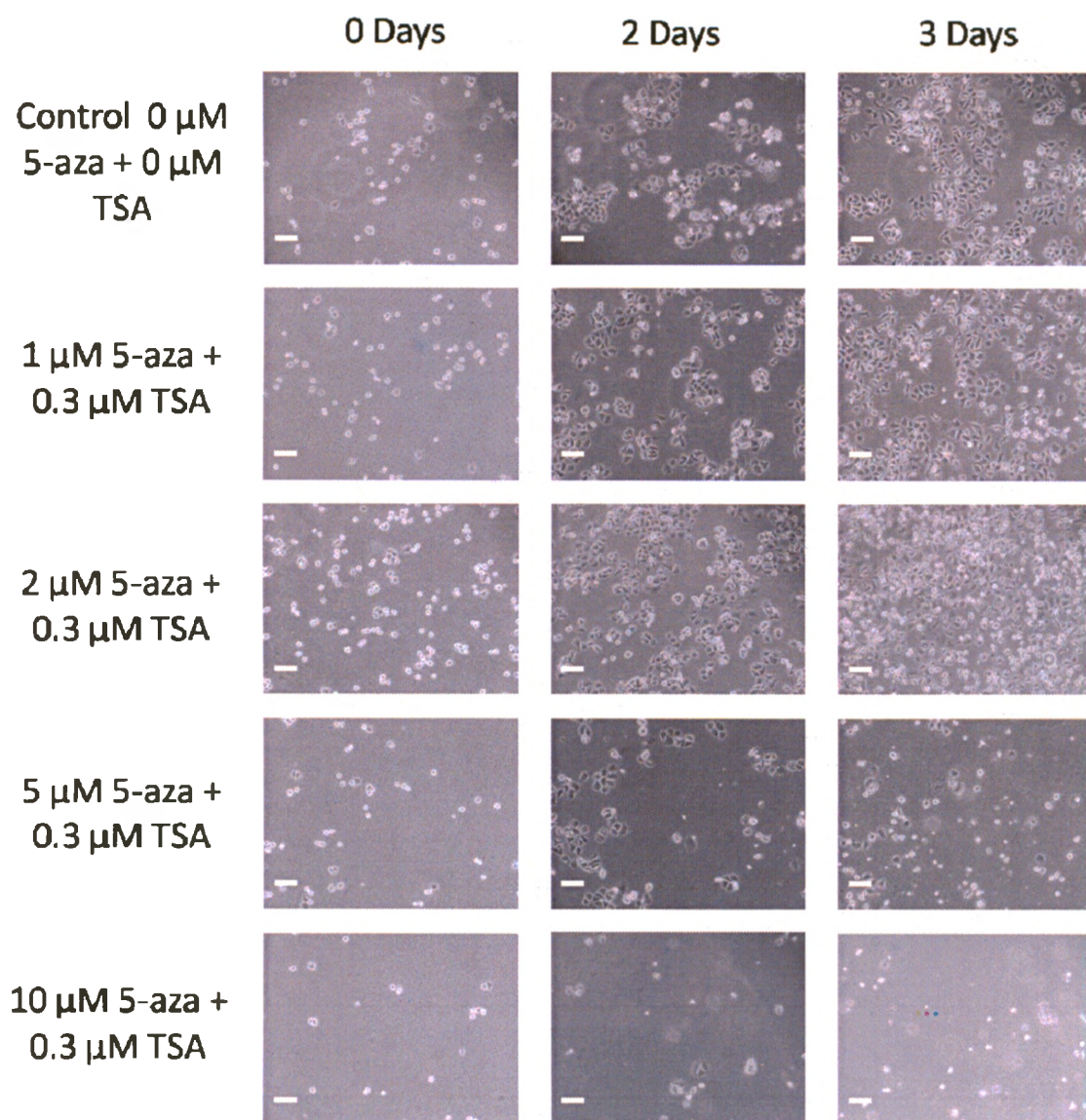
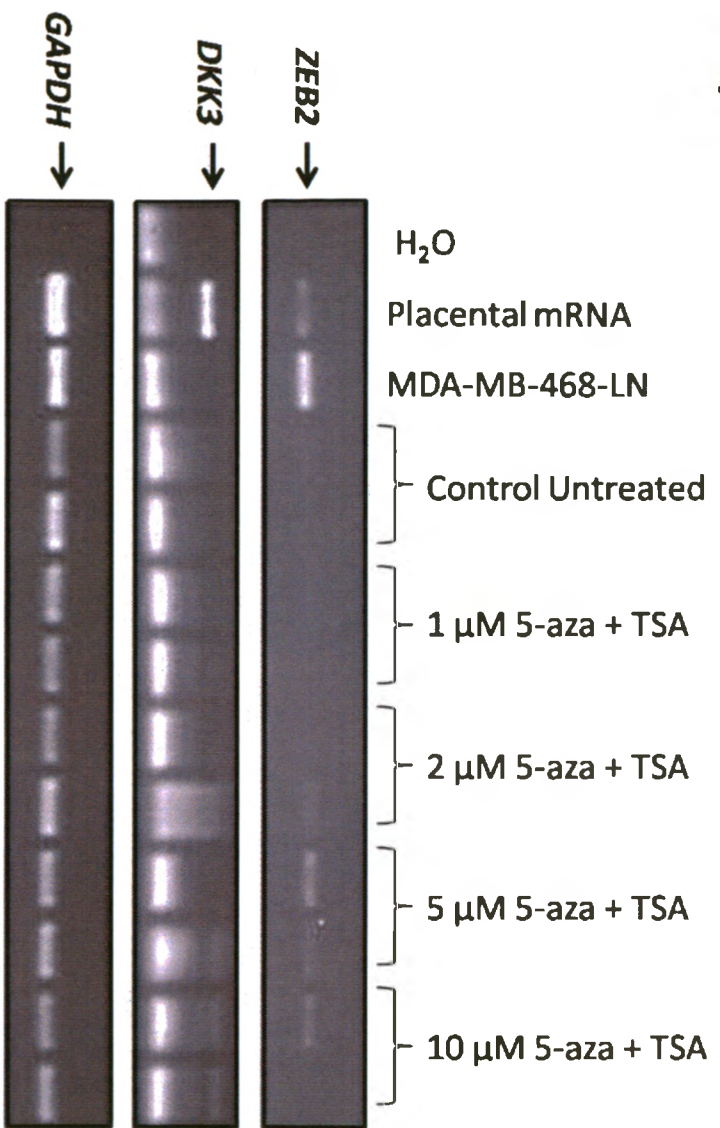
MDA-MB-468-GFP**3 Days**

Figure 3.8 5-aza-2'deoxyctidine and Trichostatin A treatment did not alter the expression of *ZEB2* in MDA-MB-468-GFP cells. MDA-MB-468-GFP cells were plated at a density of 7.1×10^3 cells/cm² on day 0. Fresh 5-aza-2'deoxyctidine (1, 2, 5 and 10 μ M) was added on day 1, 2 and 3, with the addition of Trichostatin A for the last 24 hours of culture, and cells were harvested on day 4. Levels of *ZEB2* expression were analyzed by RT-PCR. The expression of *DKK3* was shown as a positive control for 5-aza treatment. Placental cDNA was used as a positive control for *DKK3* expression. MDA-MB-468-LN cDNA was used as a positive control for *ZEB2* expression. Water was used as a no template control. The expression of *GAPDH* is shown as a positive control.



MDA-MB-468-GFP
3 Days

was analyzed by RT-PCR in both control and 5-aza and TSA treated cells (Figure 3.8). *DKK3* expression was not reactivated under any drug conditions tested. This suggests that 5-aza and TSA may not have been active, or that the MDA-MB-468-GFP cell line was not responsive, or resistant, to these drugs. The expression of *GAPDH* was used as a positive control for the cDNA synthesis and to ensure equal mRNA was used in each reaction.

To optimize the duration of 5-aza treatment necessary to induce demethylation of *ZEB2*, these experiments were also performed over 5 and 7 days. Again, MDA-MB-468-GFP cells were grown in 2D culture, and were either treated with no drug, or 1, 2, 5 or 10 μM 5-aza for 5 or 7 days. TSA (0.3 μM) was added for the last 24 hours of 5-aza treatment. To analyze morphological differences between control cells and cells treated with 5-aza and TSA, and to ensure cells were proliferating, brightfield images of cells were taken after 2, 3, 5 or 7 days of drug treatment, depending on the length of the experiment (Figure 3.9 and Figure 3.10). Again, no changes in morphology were apparent at any time or dose. MDA-MB-468-GFP cells were able to proliferate when untreated, or treated with 1 μM and 2 μM 5-aza + TSA. However, 5 μM and 10 μM 5-aza treatments were toxic to the cells in these prolonged experiments, as expected. In order to determine the effect of 5-aza and TSA treatment on *ZEB2* expression, RT-PCR was performed on all control cells, and cells treated with 5-aza and TSA (Figure 3.11). The expression of *ZEB2* was unaltered by these drug treatments. From these experiments, it was evident that prolonged 5-aza and TSA exposure did not alter the expression of *ZEB2*.

Figure 3.9 MDA-MB-468-GFP cells were proliferating during some 5 day 5-aza-2'deoxyctidine and Trichostatin A treatment conditions. MDA-MB-468-GFP cells were plated at a density of 7.1×10^3 cells/cm² on day 0. Fresh 5-aza-2'deoxyctidine (1, 2, 5 and 10 μ M) was added on day 1, 2, 3, 4 and 5, with the addition of Trichostatin A for the last 24 hours of culture, and cells were harvested on day 6. Brightfield images of cells after 2, 3 and 5 days of drug treatment are shown. White bars represent 100 μ m.

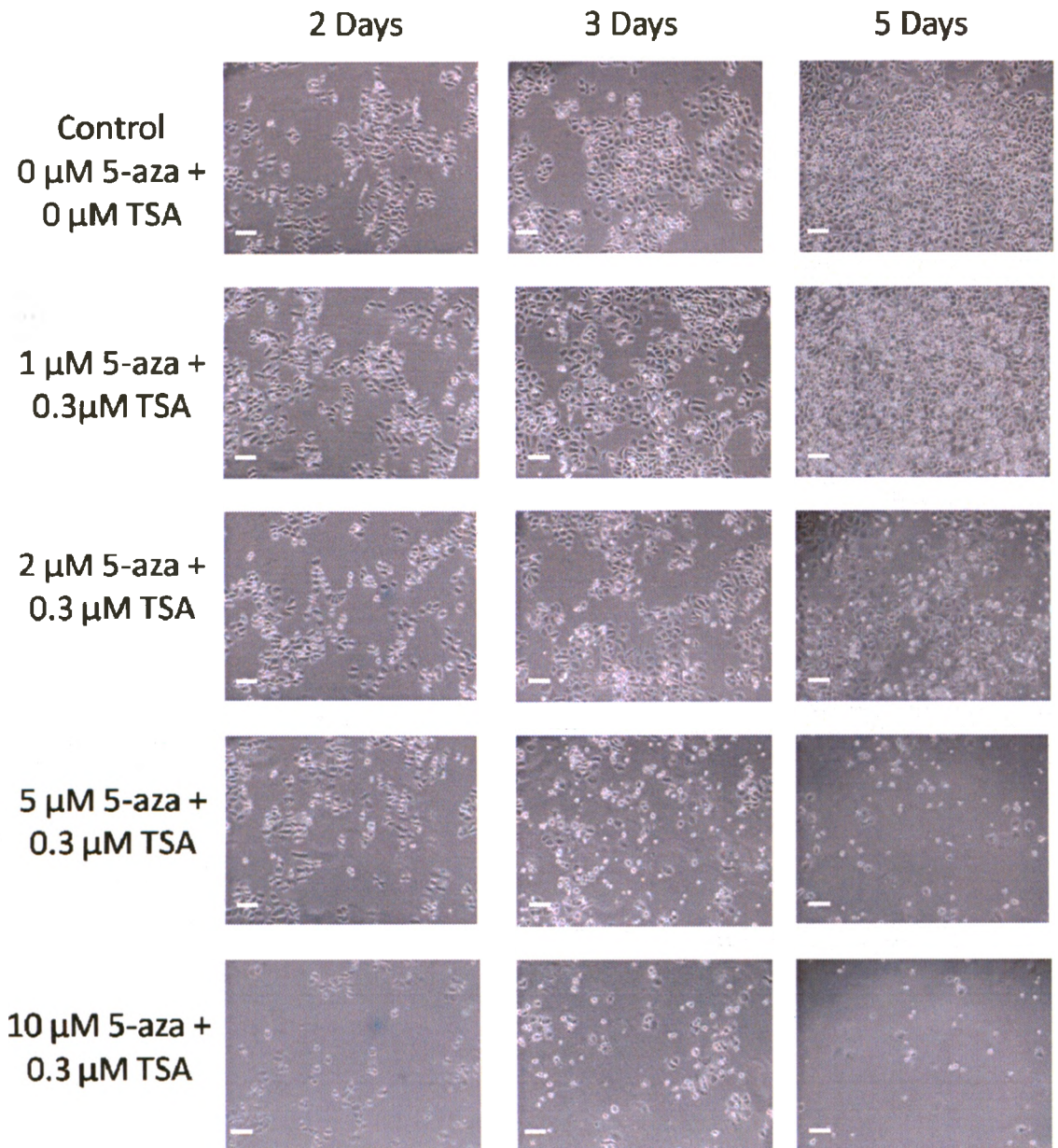
MDA-MB-468-GFP**5 Days**

Figure 3.10 MDA-MB-468-GFP cells were proliferating during some 7 day 5-aza-2'deoxyctidine and Trichostatin A treatment conditions. MDA-MB-468-GFP cells were plated at a density of 7.1×10^3 cells/cm² on day 0. Fresh 5-aza-2'deoxyctidine (1, 2, 5 and 10 μ M) was added on day 1, 2, 3, 4, 5, 6 and 7 with the addition of Trichostatin A for the last 24 hours of culture, and cells were harvested on day 8. Brightfield images of cells were obtained after 2, 3, 5 and 7 days of drug treatment. White bars represent 100 μ m.

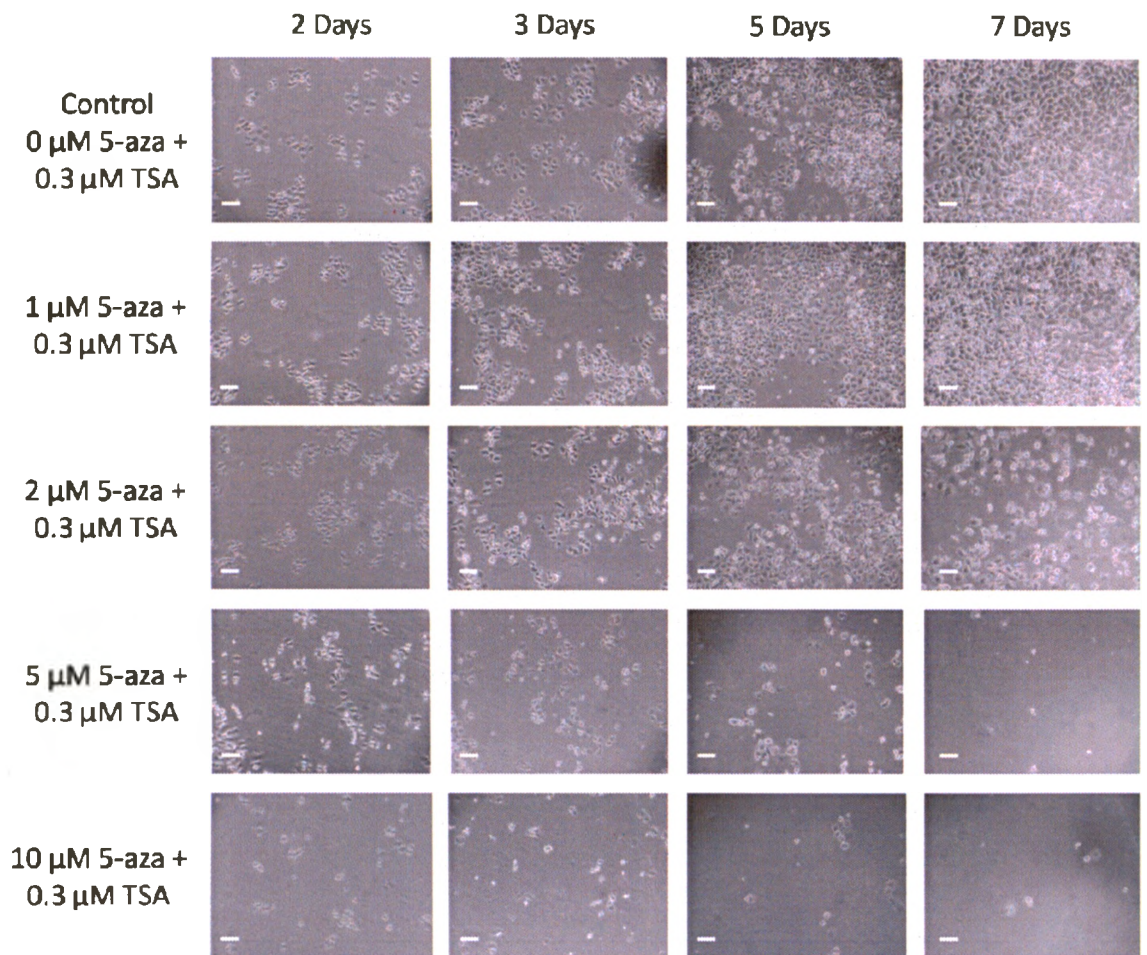
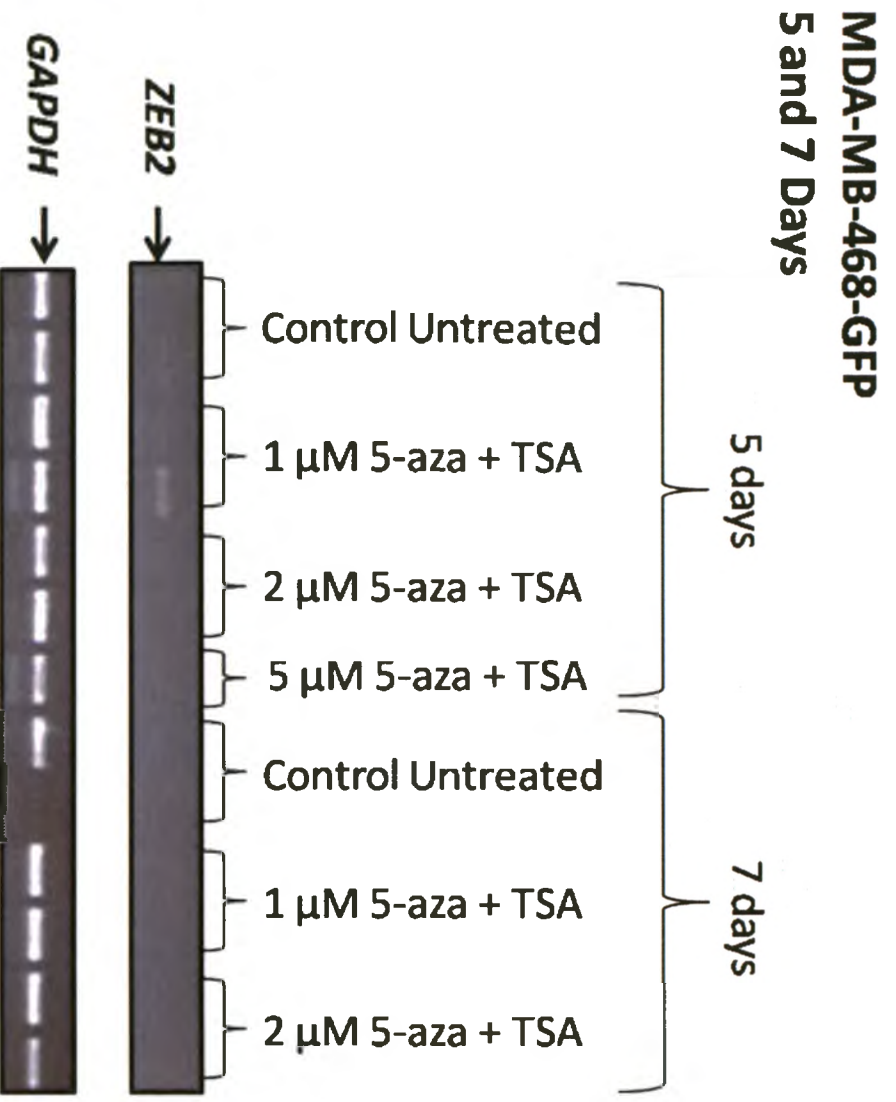
MDA-MB-468-GFP**7 Days**

Figure 3.11 5-aza-2'deoxyctidine and Trichostatin A treatment for 5 and 7 days did not alter expression of *ZEB2* in MDA-MB-468-GFP cells. MDA-MB-468-GFP cells were plated at a density of 7.1×10^3 cells/cm² on day 0. Fresh 5-aza-2'deoxyctidine (1, 2, 5 and 10 μ M) was added on day 1, 2, 3, 4, 5, (as well as day 6 and 7) with the addition of Trichostatin A for the last 24 hours of culture, and cells were harvested on day 6 (or 8 for 7 day drug treatment). Levels of *ZEB2* expression were analyzed by RT-PCR. MDA-MB-468-LN cDNA was used as a positive control for *ZEB2* expression (data not shown). Water was used as a no template control (data not shown). The expression of *GAPDH* was used as a positive control.



To confirm the effectiveness of 5-aza treatments, I also determined whether any genomic regions that I had previously analyzed were demethylated. Bisulfite genomic analysis was performed on DNA extracted from non-treated and treated cells, for CGI 1 (Figure 3.12), the most 3' region of CGI 2 (CGI 2-6) (Figure 3.13) and 5' to Exon 1 (Figure 3.14).

During analysis of CGI 1 methylation, non-specific amplification of another DNA sequence occurred, so my methods had to be modified. As well, new primers were designed to amplify a region similar to the region previously analyzed. This new primer set amplified a region that contains 37 CpG sites, 33 of which were analyzed with the original primers. No differences in *ZEB2* methylation were observed at these regions between untreated and treated groups in any of the regions analyzed. It appears that *ZEB2* is resistant to DNA methylation manipulations through the use of 5-aza and TSA at these regions analyzed, under the conditions tested.

3.7 *ZEB2* Methylation was Resistant to Demethylation by 5-Aza and TSA Treatment in MCF-7 Cells

From the previous experiments, it appeared that *ZEB2* was resistant to DNA methylation manipulation in MDA-MB-468-GFP cells. To understand whether this was a phenomenon specific to the MDA-MB-468-GFP cells, the three day 5-aza experiments were repeated with the MCF-7 cell line. This cell line had a high level of CGI 1 methylation and very low *ZEB2* expression, similar to that of the MDA-MB-468-GFP cells. As well, this cell line has been used for many 5-aza experiments previously (Rivenbark et al., 2006; Sadikovic et al., 2004; Veeck et al., 2008; Veeck et al., 2006; Zhang et al., 2005). Thus, not only is this cell line a good candidate cell line for our

Figure 3.12 MDA-MB-468-GFP cells were resistant to demethylation of CpG island 1 by 5-aza-2'deoxycytidine and Trichostatin A. MDA-MB-468-GFP cells were plated at a density of 7.1×10^3 cells/cm² on day 0. Fresh 5-aza-2'deoxycytidine (1, 2, 5 and 10 μ M) was added on day 1, 2 and 3, with the addition of Trichostatin A for the last 24 hours of culture, and cells were harvested on day 4, 6 or 8. Methylation of CGI 1 was analyzed by the bisulfite mutagenesis and sequencing assay with DNA from cells grown for 3 days with either no drug (control) or 1 μ M, 2 μ M, 5 μ M or 10 μ M 5-aza + TSA drug treatment, as well as cells grown for 5 and 7 days with no drug (control) or 2 μ M 5-aza + TSA treatment. The methylation status of the untreated MDA-MB-468-GFP cells during the 5 day experiment was analyzed using the same CGI 1 primers used in Figure 3.2 (PR1 and PR2; Table 2.1). However, the methylation status of CGI 1 after all other treatment conditions was tested with the second set of CGI 1 primers (PR31 and PR32; Table 2.1), and therefore different CpGs were analyzed.

**MDA-MB-468-GFP
CGI 1**

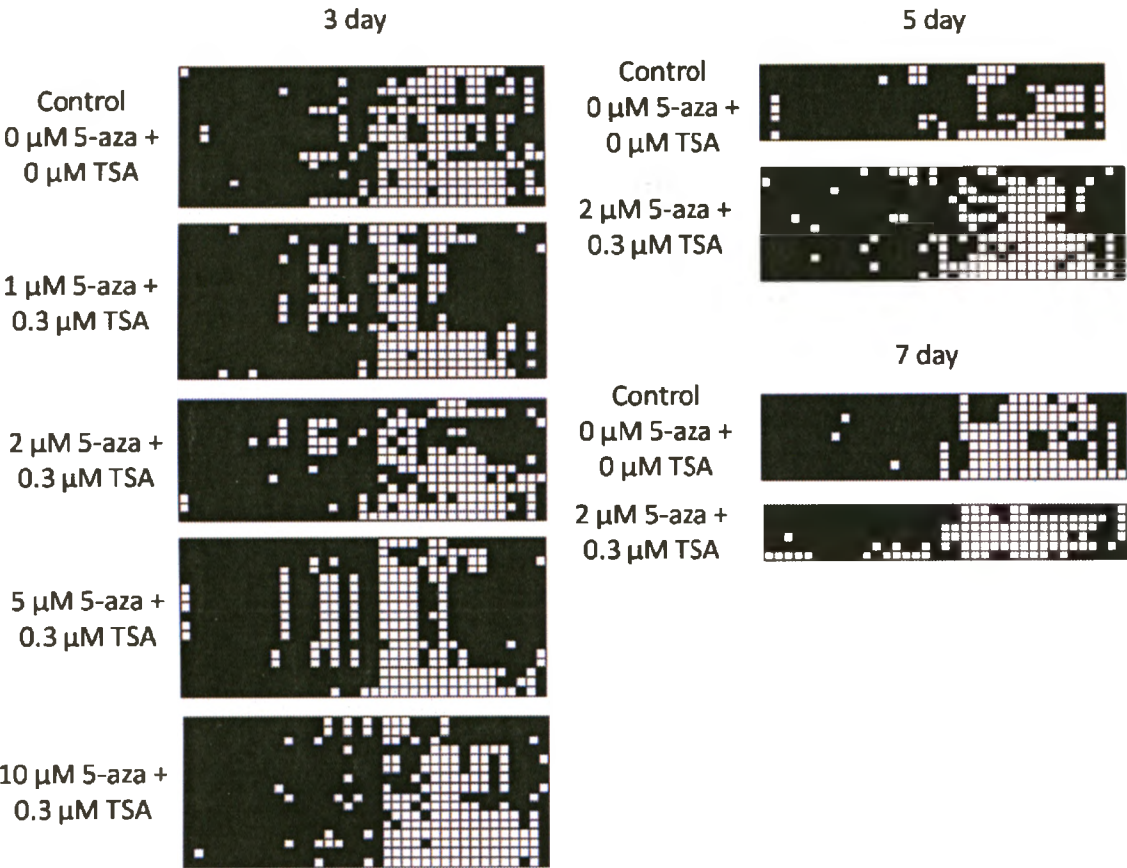


Figure 3.13 MDA-MB-468-GFP cells were resistant to demethylation of CpG island 2 by 5-aza-2'deoxyctidine and Trichostatin A. MDA-MB-468-GFP cells were plated at a density of 7.1×10^3 cells/cm² on day 0. Fresh 5-aza-2'deoxyctidine (1, 2, 5 and 10 μ M) was added on day 1, 2 and 3, with the addition of Trichostatin A for the last 24 hours of culture, and cells were harvested on day 4, 6 or 8. Bisulfite mutagenesis and sequencing of CGI 2-6 was performed with DNA extracted from cells grown for 3 days with either no drug (control) or 1 μ M, 2 μ M, 5 μ M or 10 μ M 5-aza + TSA drug treatment, as well as cells grown for 5 and 7 days with no drug (control) or 2 μ M 5-aza + TSA treatment.

**MDA-MB-468-GFP
CGI 2-6**

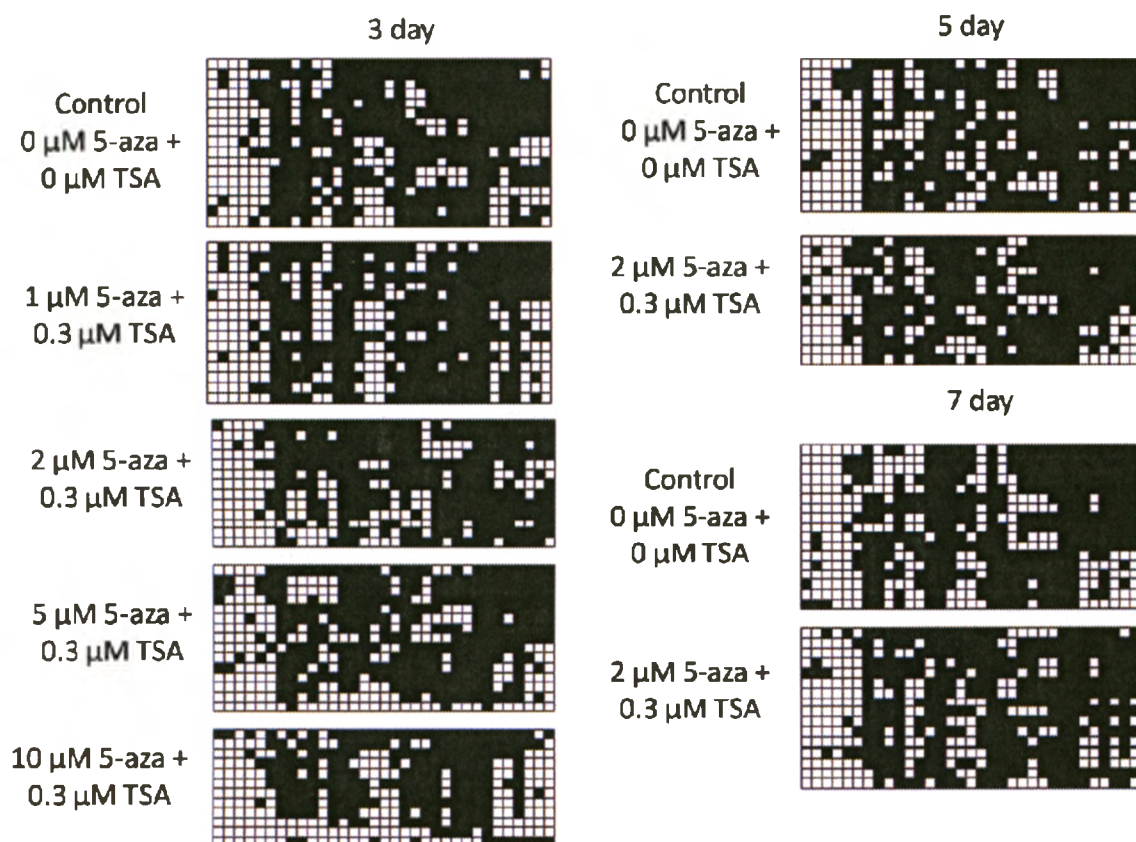


Figure 3.14 MDA-MB-468-GFP cells were resistant to demethylation of 5' to Exon 1 by 5-aza-2'deoxyctidine and Trichostatin A. MDA-MB-468-GFP cells were plated at a density of 7.1×10^3 cells/cm² on day 0. Fresh 5-aza-2'deoxyctidine (1, 2, 5 and 10 μ M) was added on day 1, 2 and 3, with the addition of Trichostatin A for the last 24 hours of culture, and cells were harvested on day 4, 6 or 8. Bisulfite mutagenesis and amplification and cloning of a subregion of 5' Exon 1 was performed with DNA extracted from cells grown for 3 days with either no drug (control) or 1 μ M, 2 μ M, 5 μ M or 10 μ M 5-aza + TSA drug treatment.

MDA-MB-468-GFP
5' to Exon 1

Control
0 μM 5-aza +
0 μM TSA



1 μM 5-aza +
0.3 μM TSA



2 μM 5-aza +
0.3 μM TSA



5 μM 5-aza +
0.3 μM TSA



10 μM 5-aza +
0.3 μM TSA



experiments, but alterations in expression of other genes shown in the literature after 5-aza treatment could be used as a positive control, to analyze the effectiveness of these 5-aza treatments. MCF-7 cells were treated with no drug, or 1, 2, 5 or 10 μM 5-aza-2'deoxyctidine for 3 days. TSA (0.3 μM) was added for the last 24 hours of 5-aza treatment. To determine morphological changes between control and 5-aza and TSA treated cells, and to ensure cells were proliferating, brightfield images of cells were taken before 5-aza treatment, 48 hours after 5-aza treatment (before TSA treatment), and 72 hours after 5-aza treatment (24 hours after TSA treatment) (Figure 3.15.). MCF-7 cells appeared more elongated in shape after TSA treatment and were able to proliferate when treated with no drug, 1 μM , 2 μM , 5 μM and 10 μM 5-aza + TSA with seemingly low toxicities. To determine the effect of 5-aza and TSA treatment on *ZEB2* expression, RT-PCR was performed on all control cells, and cells treated with 5-aza and TSA (Figure 3.16). Activation of *ZEB2* was seen after 1 μM 5-aza + TSA treatment, but no alteration in *ZEB2* expression was seen under any other condition. As a control, the expression of *DKK3* shown in the literature to be expressed after 1 μM 5-aza and 0.3 μM TSA treatment in MCF-7 cells (Veeck et al., 2008) was analyzed by RT-PCR on all control cells, and cells treated with 5-aza and TSA (Figure 3.16). *DKK3* expression was increased in cells treated with all 5-aza conditions, as expected. This indicates that the 5-aza drug was active and was capable of inducing the expression of at least one gene. The expression of *GAPDH* was used as a positive control. Thus, it appears that 5-aza was able to alter the expression of *ZEB2*, but only under a subset of the conditions tested, all of which additionally resulted in the activation of *DKK3*.

Figure 3.15 MCF-7 cells were proliferating during 5-aza-2'deoxycytidine and Trichostatin A treatment. MCF-7 cells were plated at a density of 2.1×10^4 cells/cm² on day 0. Fresh 5-aza-2'deoxycytidine (1, 2, 5 and 10 μ M) was added on day 1, 2, and 3, with the addition of Trichostatin A for the last 24 hours, and cells were harvested on day 4. Brightfield images of cells were obtained before treatment (0 days), and 2 days and 3 days after drug treatment. White bars represent 100 μ m.

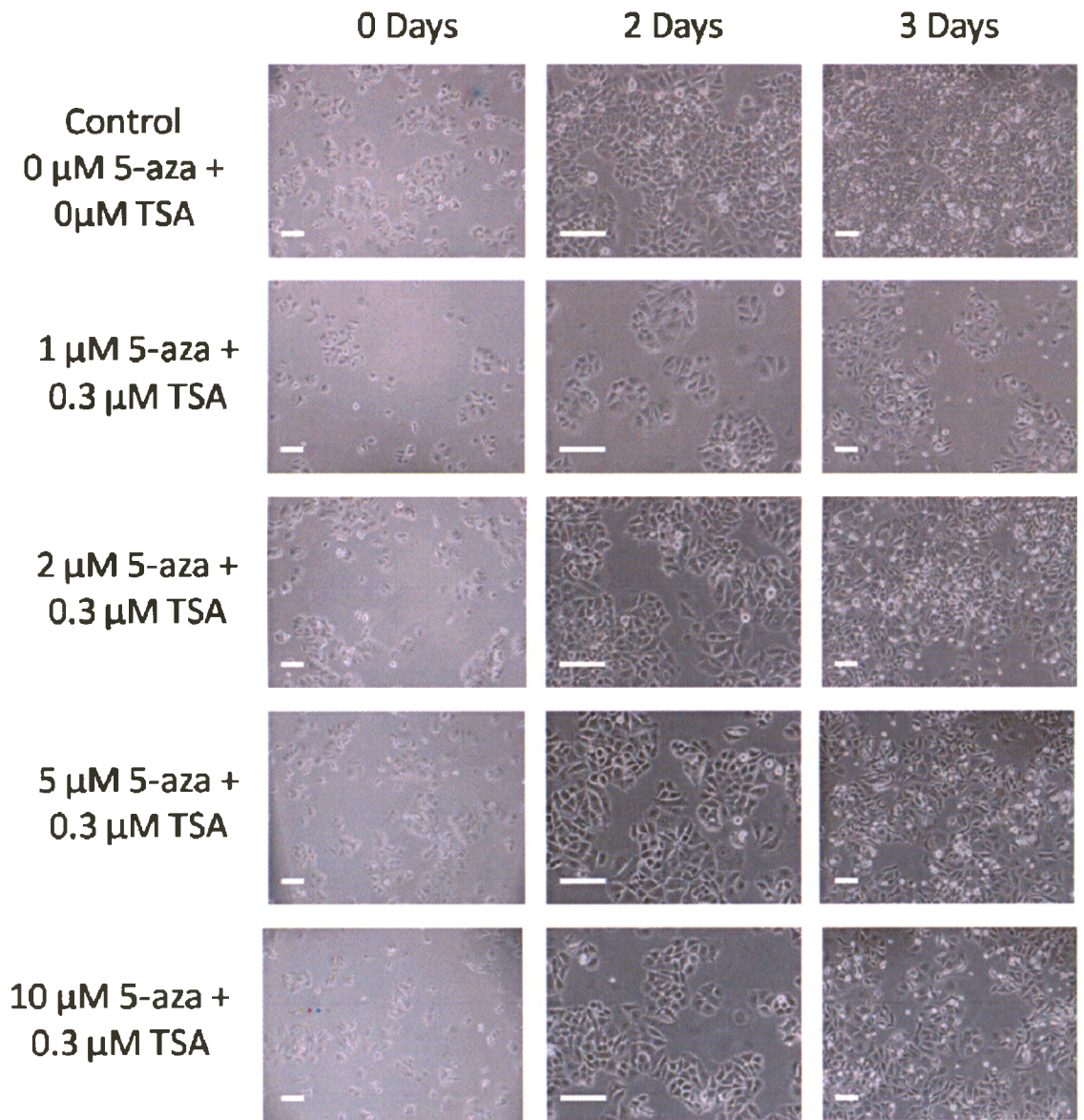
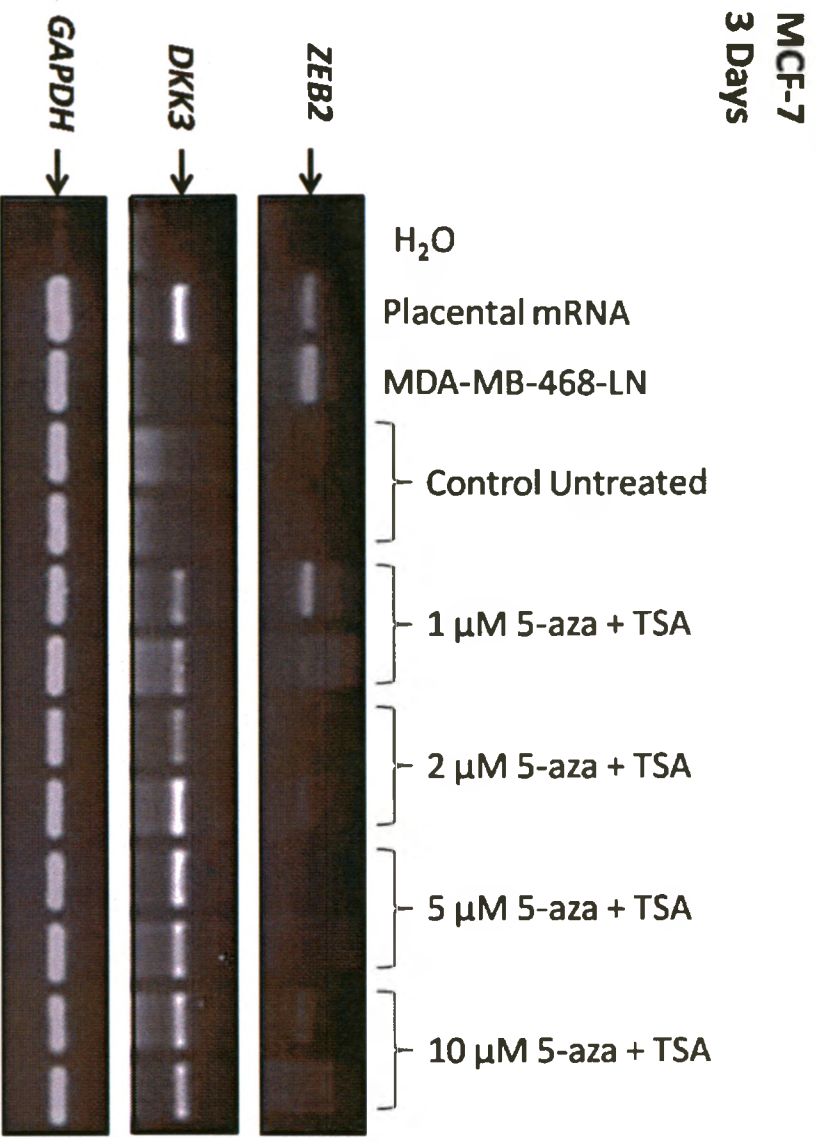
**MCF-7
3 Days**

Figure 3.16 Specific 5-aza-2'deoxyctidine and Trichostatin A treatment altered the expression of *ZEB2* in MCF-7 cells. MCF-7 cells were plated at a density of 2.1×10^4 cells/cm² on day 0. Fresh 5-aza-2'deoxyctidine (1, 2, 5 and 10 μ M) was added on day 1, 2 and 3, with the addition of Trichostatin A for the last 24 hours of culture, and cells were harvested on day 4. Levels of *ZEB2* expression was analyzed by RT-PCR. The expression of *DKK3* was shown as a positive control for 5-aza treatment. Placental cDNA was used as a positive control for *DKK3* expression. MDA-MB-468-LN cDNA was used as a positive control for *ZEB2* expression. Water was used as a no template control. The expression of *GAPDH* is shown as a positive control.



I also determined whether 5-aza treatment was able to demethylate genomic regions that may be important in the regulation of *ZEB2* in MCF-7 cells. To this end, DNA was extracted from both untreated and treated MCF-7 cells, and bisulfite mutagenesis and sequencing was performed to analyze the methylation status of three regions of the *ZEB2* gene: CGI 1 (Figure 3.17), CGI 2 (Figure 3.18) and 5' to Exon 1 (Figure 3.19). Treatment of MCF-7 cells with 1 and 2 μM 5-aza did result in a decrease in methylation at CGI 1 and CGI 2 in a subset of MCF-7 cells, but no demethylation was observed in these regions in any other drug treatment groups. The methylation of the region 5' to Exon 1 was not altered by 5-aza and TSA treatment. In summary, utilization of a DNA methylation inhibitor and a deacetylase inhibitor showed some involvement of methylation in the regulation of *ZEB2* expression. However, it is still not clear whether DNA methylation and deacetylation are a cause of *ZEB2* repression, or a consequence of *ZEB2* silencing.

3.8 *In Vitro* Methylation of hPr Diminished Promoter Activity

Experiments with 5-aza and TSA were carried out to gain a better understanding of whether *ZEB2* DNA methylation was a cause or consequence of altered *ZEB2* expression. However, the experiments were inconclusive, and thus another approach was used. I had previously shown that the regions corresponding to the promoter of *ZEB2* were differentially methylated in the MDA-MB-468-GFP and MDA-MB-468-LN cells, indicating that methylation of this region may contribute to the regulation of *ZEB2* expression. To further determine the role of methylation of this region, I manipulated the methylation of this region *in vitro*. To this end, the reporter vectors pGL3 and pGL3-hPr

Figure 3.17 MCF-7 cells were partially resistant to demethylation of CpG island 1 by 5-aza-2'deoxyctidine and Trichostatin A. MCF-7 cells were plated at a density of 2.1×10^4 cells/cm² on day 0. Fresh 5-aza-2'deoxyctidine (1, 2, 5 and 10 μ M) was added on day 1, 2 and 3, with the addition of Trichostatin A for the last 24 hours of culture, and cells were harvested on day 4. Methylation of CGI 1 was analyzed by bisulfite mutagenesis and sequencing of CGI 1, with DNA from cells grown with either no drug (control) or 1 μ M, 2 μ M, 5 μ M or 10 μ M 5-aza + TSA drug treatment.

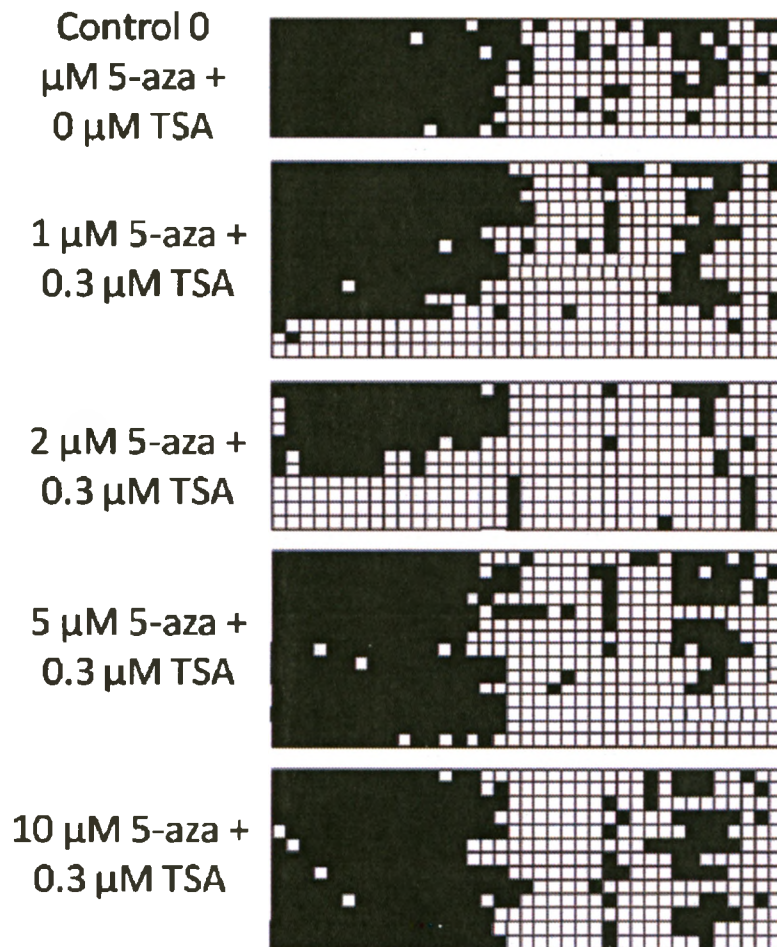
**MCF-7
CGI 1**

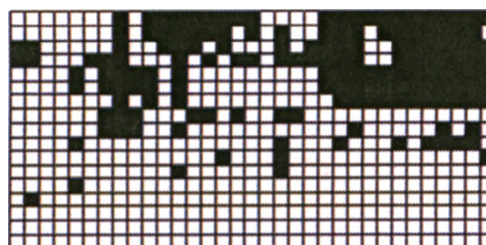
Figure 3.18 MCF-7 cells were partially resistant to demethylation of CpG island 2 by 5-aza-2'deoxyctidine and Trichostatin A. MCF-7 cells were plated at a density of 2.1×10^4 cells/cm² on day 0. Fresh 5-aza-2'deoxyctidine (1, 2, 5 and 10 μ M) was added on day 1, 2 and 3, with the addition of Trichostatin A for the last 24 hours of culture, and cells were harvested on day 4. Methylation of CGI 2-6 was analyzed by bisulfite mutagenesis and sequencing of CGI 2-6, with DNA from cells grown with either no drug (control) or 1 μ M, 2 μ M, 5 μ M or 10 μ M 5-aza + TSA drug treatment.

**MCF-7
CGI 2-6**

Control
0 μM 5-aza +
0 μM TSA



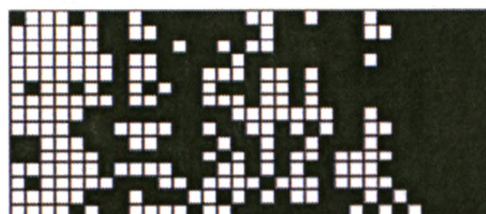
1 μM 5-aza +
0.3 μM TSA



2 μM 5-aza +
0.3 μM TSA



5 μM 5-aza +
0.3 μM TSA



10 μM 5-aza +
0.3 μM TSA



Figure 3.19 MCF-7 cells were resistant to demethylation of 5' to Exon 1 by 5-aza-2'deoxyctidine and Trichostatin A. MCF-7 cells were plated at a density of 2.1×10^4 cells/cm² on day 0. Fresh 5-aza-2'deoxyctidine (1, 2, 5 and 10 μ M) was added on day 1, 2 and 3, with the addition of Trichostatin A for the last 24 hours of culture, and cells were harvested on day 4. Bisulfite mutagenesis and sequencing of a subregion of 5' to Exon 1 was performed with DNA extracted from cells grown with either no drug (control) or 1 μ M, 2 μ M, 5 μ M or 10 μ M 5-aza + TSA drug treatment.

MCF-7
5' to Exon 1

Control
0 μ M 5-aza +
0 μ M TSA



1 μ M 5-aza +
0.3 μ M TSA



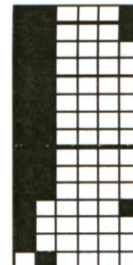
2 μ M 5-aza +
0.3 μ M TSA



5 μ M 5-aza +
0.3 μ M TSA



10 μ M 5-aza +
0.3 μ M TSA



were methylated *in vitro* and promoter activity was determined in MDA-MB-468-LN cells (Figure 3.20). Consistent with the results shown previously, there was increased luciferase activity with the mock-methylated pGL3-hPr vector compared with the mock-methylated control pGL3 vector. It was also found that the luciferase activity from the methylated pGL3-hPr vector was much lower than the mock-methylated pGL3-hPr, indicating that methylation of the plasmid resulted in decreased luciferase activity of the hPr fragment.

However, because the entire vector was methylated, non-specific methylation of the pGL3-basic backbone vector itself may account for some of this difference in luciferase activity. To test whether non-specific methylation of the vector may be contributing to this decreased activity, the hPr promoter region was removed from the vector and methylated *in vitro* ('Patch' methylation), resulting in methylation of only the hPr region. Previous results from our laboratory have demonstrated similar decreases in luciferase activity using both methylation methods in parallel (DiNardo et al., 2001), but to ensure that non-specific methylation was not causing the activity decrease seen in this system, 'patch' methylation of the vector was performed. Reporter vectors (pGL3-hPr-mock and pGL3-hPr-meth) were transfected into MDA-MB-468-LN cells (Figure 3.21). Region hPr basal luciferase activity in MDA-MB-468-LN cells was abolished when Region hPr was methylated. From these two independent methylation manipulation experiments, it appeared that methylation within this putative promoter region was one mechanism of regulation that can be functionally important in the regulation of *ZEB2*, and one that may contribute to altered expression of *ZEB2* during epithelial-mesenchymal transition.

Figure 3.20 *In vitro* methylation of Region hPr reporter plasmid diminished promoter activity. a) A table of the average relative luciferase units (RLU) for the pGL3mock, pGL3meth, pGL3-hPr-mock and pGL3-hPr-meth plasmids transfected into the MDA-MB-468-LN cell line. b) pGL3 and pGL3-hPr were methylated *in vitro* with SssI methylase. Mock-methylation of these vectors was performed in the absence of SssI methylase and S-adenosylmethionine. Methylated and mock-methylated vectors were purified and were transfected into MDA-MB-468-LN cells using Lipofectamine 2000. Forty-eight hours after transfection, cells were lysed and luciferase assays were performed. β -Galactosidase assays were performed to normalize for transfection efficiency. Bars represent the relative luciferase activity of each vector, normalized to β -Galactosidase, obtained from three separate transfections for each vector. Significant luciferase differences ($P < 0.05$) between each group tested, as determined by Analysis of Variance (ANOVA) based on ranks and the Student Newman Keuls post hoc test, are indicated by (*).

a)

Cell Line	Plasmid	RLU
MDA-MB-468-LN	pGL3mock	641
	pGL3meth	59
	pGL3-hPr-mock	14099
	pGL3-hPr-meth	483

b)

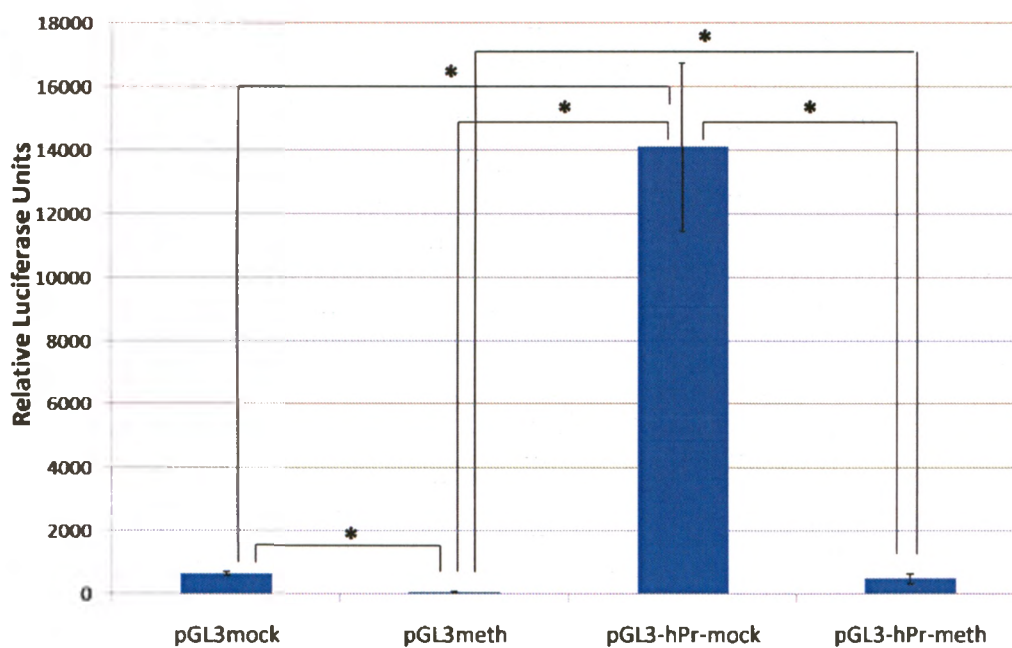
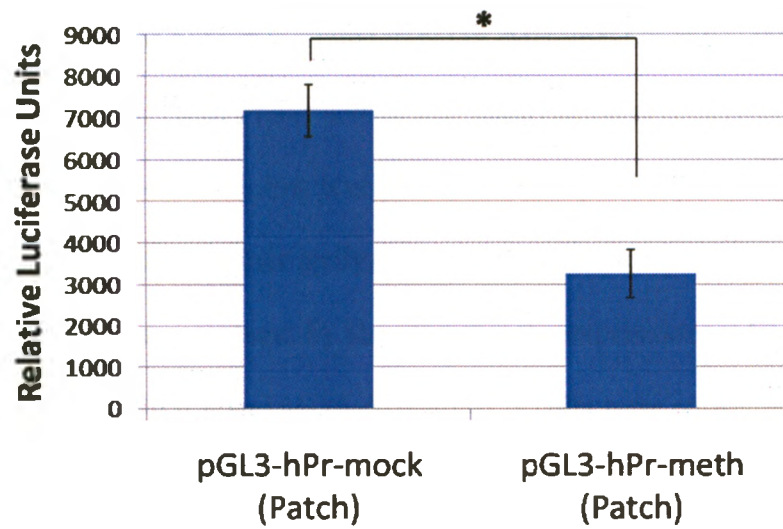


Figure 3.21 'Patch' methylation of Region hPr decreased promoter activity. a) A table of the average relative luciferase units (RLU) for the pGL3-hPr-mock (Patch) and pGL3-hPr-meth (Patch) plasmids transfected into the MDA-MB-468-LN cell line and the P-values for each cell line. b) Region hPr, contained in pGL3-hPr was digested out of the vector, and *SssI* was used to methylation Region hPr *in vitro*. Mock-methylation of Region hPr was performed in the absence of *SssI* methylase and S-adenosylmethionine. Methylated and mock-methylated Region hPr was re-ligated into pGL3. pGL3-hPr-mock (0.75 μ g) and pGL3-hPr-meth (0.75 μ g), along with a vector containing CD20 and CMV- β -Gal, were transfected into MDA-MB-468-LN cells using Lipofectamine 2000. Forty-eight hours after transfection, cells were lysed and luciferase assays were performed. β -Galactosidase assays were performed to normalize for transfection efficiency. Bars represent the relative luciferase activity of each vector, normalized to β -Galactosidase, obtained from two separate transfections for each vector. Significant luciferase activity difference of pGL3-hPr-mock (Patch) ($P < 0.05$) compared to pGL3-hPr-meth (Patch) is indicated by (*).

a)

Cell Line	Plasmid	RLU	P-value
MDA-MB-468-LN	pGL3-hPr-mock (Patch)	7170	0.02
	pGL3-hPr-meth (Patch)	3263	

b)



CHAPTER 4 – DISCUSSION AND CONCLUSIONS

4.1 Summary of Thesis Findings

In this thesis, I investigated the expression of *ZEB2* in ten human breast cancer cell lines. *ZEB2* was not expressed in most epithelial cells, but was expressed in most mesenchymal-like cells, confirming similar findings in the literature. I also demonstrated that for two CpG islands, CGI 1 and CGI 2, epithelial cells had higher levels of methylation, whereas more mesenchymal-like cells had decreased methylation, in the majority of cell lines analyzed. I identified a putative promoter of *ZEB2*, and demonstrated that this region has promoter activity in three cell lines. This promoter region was also found to be hypomethylated in MDA-MB-468-LN cells, compared to MDA-MB-468-GFP cells. Thus, I have shown that methylation inversely correlated with *ZEB2* expression, where cells with low levels of *ZEB2* methylation have high levels of *ZEB2* expression in most of cell lines analyzed. I finally validate these results in a more physiologically relevant environment, by showing that the expression and methylation patterns of MDA-MB-468-GFP and MDA-MB-468-LN cells were consistent between 2D and 3D culture.

To analyze the functional contribution of DNA methylation to the regulation of *ZEB2* expression, cells were treated with the demethylating agent 5-aza-2'-deoxycytidine and the deacetylase inhibitor Trichostatin A. I demonstrated that MDA-MB-468-GFP cells were resistant to drug-induced demethylation of *ZEB2* CpG islands and the region 5' to Exon 1. I also demonstrated that in MCF-7 cells, some drug treatments caused the demethylation of a population of cells at *ZEB2* CGI 1 and CGI 2. MCF-7 cells treated

with drug were able to proliferate, and I was furthermore able to concurrently induce the expression of *DKK3*, a gene previously shown to be responsive to 5-aza treatment (Veeck et al., 2008). However, unlike the robust response seen with *DKK3*, *ZEB2* expression was altered under only one condition of 5-aza treatment that I tested. These results were inconclusive, and by using another approach to study the functionality of *ZEB2* DNA methylation, I demonstrated that two separate methods of *in vitro* methylation of the *ZEB2* promoter diminished promoter activity using luciferase assays.

Taken together, these results indicate that DNA methylation may contribute to the regulation of *ZEB2*, but it remains unclear whether it plays a causal role, or is a consequence of *ZEB2* expression. DNA methylation and *ZEB2* expression are inversely correlated, and while I have also shown that CpG islands proximal to the *ZEB2* gene were at least partially resistant to drug-induced demethylation I have confirmed a *ZEB2* promoter region that was differentially methylated in MDA-MB-468-GFP and MDA-MB-468-LN cell lines, and that *in vitro* methylation of this promoter region diminished promoter activity. Therefore, I conclude that DNA methylation of the *ZEB2* promoter and CpG islands may play a role in the regulation of this gene.

4.2 Expression of *ZEB2* in Mesenchymal Cells

ZEB2 is a transcription factor important in development. It regulates the movement of neural cells for proper neuronal development, and in the absence of this protein, mice die at embryonic day E9.5 (Van de Putte et al., 2003). Given that *ZEB2* plays such a crucial role in the migration of these cells, it seems logical that the aberrant expression of *ZEB2* can cause similar migratory behaviours in cancer cells. In fact, *ZEB2*

expression is increased in a number of cancers (Elloul et al., 2005; Isohata et al., 2009; Kojc et al., 2009; Ohta et al., 2008; Yoshida et al., 2009; Yoshihara et al., 2009). Upregulation of *ZEB2* has also been implicated in epithelial-mesenchymal transition (EMT), a process implicated in metastasis. Many studies have shown that *ZEB2* can regulate key genes in this process, such as E-cadherin and vimentin (Bindels et al., 2006; Comijn et al., 2001). As well, it has been shown that *ZEB2* also downregulates other junctional proteins, and can increase the expression of matrix metalloproteinases (Miyoshi et al., 2004; Vandewalle et al., 2005). It was therefore expected that in the 10 human cancer cell lines analyzed, *ZEB2* was found to be more highly expressed in cells with high levels of vimentin and N-cadherin, and low levels of E-cadherin, indicative of a mesenchymal phenotype. The mesenchymal marker fibronectin did not possess a particular expression pattern in the cell lines analyzed. The pattern of *ZEB2* expression observed was consistent with previous studies that demonstrated that the *ZEB2* transcript was absent in T47D and MCF-7 cells, but was present in MDA-MB-231 and MDA-MB-435S cells (Bindels et al., 2006; Comijn et al., 2001; van Grunsven et al., 2003). Furthermore, the levels of the EMT markers E-cadherin, vimentin and N-cadherin found in the cell lines analyzed, and the morphology of these cells, were consistent with the literature. MDA-MB-231 and MDA-MB-435 cells typically express vimentin, but not E-cadherin, are of a fibroblastic phenotype, and possess some invasive characteristics (Blick et al., 2008; Hollestelle et al., 2009). In contrast, MCF-7, MDA-MB-468, T47D and HCC1806 cells were typically found to be of an epithelial phenotype, with low vimentin expression, high levels of E-cadherin, and typically low in invasive abilities (Blick et al., 2008; Gazdar et al., 1998; Hollestelle et al., 2009). My results are consistent

with these findings, and support my decision to group these sets of cell lines into cells of either epithelial or mesenchymal phenotype. Furthermore, I have further supported the notion that *ZEB2* expression is often elevated in cells of a more mesenchymal-like nature compared to epithelial-like cells. However, it is important to note that only mRNA levels were investigated, due to the lack of good quality antibodies for Western blotting and immunofluorescence procedures. RNA levels are not necessarily reflective of protein abundance, and therefore protein analyses should be performed in the future.

4.3 The *ZEB2* Promoter

Over the last few years, the identification of multiple antisense transcripts has shed some light onto the regulation of the human *ZEB2* gene. A natural antisense transcript (NAT) exists, that when expressed, causes the maintenance of Intron 1, resulting in increased production of the *ZEB2* protein (Beltran et al., 2008). Alternatively, several microRNAs have been identified that are capable of downregulating *ZEB2* (Bracken et al., 2008; Christoffersen et al., 2007; Cochrane et al., 2009; Gandellini et al., 2009; Gregory et al., 2008; Kong et al., 2009; Korpala et al., 2008; Park et al., 2008; Tryndyak et al., 2009). Despite this extensive knowledge, much remains unknown as to which transcription factors may be influencing the expression of *ZEB2*. There has been some evidence to suggest that NF- κ B, ETS1 induced by TGF β , Snail, Churchill, GLI1 in hedgehog signalling, and HIF-1 may play a role in regulating *ZEB2* (Chua et al., 2007; Criswell and Arteaga, 2007; Isohata et al., 2009; Krishnamachary et al., 2006; Ohta et al., 2008; Sheng et al., 2003; Shirakihara et al., 2007; Takkunen et al., 2006). However, due to the lack of identification of the *ZEB2* minimum promoter, these have not been

validated through promoter association methods. In fact, little is known about the human *ZEB2* promoter itself. Three promoters have been identified for the mouse gene (P1, P2 and P3; Figure 1.6b), with P2 showing high promoter activity (Nelles et al., 2003). It has been suggested that P1 and P2 do exist in humans, and that human *ZEB2* transcripts are derived from both promoters. However the majority of transcripts are thought to result from the activation of the main P2 promoter) (Katoh, 2009). To date, these promoter regions have not been confirmed experimentally for the human *ZEB2* gene.

To gain a better understanding of the mechanisms by which *ZEB2* expression is regulated, promoter assays were performed on an 810 bp region of the *ZEB2* gene that spans from -399 bp + to -411 bp, corresponding to a large portion of the region of the mouse *ZEB2* promoter (-960 bp to + 297 bp; (Nelles et al., 2003)). This region did possess promoter activity, as expected, as this region of DNA contains conserved transcription factor binding sites for ETS-SMAD and SP1 (Figure 1.6b) (Katoh, 2009). This activity was greater in the MDA-MB-468-LN and MDA-MB-453 cells as compared to the MCF-7 cells. This may be because *ZEB2* is endogenously expressed in the former two cell lines, and thus, all the necessary machinery for *ZEB2* transcription is presumably present. Promoter activity is still seen in MCF-7 cells despite the fact that this cell line does not usually express *ZEB2*, perhaps because the machinery for *ZEB2* transcription is present. DNA methylation and chromatin structure, as well as the expression of microRNAs, may be at least partially responsible for the lack of *ZEB2* expression in this cell line.

4.4 DNA Methylation in the Regulation of *ZEB2*

ZEB2 is not normally expressed in mammary glands (Cacheux et al., 2001). However, as previously discussed, *ZEB2* expression was increased in a number of human carcinomas, often in cells of a mesenchymal phenotype. Some studies have suggested that this increase in *ZEB2* expression may be the result of decreases in microRNAs capable of downregulating *ZEB2* (Bracken et al., 2008; Christoffersen et al., 2007; Cochrane et al., 2009; Gandellini et al., 2009; Gregory et al., 2008; Kong et al., 2009; Korpál et al., 2008; Park et al., 2008; Tryndyak et al., 2009). However, very little is known about the *ZEB2* promoter and the interplay between transcription factors and epigenetics in the regulation of *ZEB2*. Previous work from our laboratory suggested that DNA methylation may play a role in the regulation of *ZEB2* (Esteller, 2008; Rodenhiser et al., 2008).

DNA methylation can occur in the promoter of genes, and often in CpG islands, which are regions rich in CpGs. The presence or absence of DNA methylation in the promoter of genes can influence the ability of a gene to be transcribed; methylation can hinder the binding of transcription factors necessary for transcription of a gene, and can facilitate the binding of methyl-binding proteins, which can then recruit co-repressor complexes, resulting in the repression of gene transcription. The aberrant hypermethylation or hypomethylation of promoters has been shown to contribute to both cancer and metastasis (Esteller, 2008; Rodenhiser, 2009), and thus, has been further examined here in the context of *ZEB2* regulation.

Interestingly, there are two CpG islands proximal to the *ZEB2* gene, one approximately 4 kb upstream of the *ZEB2* transcriptional start site (CGI 1), and a second,

larger island approximately 3 kb downstream of the transcriptional start site, including Exon 2 (CGI 2). Bisulfite mutagenesis of CGI 1 demonstrated differential methylation patterns among the 10 breast cancer cell lines analyzed. Interestingly, most cells of an epithelial nature appeared to have high levels of *ZEB2* methylation, and most cells of a mesenchymal nature appeared to lack methylation. The methylation status of CGI 2 and two regions of the putative *ZEB2* promoter (5' to Exon 1, and Exon 1) were also analyzed in the MDA-MB-468-GFP and MDA-MB-468-LN cell lines. The methylation patterns found at CGI 2 and the putative promoter mimicked those seen at CGI 1 for these cell lines, where hypomethylation was seen in cells of a more mesenchymal nature. In fact, methylated marks were mainly located at the most 5' CpG sites within the region 5' to Exon 1 (Figure 3.4). This may be due to the presence of SP1 binding sites which overlap CpG site 3 and 4 of this region, which have been previously shown to act as a methylation boundary element, important in maintaining genomic integrity (Butcher et al., 2004; Siegfried et al., 1999). The CpG islands found in the *ZEB2* gene are several kilobases upstream and downstream of the putative human *ZEB2* promoter. These CpG islands may not influence the ability of transcription factors to bind to the promoter of a gene, as typical CpG islands found in the promoter of genes do. Instead, these CpG islands may play an important role in the regulation of *ZEB2* by acting as enhancers, a suggested potential role of distal CpG islands (Schmidl et al., 2009).

CGI 2 is found downstream of the *ZEB2* transcriptional start site. This CpG island is present within the promoter of the natural antisense transcript (NAT) that has been previously described for *ZEB2* (Beltran et al., 2008). The promoter of this NAT is located at the 5' end of CpG island 2. Thus, this CpG island may also regulate the binding of

transcription factors to the promoter of the NAT, or act as an enhancer for the NAT, rather than the *ZEB2* gene itself. Expression analysis of the NAT would be necessary to determine whether methylation of this CpG island would impact transcription factor binding to the promoter, or act as an enhancer, of the NAT. Both CpG islands may also be important in regulating the chromatin structure in this region, influencing the state of compaction and ability of *ZEB2* to be transcribed. Nevertheless, given the correlation between methylation and *ZEB2* expression, the methylation of these CpG islands probably has an important role in the *ZEB2* regulation.

In some cell lines, the methylation status of *ZEB2* did not inversely correlate with *ZEB2* expression. For example, in the MDA-MB-231 cell line, moderate levels of *ZEB2* were observed and extremely high levels of CGI 1 and CGI 2 methylation were found. This inconsistency could be due to the fact that every cancer cell line has its own unique combination of mutations and cellular signalling aberrations. The regulation of *ZEB2* in the MDA-MB-231 cell line may not be identical to that of the other cell lines and may involve alternate modes of regulation, such as miRNA and the *ZEB2* NAT. In addition, we did not sequence the full *ZEB2* gene in the MDA-MB-231 cell line, raising the possibility that chromosomal translocations of the *ZEB2* gene (dissociating it from the putative promoter), or large mutations may have occurred, contributing to the dysregulation of *ZEB2* expression, explaining the high levels of DNA methylation and increased *ZEB2* expression that we observe.

My experiments examining the methylation status and expression of *ZEB2* were carried out using immortalized cell lines grown in 2D culture. The behaviour of these cultured cells in 2D did not necessarily reflect the behaviour of cancerous cells in a

tumour. 3D studies can be used to mimic many aspects of the natural physiological environment, and Matrigel is often used to study epithelial cell behaviour because it contains many components of the basement membrane such as extracellular matrix proteins and growth factors (Yamada and Cukierman, 2007). Cells grown under these conditions have been shown to possess different morphology, cell-cell contacts and cell-matrix contacts (Debnath et al., 2003; Petersen et al., 1992; Yamada and Cukierman, 2007). In the 3D Matrigel model system, the MDA-MB-468-GFP and MDA-MB-468-LN cells had similar expression of *ZEB2* and CpG island 1 methylation patterns, suggesting that the expression of *ZEB2* and the methylation of this gene may be clinically important. However, these 3D environments are still artificial and lack many aspects of the *in vivo* environment, such as other cell-cell interactions and host responses (Yamada and Cukierman, 2007). To more fully understand how DNA methylation may be contributing to the regulation of *ZEB2* in patients, future studies should address *ZEB2* expression and epigenetic regulation in normal and cancerous mammary tissue.

Nevertheless, the maintenance of aberrant methylation, not only among cell lines having similar *ZEB2* expression patterns, but also within the *ZEB2* gene, suggest these DNA methylation patterns may be important in the regulation of this gene. Even more important is the correlation between these methylation patterns and the expression of *ZEB2* that has now been demonstrated. However, these correlative studies have not demonstrated the specific role DNA methylation is playing in the context of *ZEB2* regulation.

Functional analyses were performed using 5-aza-5'-deoxycytidine and Trichostatin A in order to elucidate whether DNA methylation was playing a causative role in *ZEB2*

expression, or whether methylation was a consequence of *ZEB2* expression. 5-aza-2'-deoxycytidine (5-aza) is an agent capable of inhibiting DNA methyltransferases, resulting in global demethylation of the genome (Gabbara and Bhagwat, 1995; Santi et al., 1984). Experiments using 5-aza are often performed with the addition of the histone deacetylase inhibitor Trichostatin A (TSA) (Yoshida et al., 1990), which can work synergistically with 5-aza to cause the activation of genes (Chiurazzi et al., 1999; Meng et al., 2007; Veeck et al., 2008; Zhang et al., 2005).

MDA-MB-468-GFP cells were treated with 5-aza and TSA. However, the MDA-MB-468-GFP cell line was resistant to demethylation of the *ZEB2* gene under the conditions tested, in the regions of the *ZEB2* gene analyzed. These drug conditions did not result in the activation of *ZEB2* or *DKK3*, a gene previously shown to be responsive to 5-aza and TSA treatment in MCF-7 cells (Veeck et al., 2008). The very low expression of *ZEB2* observed at the highest concentrations of 5-aza and TSA could be due to a toxicity response of this drug, as cells grown under these conditions did not proliferate and appeared to be less viable. The lack of robust activation of *ZEB2* or *DKK3* was not due to non-proliferative conditions, as MDA-MB-468-GFP cells were shown to proliferate over the course of these experiments, with the exception of the 5 and 10 μ M conditions in the MDA-MB-468-GFP cells. Additionally, the duration of exposure did not seem to be a factor in this resistance, as MDA-MB-468-GFP cells treated for 5 and 7 days (as opposed to the 3 day treatment) did not result in increased *ZEB2* expression or decreased *ZEB2* methylation. It is possible that demethylation was occurring at other regions within the *ZEB2* gene we have not analyzed. However, the data suggest that either the drugs may not have been active, or the MDA-MB-468-GFP cell line may be

unresponsive to these drugs. The former is not likely true, as the drug was demonstrated to be functional by the partial activation of *ZEB2* and the activation of *DKK3* in MCF-7 cells. Thus, it is likely that MDA-MB-468-GFP cells were unresponsive to these drugs. It has been shown that some human cancer cells are resistance to nucleoside analogues (Kroep et al., 2002; Qin et al., 2009; Stegmann et al., 1995). Work investigating the mechanisms of resistance has suggested that insufficient incorporation of these drugs into the DNA can lead to this resistance (Qin et al., 2009). This may be due to a reduction in deoxycytidine kinase activity, or due to increased activity of cytidine deaminase, an enzyme which can inactivate this drug (Momparker, 2005). As well, the unresponsiveness of these cells to TSA, resulting in the maintenance of tightly compact chromatin may also be contributing to a lack of a response. Further studies utilizing 5-aza and TSA individually, and together, will help to demonstrate the relationship between these two drugs and the resistance that is seen in the MDA-MB-468-GFP cells.

Interestingly, some of the same drug combinations (1 and 2 μM 5-aza) used to treat the MDA-MB-468-GFP cells were able to cause demethylation in a population of MCF-7 cells. In fact, this demethylation did correlate with increased *ZEB2* expression by treatment with 1 μM 5-aza and TSA, but *ZEB2* expression was not increased after 2 μM 5-aza and TSA treatment. The apparent *ZEB2* expression observed at 1 μM 5-aza and TSA could also be the result of genomic DNA contamination of the RNA sample. A no-RT control would be necessary to elucidate whether genomic DNA contamination does exist in this sample. This demethylation, but lack of increased *ZEB2* expression, suggests altered chromatin organization may not alone be sufficient for *ZEB2* regulation. Under the same conditions, *DKK3* was re-expressed due to 5-aza and TSA treatment in MCF-7

cells, clearly demonstrating that the drug was active during these treatments. However, despite this, it is clear that the MCF-7 cells are at least partially resistant to demethylation of *ZEB2* by 5-aza and TSA treatment, as demethylation was only seen in a small population of cells treated with the lowest concentrations of 5-aza. In addition, demethylation was not seen at higher doses of 5-aza, opposite to what is often observed, and the region 5' to Exon 1 was not demethylated under any drug treatment conditions. Cellular resistance to these drugs cannot explain the resistance to demethylation of *ZEB2* observed in the MCF-7 cell line, as it is evident that the drugs were able to elicit a cellular response, demonstrated by the activation of *DKK3*. However, complex regulation of this region of DNA may be hindering the ability of 5-aza to be incorporated. The resistance to demethylation of this gene by 5-aza in MCF-7 cells suggests that perhaps DNA methylation is a consequence of *ZEB2* expression, rather than a cause of altered *ZEB2* expression and that the expression of *ZEB2* may be required to induce a chromatin remodelling response, through signalling and activation of particular factors that are not induced through 5-aza and TSA treatment. Little is understood about gene specific resistance to particular drugs, and our laboratory is currently investigating methods to address this question. However, it remains possible that we have not identified the optimal treatment conditions to sufficiently demethylate *ZEB2*. Thus, further studies using additional concentrations of these drugs, with and other DNMT and HDAC inhibitors may result in a stronger response. Also, it has been suggested that there are regions of the genome that are more susceptible to hypomethylation than others, such as repeat regions (El-Osta, 2003; Narayan et al., 1998; Sadikovic et al., 2004). Alternatively, demethylation of particular regions of genomic DNA may result in detrimental

consequences for the cell, causing genomic instability or inappropriate gene expression, and thus, the cell may be actively acting to protect specific sequences from inappropriate demethylation (El-Osta, 2003; Sadikovic et al., 2004). Finally, the state of histone modifications was not analyzed throughout these experiments. It is plausible that there was insufficient inhibition of deacetylation, or the lack of other histone modifications in this chromatin region, causing the inability of this gene to be activated. Thus, this resistance to demethylation may be a *ZEB2* gene specific response, or it may be a consequence of inadequate testing conditions.

Functional analysis through 5-aza and TSA treatment were inconclusive, due to the lack of responsiveness of the cell lines or the resistance of *ZEB2* demethylation and potentially histone deacetylase inhibition. Therefore, another approach was taken to study the influence of DNA methylation on *ZEB2* expression. The *ZEB2* promoter region was differentially methylated among cell lines of epithelial and mesenchymal phenotype. Testing whether this methylation could functionally impact the activity of this promoter by *in vitro* methylation of promoter constructs and luciferase assays demonstrated that *in vitro* methylation could diminish the activity of this promoter region. These two methods of *in vitro* methylation resulted in different levels of promoter activity decrease. This can be partially due to non-specific methylation of the pGL3-basic vector itself during the whole vector methylation process. As well, the 'patch' methylation experiment was complicated by the complexity and numerous steps of the procedure, resulting in very low yields of end products. Because of this, the quantity of reporter vector transfected into the cells for luciferase activities was much less than that of the whole vector methylation experiments. Thus, these two experiments cannot be adequately compared.

Nevertheless, both experiments yielded similar trends, indicating that *in vitro* methylation was capable of decreasing the activity of the *ZEB2* promoter. These results support a role for DNA methylation in the regulation of *ZEB2* transcription.

Taken together, the results presented appear contradictory. *ZEB2* appeared to be resistant to demethylation, suggesting that DNA methylation may be a consequence of *ZEB2* expression. However, the *in vitro* promoter methylation data suggest that DNA methylation can alter the activity of this gene, and therefore may play a causative role on *ZEB2* expression. The lack of a clear conclusion from these experiments is likely due to the complex nature of the regulation of the *ZEB2* gene. Not only does *ZEB2* have an atypical gene structure, with two CpG islands found distal to the promoter and a long 5' untranslated region, but its regulation is also complex. The mouse *Zeb2* gene has multiple alternate transcripts and promoter regions (Nelles et al., 2003). As well, the effects of the NAT on the regulation of *ZEB2* have not been fully elucidated. MicroRNAs have also been shown to contribute to the regulation of *ZEB2* expression (Bracken et al., 2008; Christoffersen et al., 2007; Cochrane et al., 2009; Gandellini et al., 2009; Gregory et al., 2008; Kong et al., 2009; Korpil et al., 2008; Park et al., 2008; Tryndyak et al., 2009). However, no studies have investigated the combined influence of each of these modes of regulation on each other. To fully understand the specific role DNA methylation plays on the regulation of *ZEB2*, the expression of the miRNAs and NAT must also be examined in these cell lines. Information as to the interaction between these antisense transcripts, as well as how they may influence DNA methylation must be studied. Furthermore, it is not known whether these forms of regulation are mutually exclusive, or if they influence the activity of each other. The DNA methylation patterns observed in the cell lines may in

fact be influencing the activity of the NAT, or the ability of the miRNAs to bind to the *ZEB2* transcript. Furthermore, the influence of each of these modes of regulation on transcription factor binding has not been analyzed. Thus, a thorough understanding of the interaction between all of these modes of *ZEB2* regulation is necessary to fully understand what the specific role of DNA methylation plays in this regulation.

4.5 Future Directions

The experiments described above suggest that DNA methylation may play a role in the regulation of *ZEB2* expression. However, to fully understand this potential regulation, many aspects of this regulation should be analyzed. Firstly, the *ZEB2* gene spans a great distance, and while extensive analysis of the methylation status of CGI 1, CGI 2 and the promoter region of *ZEB2* have been performed, there may be other important regulatory regions that have yet to be identified. The luciferase assays performed in this thesis have sufficiently demonstrated a promoter of the human *ZEB2* gene. Further studies must be performed to elucidate the minimum essential sequence for promoter activity. Cloning of regions where more transcription factors are found to bind will help to identify key regulatory regions, and elucidate the roles of these transcription factors. The inclusion of the two CpG islands into reporter vectors will also demonstrate the importance of these sequences, perhaps acting as enhancers of the *ZEB2* promoter. Furthermore, functional analysis of the ability of many transcription factors identified as having a potential role for *ZEB2* regulation, and those with conserved binding sites within the *ZEB2* gene, should be analyzed. This can be done *in vitro* using gel mobility shift assays, and *in vivo* through chromatin immunoprecipitation experiments, to determine

whether these factors actually bind to specific sequences of the *ZEB2* promoter. The role of methylation in the ability of specific factors to bind can be further studied through gel mobility shift assays, where variable methylated oligonucleotides containing the sequence of interest, can be used. This will indicate whether the binding of specific transcription factors is influenced by DNA methylation, and identify the specific CpGs that are important in the binding of these factors. Thus, identification of specific regulatory regions, and the methylation status of these regions, might lend insight into function of DNA methylation in the regulation of this gene.

This thesis has demonstrated that DNA methylation is implicated in the regulation of *ZEB2*, but has also shown that it is also necessary to investigate histone modifications (such as methylation and acetylation) at various locations within this gene and promoter, to fully understand the interplay between these epigenetic modifications. It may be that the chromatin structure at this region is complex, and other inhibitors are required to activate genes in this region. As well, histone acetylation should be analyzed after 5-aza and TSA treatment to fully elucidate the activity of TSA and the influence of these drugs treatments on chromatin structure throughout these experiments.

The MDA-MB-468-GFP cell lined appeared completely resistant to *ZEB2* demethylation by treatment with 5-aza-2'deoxyctidine and Trichostatin A, potentially due to the unresponsiveness of this cell line to these drugs. Studies into the potential mechanism for resistance to demethylation could be attempted, by looking at the levels of deoxycytidine kinase and cytidine deaminase activity in MDA-MB-468-GFP cells. MCF-7 cells showed some degree of resistance to *ZEB2* demethylation by treatment with these drugs. While it is evident that these treatment conditions were sufficient for activation of

the control gene *DKK3*, in MCF-7 cells, perhaps this is not sufficient for *ZEB2* demethylation. This either suggests that the conditions were not sufficient for demethylation of *ZEB2*, or may imply that DNA methylation is more of a consequence of *ZEB2* expression rather than a cause. Further experiments testing alternate drug treatment conditions, including alternate drug concentrations, differential treatment times, and different combinations of epigenetic drugs may result in more efficient demethylation of this particular region of DNA. Performing these experiments with 5-aza or TSA alone will also help to elucidate mechanisms of resistance, or the influence of each specific epigenetic modification on the regulation of *ZEB2*. However, the lack of responsiveness of *ZEB2* to these drugs may be due to gene specific resistance. There may be groups of genes that are more susceptible to resistance than others, and we are currently working to address this question, as there is very little information about gene specific resistance to 5-aza.

To gain a better understanding of the overall regulation of *ZEB2*, the levels of miRNAs and the *ZEB2* NAT should also be analyzed. These levels should be correlated with the expression of *ZEB2*, and the methylation of the *ZEB2* gene. The influence of all of these modes of regulation on each other is not understood, and the interaction between these modes of regulation and requirements of each of these must be defined. Studies manipulating these levels of regulation should be performed, and the consequence of these alterations on the levels and activities of the other modes of regulation should be analyzed. The levels of these transcripts and DNA methylation should also be analyzed after manipulation of *ZEB2* levels in order to determine if *ZEB2* can impact the methylation status of its promoter.

Finally, it is important to understand how the data presented in this thesis relates to clinical practice. Therefore, *ZEB2* expression and the methylation status of at least the regions analyzed in this thesis should be analyzed in both normal human mammary tissue, where *ZEB2* is not normally expressed, and in normal human brain tissue, where *ZEB2* expression is found (Cacheux et al., 2001). This will lend information as to whether DNA methylation is responsible for the tissue-specific expression of this gene. Finally, to fully elucidate the role of aberrant DNA methylation in the expression of *ZEB2* and the induction (or maintenance) of a more mesenchymal (or invasive) phenotype, *ZEB2* expression and methylation should also be analyzed in human breast carcinoma tissues of differing stage, grade and lymph node status, ideally with matched normal tissue. These experiments will strengthen the notion that aberrant DNA methylation of the *ZEB2* gene may be contributing to increased aggressiveness of some cancers, and may prove useful as a prognostic or diagnostic tool.

4.6 Conclusions

DNA methylation may play a role in the regulation of *ZEB2* expression and altered methylation patterns may contribute to the re-expression of *ZEB2* in cells which will, or have, undergone epithelial to mesenchymal transition. I propose that the *ZEB2* CpG islands and the *ZEB2* promoter are methylated in a tissue-specific manner, in order to maintain low levels of this transcription factor in epithelial cells. However, I believe that aberrant hypomethylation of the *ZEB2* gene can occur, and through interactions with the actions of the NAT and miRNAs and transcription factors, results in increased *ZEB2* expression. Maintaining high levels of *ZEB2* results in the downregulation of E-cadherin

and other junctional proteins, and causes the upregulation of vimentin, N-cadherin and matrix metalloproteinases. All of these changes contribute to the maintenance of a mesenchymal phenotype, which can lead to increased invasiveness of some cells. Despite the inability to conclude whether DNA methylation plays a causative role in the regulation of *ZEB2*, or whether it is a consequence of altered *ZEB2* expression, acting to maintain *ZEB2* activation, it is evident that DNA methylation can influence the regulation of this gene, and likely plays a role in the aberrant expression of this gene during the progression of breast cancer cells to an invasive phenotype.

REFERENCES

- Bachman, K.E., Park, B.H., Rhee, I., Rajagopalan, H., Herman, J.G., Baylin, S.B., Kinzler, K.W., and Vogelstein, B. (2003). Histone modifications and silencing prior to DNA methylation of a tumor suppressor gene. *Cancer Cell* 3, 89-95.
- Beltran, M., Puig, I., Pena, C., Garcia, J.M., Alvarez, A.B., Pena, R., Bonilla, F., and de Herreros, A.G. (2008). A natural antisense transcript regulates Zeb2/Sip1 gene expression during Snail1-induced epithelial-mesenchymal transition. *Genes Dev* 22, 756-769.
- Benvenuti, S., and Comoglio, P.M. (2007). The MET receptor tyrosine kinase in invasion and metastasis. *J Cell Physiol* 213, 316-325.
- Berx, G., Cleton-Jansen, A.M., Nollet, F., de Leeuw, W.J., van de Vijver, M., Cornelisse, C., and van Roy, F. (1995). E-cadherin is a tumour/invasion suppressor gene mutated in human lobular breast cancers. *EMBO J* 14, 6107-6115.
- Berx, G., Raspe, E., Christofori, G., Thiery, J.P., and Sleeman, J.P. (2007). Pre-EMTing metastasis? Recapitulation of morphogenetic processes in cancer. *Clin Exp Metastasis* 24, 587-597.
- Bestor, T.H. (1992). Activation of mammalian DNA methyltransferase by cleavage of a Zn binding regulatory domain. *EMBO J* 11, 2611-2617.
- Bienz, M. (2005). beta-Catenin: a pivot between cell adhesion and Wnt signalling. *Curr Biol* 15, R64-67.
- Bindels, S., Mestdagt, M., Vandewalle, C., Jacobs, N., Volders, L., Noel, A., van Roy, F., Berx, G., Foidart, J.M., and Gilles, C. (2006). Regulation of vimentin by SIP1 in human epithelial breast tumor cells. *Oncogene* 25, 4975-4985.
- Blick, T., Widodo, E., Hugo, H., Waltham, M., Lenburg, M.E., Neve, R.M., and Thompson, E.W. (2008). Epithelial mesenchymal transition traits in human breast cancer cell lines. *Clin Exp Metastasis* 25, 629-642.
- Bolden, J.E., Peart, M.J., and Johnstone, R.W. (2006). Anticancer activities of histone deacetylase inhibitors. *Nat Rev Drug Discov* 5, 769-784.
- Bolos, V., Peinado, H., Perez-Moreno, M.A., Fraga, M.F., Esteller, M., and Cano, A. (2003). The transcription factor Slug represses E-cadherin expression and induces epithelial to mesenchymal transitions: a comparison with Snail and E47 repressors. *J Cell Sci* 116, 499-511.
- Bourc'his, D., and Bestor, T.H. (2004). Meiotic catastrophe and retrotransposon reactivation in male germ cells lacking Dnmt3L. *Nature* 431, 96-99.

- Bracken, C.P., Gregory, P.A., Kolesnikoff, N., Bert, A.G., Wang, J., Shannon, M.F., and Goodall, G.J. (2008). A double-negative feedback loop between ZEB1-SIP1 and the microRNA-200 family regulates epithelial-mesenchymal transition. *Cancer Res* 68, 7846-7854.
- Brueckner, B., Garcia Boy, R., Siedlecki, P., Musch, T., Kliem, H.C., Zielenkiewicz, P., Suhai, S., Wiessler, M., and Lyko, F. (2005). Epigenetic reactivation of tumor suppressor genes by a novel small-molecule inhibitor of human DNA methyltransferases. *Cancer Res* 65, 6305-6311.
- Butcher, D.T., Mancini-DiNardo, D.N., Archer, T.K., and Rodenhiser, D.I. (2004). DNA binding sites for putative methylation boundaries in the unmethylated region of the BRCA1 promoter. *Int J Cancer* 111, 669-678.
- Cacheux, V., Dastot-Le Moal, F., Kaariainen, H., Bondurand, N., Rintala, R., Boissier, B., Wilson, M., Mowat, D., and Goossens, M. (2001). Loss-of-function mutations in SIP1 Smad interacting protein 1 result in a syndromic Hirschsprung disease. *Hum Mol Genet* 10, 1503-1510.
- Canadian Cancer Society's Steering Committee: Canadian Cancer Statistics 2009. Toronto: Canadian Cancer Society.
- Cano, A., Perez-Moreno, M.A., Rodrigo, I., Locascio, A., Blanco, M.J., del Barrio, M.G., Portillo, F., and Nieto, M.A. (2000). The transcription factor snail controls epithelial-mesenchymal transitions by repressing E-cadherin expression. *Nat Cell Biol* 2, 76-83.
- Caulin, C., Scholl, F.G., Frontelo, P., Gamallo, C., and Quintanilla, M. (1995). Chronic exposure of cultured transformed mouse epidermal cells to transforming growth factor-beta 1 induces an epithelial-mesenchymal transdifferentiation and a spindle tumoral phenotype. *Cell Growth Differ* 6, 1027-1035.
- Chambers, A.F., Groom, A.C., and MacDonald, I.C. (2002). Dissemination and growth of cancer cells in metastatic sites. *Nat Rev Cancer* 2, 563-572.
- Cheng, J.C., Yoo, C.B., Weisenberger, D.J., Chuang, J., Wozniak, C., Liang, G., Marquez, V.E., Greer, S., Orntoft, T.F., Thykjaer, T., *et al.* (2004). Preferential response of cancer cells to zebularine. *Cancer Cell* 6, 151-158.
- Chiurazzi, P., Pomponi, M.G., Pietrobono, R., Bakker, C.E., Neri, G., and Oostra, B.A. (1999). Synergistic effect of histone hyperacetylation and DNA demethylation in the reactivation of the FMR1 gene. *Hum Mol Genet* 8, 2317-2323.
- Christoffersen, N.R., Silahatoglu, A., Orom, U.A., Kauppinen, S., and Lund, A.H. (2007). miR-200b mediates post-transcriptional repression of ZFH1B. *RNA* 13, 1172-1178.
- Chua, H.L., Bhat-Nakshatri, P., Clare, S.E., Morimiya, A., Badve, S., and Nakshatri, H. (2007). NF-kappaB represses E-cadherin expression and enhances epithelial to

mesenchymal transition of mammary epithelial cells: potential involvement of ZEB-1 and ZEB-2. *Oncogene* 26, 711-724.

Cochrane, D.R., Spoelstra, N.S., Howe, E.N., Nordeen, S.K., and Richer, J.K. (2009). MicroRNA-200c mitigates invasiveness and restores sensitivity to microtubule-targeting chemotherapeutic agents. *Mol Cancer Ther*.

Comijn, J., Berx, G., Vermassen, P., Verschueren, K., van Grunsven, L., Bruyneel, E., Mareel, M., Huylebroeck, D., and van Roy, F. (2001). The two-handed E box binding zinc finger protein SIP1 downregulates E-cadherin and induces invasion. *Mol Cell* 7, 1267-1278.

Coulondre, C., Miller, J.H., Farabaugh, P.J., and Gilbert, W. (1978). Molecular basis of base substitution hotspots in *Escherichia coli*. *Nature* 274, 775-780.

Criswell, T.L., and Arteaga, C.L. (2007). Modulation of NFkappaB activity and E-cadherin by the type III transforming growth factor beta receptor regulates cell growth and motility. *J Biol Chem* 282, 32491-32500.

Debnath, J., Muthuswamy, S.K., and Brugge, J.S. (2003). Morphogenesis and oncogenesis of MCF-10A mammary epithelial acini grown in three-dimensional basement membrane cultures. *Methods* 30, 256-268.

DiNardo, D.N., Butcher, D.T., Robinson, D.P., Archer, T.K., and Rodenhiser, D.I. (2001). Functional analysis of CpG methylation in the BRCA1 promoter region. *Oncogene* 20, 5331-5340.

Eden, A., Gaudet, F., Waghmare, A., and Jaenisch, R. (2003). Chromosomal instability and tumors promoted by DNA hypomethylation. *Science* 300, 455.

Eger, A., Aigner, K., Sonderegger, S., Dampier, B., Oehler, S., Schreiber, M., Berx, G., Cano, A., Beug, H., and Foisner, R. (2005). DeltaEF1 is a transcriptional repressor of E-cadherin and regulates epithelial plasticity in breast cancer cells. *Oncogene* 24, 2375-2385.

Eisaki, A., Kuroda, H., Fukui, A., and Asashima, M. (2000). XSIPI1, a member of two-handed zinc finger proteins, induced anterior neural markers in *Xenopus laevis* animal cap. *Biochem Biophys Res Commun* 271, 151-157.

El-Osta, A. (2003). DNMT cooperativity--the developing links between methylation, chromatin structure and cancer. *Bioessays* 25, 1071-1084.

Elloul, S., Elstrand, M.B., Nesland, J.M., Trope, C.G., Kvalheim, G., Goldberg, I., Reich, R., and Davidson, B. (2005). Snail, Slug, and Smad-interacting protein 1 as novel parameters of disease aggressiveness in metastatic ovarian and breast carcinoma. *Cancer* 103, 1631-1643.

Esteller, M. (2008). Epigenetics in cancer. *N Engl J Med* 358, 1148-1159.

- Ewing, J. (1928). In *Neoplastic Diseases A treatise on Tumors* (W. B. Saunders Co., Philadelphia and London), pp. 77-89.
- Feinberg, A.P., Gehrke, C.W., Kuo, K.C., and Ehrlich, M. (1988). Reduced genomic 5-methylcytosine content in human colonic neoplasia. *Cancer Res* 48, 1159-1161.
- Franke, W.W., Appelhans, B., Schmid, E., Freudenstein, C., Osborn, M., and Weber, K. (1979). Identification and characterization of epithelial cells in mammalian tissues by immunofluorescence microscopy using antibodies to prekeratin. *Differentiation* 15, 7-25.
- Franke, W.W., Schmid, E., Osborn, M., and Weber, K. (1978). Different intermediate-sized filaments distinguished by immunofluorescence microscopy. *Proc Natl Acad Sci U S A* 75, 5034-5038.
- Gabbara, S., and Bhagwat, A.S. (1995). The mechanism of inhibition of DNA (cytosine-5-)-methyltransferases by 5-azacytosine is likely to involve methyl transfer to the inhibitor. *Biochem J* 307 (Pt 1), 87-92.
- Gandellini, P., Folini, M., Longoni, N., Pennati, M., Binda, M., Colecchia, M., Salvioni, R., Supino, R., Moretti, R., Limonta, P., *et al.* (2009). miR-205 Exerts tumor-suppressive functions in human prostate through down-regulation of protein kinase Cepsilon. *Cancer Res* 69, 2287-2295.
- Garavelli, L., Zollino, M., Mainardi, P.C., Gurrieri, F., Rivieri, F., Soli, F., Verri, R., Albertini, E., Favaron, E., Zignani, M., *et al.* (2009). Mowat-Wilson syndrome: facial phenotype changing with age: study of 19 Italian patients and review of the literature. *Am J Med Genet A* 149A, 417-426.
- Gardiner-Garden, M., and Frommer, M. (1987). CpG islands in vertebrate genomes. *J Mol Biol* 196, 261-282.
- Gazdar, A.F., Kurvari, V., Virmani, A., Gollahon, L., Sakaguchi, M., Westerfield, M., Kodagoda, D., Stasny, V., Cunningham, H.T., Wistuba, II, *et al.* (1998). Characterization of paired tumor and non-tumor cell lines established from patients with breast cancer. *Int J Cancer* 78, 766-774.
- Giepmans, B.N., and van Ijzendoorn, S.C. (2009). Epithelial cell-cell junctions and plasma membrane domains. *Biochim Biophys Acta* 1788, 820-831.
- Greenburg, G., and Hay, E.D. (1982). Epithelia suspended in collagen gels can lose polarity and express characteristics of migrating mesenchymal cells. *J Cell Biol* 95, 333-339.
- Greenburg, G., and Hay, E.D. (1988). Cytoskeleton and thyroglobulin expression change during transformation of thyroid epithelium to mesenchyme-like cells. *Development* 102, 605-622.

- Gregory, P.A., Bert, A.G., Paterson, E.L., Barry, S.C., Tsykin, A., Farshid, G., Vadas, M.A., Khew-Goodall, Y., and Goodall, G.J. (2008). The miR-200 family and miR-205 regulate epithelial to mesenchymal transition by targeting ZEB1 and SIP1. *Nat Cell Biol.*
- Gronbaek, K., Hother, C., and Jones, P.A. (2007). Epigenetic changes in cancer. *APMIS* 115, 1039-1059.
- Guil, S., and Esteller, M. (2009). DNA methylomes, histone codes and miRNAs: tying it all together. *Int J Biochem Cell Biol* 41, 87-95.
- Hanahan, D., and Weinberg, R.A. (2000). The hallmarks of cancer. *Cell* 100, 57-70.
- Heard, E., Clerc, P., and Avner, P. (1997). X-chromosome inactivation in mammals. *Annu Rev Genet* 31, 571-610.
- Hellebrekers, D.M., Griffioen, A.W., and van Engeland, M. (2007). Dual targeting of epigenetic therapy in cancer. *Biochim Biophys Acta* 1775, 76-91.
- Herman, J.G., and Baylin, S.B. (2003). Gene silencing in cancer in association with promoter hypermethylation. *N Engl J Med* 349, 2042-2054.
- Hesson, L.B., Dunwell, T.L., Cooper, W.N., Catchpoole, D., Brini, A.T., Chiaramonte, R., Griffiths, M., Chalmers, A.D., Maher, E.R., and Latif, F. (2009). The novel RASSF6 and RASSF10 candidate tumour suppressor genes are frequently epigenetically inactivated in childhood leukaemias. *Mol Cancer* 8, 42.
- Higashi, Y., Maruhashi, M., Nelles, L., Van de Putte, T., Verschueren, K., Miyoshi, T., Yoshimoto, A., Kondoh, H., and Huylebroeck, D. (2002). Generation of the floxed allele of the SIP1 (Smad-interacting protein 1) gene for Cre-mediated conditional knockout in the mouse. *Genesis* 32, 82-84.
- Hollestelle, A., Nagel, J.H., Smid, M., Lam, S., Elstrodt, F., Wasielewski, M., Ng, S.S., French, P.J., Peeters, J.K., Rozendaal, M.J., *et al.* (2009). Distinct gene mutation profiles among luminal-type and basal-type breast cancer cell lines. *Breast Cancer Res Treat.*
- Imamichi, Y., Konig, A., Gress, T., and Menke, A. (2007). Collagen type I-induced Smad-interacting protein 1 expression downregulates E-cadherin in pancreatic cancer. *Oncogene* 26, 2381-2385.
- Isohata, N., Aoyagi, K., Mabuchi, T., Daiko, H., Fukaya, M., Ohta, H., Ogawa, K., Yoshida, T., and Sasaki, H. (2009). Hedgehog and epithelial-mesenchymal transition signaling in normal and malignant epithelial cells of the esophagus. *Int J Cancer.*
- Jones, P.A., and Taylor, S.M. (1980). Cellular differentiation, cytidine analogs and DNA methylation. *Cell* 20, 85-93.

- Katoh, M. (2009). Integrative genomic analyses of ZEB2: Transcriptional regulation of ZEB2 based on SMADs, ETS1, HIF1alpha, POU/OCT, and NF-kappaB. *Int J Oncol* 34, 1737-1742.
- Kojc, N., Zidar, N., Gale, N., Poljak, M., Fujs Komlos, K., Cardesa, A., Hofler, H., and Becker, K.F. (2009). Transcription factors Snail, Slug, Twist, and SIP1 in spindle cell carcinoma of the head and neck. *Virchows Arch* 454, 549-555.
- Kong, D., Li, Y., Wang, Z., Banerjee, S., Ahmad, A., Kim, H.R., and Sarkar, F.H. (2009). The MiR-200 Regulates PDGF-D Mediated Epithelial-Mesenchymal Transition, Adhesion and Invasion of Prostate Cancer Cells. *Stem Cells*.
- Kongkham, P.N., Northcott, P.A., Ra, Y.S., Nakahara, Y., Mainprize, T.G., Croul, S.E., Smith, C.A., Taylor, M.D., and Rutka, J.T. (2008). An epigenetic genome-wide screen identifies SPINT2 as a novel tumor suppressor gene in pediatric medulloblastoma. *Cancer Res* 68, 9945-9953.
- Korpala, M., Lee, E.S., Hu, G., and Kang, Y. (2008). The miR-200 family inhibits epithelial-mesenchymal transition and cancer cell migration by direct targeting of E-cadherin transcriptional repressors ZEB1 and ZEB2. *J Biol Chem* 283, 14910-14914.
- Kouzarides, T. (2007). Chromatin modifications and their function. *Cell* 128, 693-705.
- Krishnamachary, B., Zagzag, D., Nagasawa, H., Rainey, K., Okuyama, H., Baek, J.H., and Semenza, G.L. (2006). Hypoxia-inducible factor-1-dependent repression of E-cadherin in von Hippel-Lindau tumor suppressor-null renal cell carcinoma mediated by TCF3, ZFHX1A, and ZFHX1B. *Cancer Res* 66, 2725-2731.
- Kroep, J.R., Loves, W.J., van der Wilt, C.L., Alvarez, E., Talianidis, I., Boven, E., Braakhuis, B.J., van Groeningen, C.J., Pinedo, H.M., and Peters, G.J. (2002). Pretreatment deoxycytidine kinase levels predict in vivo gemcitabine sensitivity. *Mol Cancer Ther* 1, 371-376.
- LaGamba, D., Nawshad, A., and Hay, E.D. (2005). Microarray analysis of gene expression during epithelial-mesenchymal transformation. *Dev Dyn* 234, 132-142.
- Lee, J.M., Dedhar, S., Kalluri, R., and Thompson, E.W. (2006). The epithelial-mesenchymal transition: new insights in signaling, development, and disease. *J Cell Biol* 172, 973-981.
- Leonhardt, H., Page, A.W., Weier, H.U., and Bestor, T.H. (1992). A targeting sequence directs DNA methyltransferase to sites of DNA replication in mammalian nuclei. *Cell* 71, 865-873.
- Lo, P.K., and Sukumar, S. (2008). Epigenomics and breast cancer. *Pharmacogenomics* 9, 1879-1902.

- Long, J., Zuo, D., and Park, M. (2005). Pc2-mediated sumoylation of Smad-interacting protein 1 attenuates transcriptional repression of E-cadherin. *J Biol Chem* *280*, 35477-35489.
- Maruhashi, M., Van De Putte, T., Huylebroeck, D., Kondoh, H., and Higashi, Y. (2005). Involvement of SIP1 in positioning of somite boundaries in the mouse embryo. *Dev Dyn* *234*, 332-338.
- Mejlvang, J., Kriaievska, M., Vandewalle, C., Chernova, T., Sayan, A.E., Berx, G., Mellon, J.K., and Tulchinsky, E. (2007). Direct repression of cyclin D1 by SIP1 attenuates cell cycle progression in cells undergoing an epithelial mesenchymal transition. *Mol Biol Cell* *18*, 4615-4624.
- Meng, C.F., Zhu, X.J., Peng, G., and Dai, D.Q. (2007). Re-expression of methylation-induced tumor suppressor gene silencing is associated with the state of histone modification in gastric cancer cell lines. *World J Gastroenterol* *13*, 6166-6171.
- Miquelajauregui, A., Van de Putte, T., Polyakov, A., Nityanandam, A., Boppana, S., Seuntjens, E., Karabinos, A., Higashi, Y., Huylebroeck, D., and Tarabykin, V. (2007). Smad-interacting protein-1 (*Zfhx1b*) acts upstream of Wnt signaling in the mouse hippocampus and controls its formation. *Proc Natl Acad Sci U S A* *104*, 12919-12924.
- Miyoshi, A., Kitajima, Y., Sumi, K., Sato, K., Hagiwara, A., Koga, Y., and Miyazaki, K. (2004). Snail and SIP1 increase cancer invasion by upregulating MMP family in hepatocellular carcinoma cells. *Br J Cancer* *90*, 1265-1273.
- Momparler, R.L. (2005). Pharmacology of 5-Aza-2'-deoxycytidine (decitabine). *Semin Hematol* *42*, S9-16.
- Monk, M., Boubelik, M., and Lehnert, S. (1987). Temporal and regional changes in DNA methylation in the embryonic, extraembryonic and germ cell lineages during mouse embryo development. *Development* *99*, 371-382.
- Mowat, D.R., Croaker, G.D., Cass, D.T., Kerr, B.A., Chaitow, J., Ades, L.C., Chia, N.L., and Wilson, M.J. (1998). Hirschsprung disease, microcephaly, mental retardation, and characteristic facial features: delineation of a new syndrome and identification of a locus at chromosome 2q22-q23. *J Med Genet* *35*, 617-623.
- Narayan, A., Ji, W., Zhang, X.Y., Marrogi, A., Graff, J.R., Baylin, S.B., and Ehrlich, M. (1998). Hypomethylation of pericentromeric DNA in breast adenocarcinomas. *Int J Cancer* *77*, 833-838.
- Nelles, L., Van de Putte, T., van Grunsven, L., Huylebroeck, D., and Verschuere, K. (2003). Organization of the mouse *Zfhx1b* gene encoding the two-handed zinc finger repressor Smad-interacting protein-1. *Genomics* *82*, 460-469.
- Nitta, K.R., Takahashi, S., Haramoto, Y., Fukuda, M., Tanegashima, K., Onuma, Y., and Asashima, M. (2007). The N-terminus zinc finger domain of Xenopus SIP1 is important

for neural induction, but not for suppression of Xbra expression. *Int J Dev Biol* 51, 321-325.

Ohta, H., Aoyagi, K., Fukaya, M., Danjoh, I., Ohta, A., Isohata, N., Saeki, N., Taniguchi, H., Sakamoto, H., Shimoda, T., *et al.* (2008). Cross talk between hedgehog and epithelial-mesenchymal transition pathways in gastric pit cells and in diffuse-type gastric cancers. *Br J Cancer*.

Okano, M., Bell, D.W., Haber, D.A., and Li, E. (1999). DNA methyltransferases Dnmt3a and Dnmt3b are essential for de novo methylation and mammalian development. *Cell* 99, 247-257.

Overton, J. (1977). Response of epithelial and mesenchymal cells to culture on basement lamella observed by scanning microscopy. *Exp Cell Res* 105, 313-323.

Ozawa, M., Baribault, H., and Kemler, R. (1989). The cytoplasmic domain of the cell adhesion molecule uvomorulin associates with three independent proteins structurally related in different species. *EMBO J* 8, 1711-1717.

Ozturk, N., Erdal, E., Mumcuoglu, M., Akcali, K.C., Yalcin, O., Senturk, S., Arslan-Ergul, A., Gur, B., Yulug, I., Cetin-Atalay, R., *et al.* (2006). Reprogramming of replicative senescence in hepatocellular carcinoma-derived cells. *Proc Natl Acad Sci U S A* 103, 2178-2183.

Paget, S. (1889). The distribution of secondary growths in cancer of the breast. 1889. *Cancer Metastasis Rev* 8, 98-101.

Pandit, T.S., Kennette, W., Mackenzie, L., Zhang, G., Al-Katib, W., Andrews, J., Vantyghem, S.A., Ormond, D.G., Allan, A.L., Rodenhiser, D.I., *et al.* (2009). Lymphatic metastasis of breast cancer cells is associated with differential gene expression profiles that predict cancer stem cell-like properties and the ability to survive, establish and grow in a foreign environment. *Int J Oncol* 35, 297-308.

Park, S.M., Gaur, A.B., Lengyel, E., and Peter, M.E. (2008). The miR-200 family determines the epithelial phenotype of cancer cells by targeting the E-cadherin repressors ZEB1 and ZEB2. *Genes Dev* 22, 894-907.

Perez-Moreno, M.A., Locascio, A., Rodrigo, I., Dhondt, G., Portillo, F., Nieto, M.A., and Cano, A. (2001). A new role for E12/E47 in the repression of E-cadherin expression and epithelial-mesenchymal transitions. *J Biol Chem* 276, 27424-27431.

Petersen, O.W., Ronnov-Jessen, L., Howlett, A.R., and Bissell, M.J. (1992). Interaction with basement membrane serves to rapidly distinguish growth and differentiation pattern of normal and malignant human breast epithelial cells. *Proc Natl Acad Sci U S A* 89, 9064-9068.

Peterson, C.L., and Laniel, M.A. (2004). Histones and histone modifications. *Curr Biol* 14, R546-551.

- Postigo, A.A. (2003). Opposing functions of ZEB proteins in the regulation of the TGFbeta/BMP signaling pathway. *EMBO J* 22, 2443-2452.
- Postigo, A.A., and Dean, D.C. (2000). Differential expression and function of members of the *zfh-1* family of zinc finger/homeodomain repressors. *Proc Natl Acad Sci U S A* 97, 6391-6396.
- Postigo, A.A., Depp, J.L., Taylor, J.J., and Kroll, K.L. (2003). Regulation of Smad signaling through a differential recruitment of coactivators and corepressors by ZEB proteins. *EMBO J* 22, 2453-2462.
- Qin, T., Jelinek, J., Si, J., Shu, J., and Issa, J.P. (2009). Mechanisms of resistance to 5-aza-2'-deoxycytidine in human cancer cell lines. *Blood* 113, 659-667.
- Qu, G.Z., Grundy, P.E., Narayan, A., and Ehrlich, M. (1999). Frequent hypomethylation in Wilms tumors of pericentromeric DNA in chromosomes 1 and 16. *Cancer Genet Cytogenet* 109, 34-39.
- Remacle, J.E., Kraft, H., Lerchner, W., Wuytens, G., Collart, C., Verschueren, K., Smith, J.C., and Huylebroeck, D. (1999). New mode of DNA binding of multi-zinc finger transcription factors: deltaEF1 family members bind with two hands to two target sites. *EMBO J* 18, 5073-5084.
- Rivenbark, A.G., Jones, W.D., Risher, J.D., and Coleman, W.B. (2006). DNA methylation-dependent epigenetic regulation of gene expression in MCF-7 breast cancer cells. *Epigenetics* 1, 32-44.
- Rodenhiser, D., and Mann, M. (2006). Epigenetics and human disease: translating basic biology into clinical applications. *CMAJ* 174, 341-348.
- Rodenhiser, D.I. (2009). Epigenetic contributions to cancer metastasis. *Clin Exp Metastasis* 26, 5-18.
- Rodenhiser, D.I., Andrews, J., Kennette, W., Sadikovic, B., Mendlowitz, A., Tuck, A.B., and Chambers, A.F. (2008). Epigenetic mapping and functional analysis in a breast cancer metastasis model using whole-genome promoter tiling microarrays. *Breast Cancer Res* 10, R62.
- Rosivatz, E., Becker, I., Specht, K., Fricke, E., Lubber, B., Busch, R., Hofler, H., and Becker, K.F. (2002). Differential expression of the epithelial-mesenchymal transition regulators snail, SIP1, and twist in gastric cancer. *Am J Pathol* 161, 1881-1891.
- Rountree, M.R., Bachman, K.E., Herman, J.G., and Baylin, S.B. (2001). DNA methylation, chromatin inheritance, and cancer. *Oncogene* 20, 3156-3165.
- Sadikovic, B., Haines, T.R., Butcher, D.T., and Rodenhiser, D.I. (2004). Chemically induced DNA hypomethylation in breast carcinoma cells detected by the amplification of intermethylated sites. *Breast Cancer Res* 6, R329-337.

- Santi, D.V., Norment, A., and Garrett, C.E. (1984). Covalent bond formation between a DNA-cytosine methyltransferase and DNA containing 5-azacytosine. *Proc Natl Acad Sci U S A* *81*, 6993-6997.
- Schmidl, C., Klug, M., Boeld, T.J., Andreesen, R., Hoffmann, P., Edinger, M., and Rehli, M. (2009). Lineage-specific DNA methylation in T cells correlates with histone methylation and enhancer activity. *Genome Res* *19*, 1165-1174.
- Schorderet, D.F., and Gartler, S.M. (1992). Analysis of CpG suppression in methylated and nonmethylated species. *Proc Natl Acad Sci U S A* *89*, 957-961.
- Seder, C.W., Hartojo, W., Lin, L., Silvers, A.L., Wang, Z., Thomas, D.G., Giordano, T.J., Chen, G., Chang, A.C., Orringer, M.B., *et al.* (2009). INHBA overexpression promotes cell proliferation and may be epigenetically regulated in esophageal adenocarcinoma. *J Thorac Oncol* *4*, 455-462.
- Segura-Pacheco, B., Trejo-Becerril, C., Perez-Cardenas, E., Taja-Chayeb, L., Mariscal, I., Chavez, A., Acuna, C., Salazar, A.M., Lizano, M., and Duenas-Gonzalez, A. (2003). Reactivation of tumor suppressor genes by the cardiovascular drugs hydralazine and procainamide and their potential use in cancer therapy. *Clin Cancer Res* *9*, 1596-1603.
- Sheng, G., dos Reis, M., and Stern, C.D. (2003). Churchill, a zinc finger transcriptional activator, regulates the transition between gastrulation and neurulation. *Cell* *115*, 603-613.
- Shirakihara, T., Saitoh, M., and Miyazono, K. (2007). Differential regulation of epithelial and mesenchymal markers by deltaEF1 proteins in epithelial mesenchymal transition induced by TGF-beta. *Mol Biol Cell* *18*, 3533-3544.
- Siegfried, Z., Eden, S., Mendelsohn, M., Feng, X., Tsuberi, B.Z., and Cedar, H. (1999). DNA methylation represses transcription in vivo. *Nat Genet* *22*, 203-206.
- Simpson, P.T., Reis-Filho, J.S., Gale, T., and Lakhani, S.R. (2005). Molecular evolution of breast cancer. *J Pathol* *205*, 248-254.
- Song, F., Smith, J.F., Kimura, M.T., Morrow, A.D., Matsuyama, T., Nagase, H., and Held, W.A. (2005). Association of tissue-specific differentially methylated regions (TDMs) with differential gene expression. *Proc Natl Acad Sci U S A* *102*, 3336-3341.
- Stegmann, A.P., Honders, M.W., Hagemeijer, A., Hoebee, B., Willemze, R., and Landegent, J.E. (1995). In vitro-induced resistance to the deoxycytidine analogues cytarabine (AraC) and 5-aza-2'-deoxycytidine (DAC) in a rat model for acute myeloid leukemia is mediated by mutations in the deoxycytidine kinase (dck) gene. *Ann Hematol* *71*, 41-47.
- Stirzaker, C., Song, J.Z., Davidson, B., and Clark, S.J. (2004). Transcriptional gene silencing promotes DNA hypermethylation through a sequential change in chromatin modifications in cancer cells. *Cancer Res* *64*, 3871-3877.

Szabo, C.I., and King, M.C. (1995). Inherited breast and ovarian cancer. *Hum Mol Genet 4 Spec No*, 1811-1817.

Takkunen, M., Grenman, R., Hukkanen, M., Korhonen, M., Garcia de Herreros, A., and Virtanen, I. (2006). Snail-dependent and -independent epithelial-mesenchymal transition in oral squamous carcinoma cells. *J Histochem Cytochem 54*, 1263-1275.

Thiery, J.P. (2002). Epithelial-mesenchymal transitions in tumour progression. *Nat Rev Cancer 2*, 442-454.

Thiery, J.P., and Sleeman, J.P. (2006). Complex networks orchestrate epithelial-mesenchymal transitions. *Nat Rev Mol Cell Biol 7*, 131-142.

Tryndyak, V.P., Ross, S.A., Beland, F.A., and Pogribny, I.P. (2009). Down-regulation of the microRNAs miR-34a, miR-127, and miR-200b in rat liver during hepatocarcinogenesis induced by a methyl-deficient diet. *Mol Carcinog 48*, 479-487.

Tuck, A.B., Arsenault, D.M., O'Malley, F.P., Hota, C., Ling, M.C., Wilson, S.M., and Chambers, A.F. (1999). Osteopontin induces increased invasiveness and plasminogen activator expression of human mammary epithelial cells. *Oncogene 18*, 4237-4246.

Tylzanowski, P., Verschueren, K., Huylebroeck, D., and Luyten, F.P. (2001). Smad-interacting protein 1 is a repressor of liver/bone/kidney alkaline phosphatase transcription in bone morphogenetic protein-induced osteogenic differentiation of C2C12 cells. *J Biol Chem 276*, 40001-40007.

Vaissiere, T., Sawan, C., and Herceg, Z. (2008). Epigenetic interplay between histone modifications and DNA methylation in gene silencing. *Mutat Res 659*, 40-48.

Valles, A.M., Boyer, B., Badet, J., Tucker, G.C., Barritault, D., and Thiery, J.P. (1990). Acidic fibroblast growth factor is a modulator of epithelial plasticity in a rat bladder carcinoma cell line. *Proc Natl Acad Sci U S A 87*, 1124-1128.

Van de Putte, T., Maruhashi, M., Francis, A., Nelles, L., Kondoh, H., Huylebroeck, D., and Higashi, Y. (2003). Mice lacking ZFH1B, the gene that codes for Smad-interacting protein-1, reveal a role for multiple neural crest cell defects in the etiology of Hirschsprung disease-mental retardation syndrome. *Am J Hum Genet 72*, 465-470.

van Grunsven, L.A., Michiels, C., Van de Putte, T., Nelles, L., Wuytens, G., Verschueren, K., and Huylebroeck, D. (2003). Interaction between Smad-interacting protein-1 and the corepressor C-terminal binding protein is dispensable for transcriptional repression of E-cadherin. *J Biol Chem 278*, 26135-26145.

van Grunsven, L.A., Papin, C., Avalosse, B., Opdecamp, K., Huylebroeck, D., Smith, J.C., and Bellefroid, E.J. (2000). XSIP1, a Xenopus zinc finger/homeodomain encoding gene highly expressed during early neural development. *Mech Dev 94*, 189-193.

- Vandewalle, C., Comijn, J., De Craene, B., Vermassen, P., Bruyneel, E., Andersen, H., Tulchinsky, E., Van Roy, F., and Berx, G. (2005). SIP1/ZEB2 induces EMT by repressing genes of different epithelial cell-cell junctions. *Nucleic Acids Res* 33, 6566-6578.
- Vantyghem, S.A., Allan, A.L., Postenka, C.O., Al-Katib, W., Keeney, M., Tuck, A.B., and Chambers, A.F. (2005). A new model for lymphatic metastasis: development of a variant of the MDA-MB-468 human breast cancer cell line that aggressively metastasizes to lymph nodes. *Clin Exp Metastasis* 22, 351-361.
- Veeck, J., Bektas, N., Hartmann, A., Kristiansen, G., Heindrichs, U., Knuchel, R., and Dahl, E. (2008). Wnt signalling in human breast cancer: expression of the putative Wnt inhibitor Dickkopf-3 (DKK3) is frequently suppressed by promoter hypermethylation in mammary tumours. *Breast Cancer Res* 10, R82.
- Veeck, J., Niederacher, D., An, H., Klopocki, E., Wiesmann, F., Betz, B., Galm, O., Camara, O., Durst, M., Kristiansen, G., *et al.* (2006). Aberrant methylation of the Wnt antagonist SFRP1 in breast cancer is associated with unfavourable prognosis. *Oncogene* 25, 3479-3488.
- Verona, R.I., Mann, M.R., and Bartolomei, M.S. (2003). Genomic imprinting: intricacies of epigenetic regulation in clusters. *Annu Rev Cell Dev Biol* 19, 237-259.
- Verschueren, K., Remacle, J.E., Collart, C., Kraft, H., Baker, B.S., Tylzanowski, P., Nelles, L., Wuytens, G., Su, M.T., Bodmer, R., *et al.* (1999). SIP1, a novel zinc finger/homeodomain repressor, interacts with Smad proteins and binds to 5'-CACCT sequences in candidate target genes. *J Biol Chem* 274, 20489-20498.
- Weaver, V.M., and Bissell, M.J. (1999). Functional culture models to study mechanisms governing apoptosis in normal and malignant mammary epithelial cells. *J Mammary Gland Biol Neoplasia* 4, 193-201.
- Weber, M., Davies, J.J., Wittig, D., Oakeley, E.J., Haase, M., Lam, W.L., and Schubeler, D. (2005). Chromosome-wide and promoter-specific analyses identify sites of differential DNA methylation in normal and transformed human cells. *Nat Genet* 37, 853-862.
- Wellings, S.R., Jensen, H.M., and Marcum, R.G. (1975). An atlas of subgross pathology of the human breast with special reference to possible precancerous lesions. *J Natl Cancer Inst* 55, 231-273.
- Wyckoff, J.B., Jones, J.G., Condeelis, J.S., and Segall, J.E. (2000). A critical step in metastasis: in vivo analysis of intravasation at the primary tumor. *Cancer Res* 60, 2504-2511.
- Yamada, K.M., and Cukierman, E. (2007). Modeling tissue morphogenesis and cancer in 3D. *Cell* 130, 601-610.

- Yoshida-Noro, C., Suzuki, N., and Takeichi, M. (1984). Molecular nature of the calcium-dependent cell-cell adhesion system in mouse teratocarcinoma and embryonic cells studied with a monoclonal antibody. *Dev Biol* 101, 19-27.
- Yoshida, J., Horiuchi, A., Kikuchi, N., Hayashi, A., Osada, R., Ohira, S., Shiozawa, T., and Konishi, I. (2009). Changes in the expression of E-cadherin repressors, Snail, Slug, SIP1, and Twist, in the development and progression of ovarian carcinoma: the important role of Snail in ovarian tumorigenesis and progression. *Med Mol Morphol* 42, 82-91.
- Yoshida, M., Kijima, M., Akita, M., and Beppu, T. (1990). Potent and specific inhibition of mammalian histone deacetylase both in vivo and in vitro by trichostatin A. *J Biol Chem* 265, 17174-17179.
- Yoshihara, K., Tajima, A., Komata, D., Yamamoto, T., Kodama, S., Fujiwara, H., Suzuki, M., Onishi, Y., Hatae, M., Sueyoshi, K., *et al.* (2009). Gene expression profiling of advanced-stage serous ovarian cancers distinguishes novel subclasses and implicates ZEB2 in tumor progression and prognosis. *Cancer Sci.*
- Yoshimoto, A., Saigou, Y., Higashi, Y., and Kondoh, H. (2005). Regulation of ocular lens development by Smad-interacting protein 1 involving Foxe3 activation. *Development* 132, 4437-4448.
- Zhang, Y., Fatima, N., and Dufau, M.L. (2005). Coordinated changes in DNA methylation and histone modifications regulate silencing/derepression of luteinizing hormone receptor gene transcription. *Mol Cell Biol* 25, 7929-7939.